

Nitric oxide synthase mediates growth coordination during
Drosophila melanogaster imaginal disc regeneration

Jacob Stephen Jaszczak

B.S., Michigan Technological University, 2010

A Dissertation Presented to the Graduate Faculty
of the University of Virginia in Candidacy for the Degree of
Doctor of Philosophy

Department of Cell Biology

University of Virginia
August 2015

Abstract

Regulation of developmental growth is necessary to form animals of specific size and proportion. Growth coordination between organs ensures that each organ develops to the right size and proportion. The mechanisms regulating the coordination of developmental growth are not fully understood. Using *Drosophila melanogaster* regeneration as a model for developmental growth coordination, I describe a novel pathway through which tissues communicate with a central endocrine organ, the prothoracic gland, to coordinate growth. During *Drosophila* larval development, damage to imaginal discs activates a regeneration checkpoint that slows the growth of undamaged imaginal discs, coordinating regeneration of the damaged discs with developmental growth. *Drosophila* insulin-like peptide 8 (Dilp8) is secreted from regenerating imaginal discs and restricts growth of the undamaged imaginal discs. I identify nitric oxide synthase (NOS) as a target of Dilp8 signaling. During regeneration, Dilp8 activates NOS signaling in the prothoracic gland, reducing ecdysone biosynthesis to slow the growth of undamaged tissues. I also identify Lgr3 as a putative receptor for Dilp8. Lgr3 mediates growth coordination and regulates NOS signaling in the PG. Additionally, Dilp8 and Lgr3 also regulate bilateral symmetry in *Drosophila* and Lgr3 regulates organ-proportions in mammals. This suggests that the Dilp8-Lgr3-NOS pathway, which regulates organ growth through signaling in the endocrine system, may be conserved beyond *Drosophila* regeneration.

Acknowledgements

I owe lasting gratitude to many people for their tremendous support through out my time in graduate school. Foremost, I thank my advisor, Adrian Halme. This dissertation represents my first contribution to science, but even more so exemplifies Adrian's contribution to my development as a scientist.

I am also thankful to the scientific community of the Cell Biology department, of which I have been honored to be a part. To my thesis committee, Xiaowei Lu, Dougl DeSimone, and Paul Adler, thank you for your valuable time and advice in support of my scientific exploration. To my fellow graduate research comrades, thanks for all the good times and for letting me bum off your lab equipment. And thank you to all the past and present members of the Halme lab, especially Jacob Wolpe who dove right in with me and worked tirelessly on these projects.

I also thank my role model who embodies scientific enthusiasm, my Dad, and my Mom, for her sacrifice in laying the foundation of my education that has brought me to this point.

Many friendships are formed under the pressures of science and in the heat of the laboratory. In my time here, one of these friendships was forged into more; this dissertation never would have been finished without the support and love of my wife and lab partner, Becky. I dedicate this work to her and the future science we will share together.

Table of Contents

Abstract	ii
Acknowledgements	iii
Table of Contents	iv
List of Abbreviations	ix
List of Figures	xi

Chapter 1: Introducton

1.1 Developmental regulation of allometry	2
1.1.1 The importance of size and proportion	2
1.1.2 Allometry is determined through growth rate and time	3
1.1.3 Allometry requires coordination of autonomous and systemic growth	4
1.1.4 Studying of growth coordination in <i>Drosophila</i>	6
1.2 Endocrine regulation of allometry	8
1.2.1 Nutrient signaling regulates growth and time	8
1.2.2 Steroid hormones regulate growth and time	10
1.2.3 Reciprocal regulation of IIS and ecdysone	13
1.2.4 Coordination of endocrine and autonomous growth regulation	15
1.3 Nitric oxide regulation of growth	16
1.3.1 Nitric oxide synthase	16

1.3.2 Mammalian <i>NOS</i>	17
1.3.4 <i>Drosophila NOS</i>	18
1.3.4 Mechanisms of NO growth regulation	20
1.3.5 NO regulation of nuclear hormone receptors	22
1.4 Summary	24
Chapter 2: Methods	
2.1 <i>Drosophila</i> Stocks	33
2.2 <i>Drosophila</i> culture and media	33
2.3 Ionizing irradiation damage	34
2.4 DAF2-DA assay	35
2.5 Measurement of growth parameters	35
2.6 Indirect immunofluorescence	36
2.7 Ecdysone measurements	36
2.8 NADPH-diaphorase assay	36
2.9 Polymerase chain reaction (PCR)	37
2.10 Semi-quantitative PCR	37
2.11 Quantitative RT-PCR	38
2.12 Ecdysone media	38
2.13 X-gal staining	39
2.14 Calcium Imaging	39

Chapter 3: Nitric oxide synthase regulates growth coordination during *Drosophila melanogaster* imaginal disc regeneration

3.1 Abstract	41
3.2 Introduction	42
3.3 Results	45
3.3.1 Nitric oxide synthase (NOS) is necessary for growth regulation during the regeneration checkpoint	45
3.3.2 Nitric oxide synthase activity in the prothoracic gland regulates imaginal disc growth	46
3.3.4 The growth of imaginal tissues is selectively regulated during the regeneration checkpoint	49
3.3.5 NOS in the PG inhibits ecdysone biosynthesis during the larval growth phase	51
3.3.6 The regeneration checkpoint reduces growth of undamaged tissues by limiting ecdysone signaling	56
3.4 Discussion	57

Chapter 4: The leucine-rich repeat-containing G-protein-coupled receptor Lgr3 mediates growth coordination and developmental delay during regeneration

4.1 Abstract	101
4.2 Introduction	102
4.3 Results	104
4.3.1 The <i>Drosophila</i> relaxin receptor homolog, Lgr3, is required for growth coordination and delay during the regeneration checkpoint	104
4.3.2 Lgr3 mediates Dilp8 activation of NOS in the PG and is necessary for growth coordination during the regeneration checkpoint	106
4.3.3 Lgr3 functions in neurons to regulate ecdysone production and imaginal tissue growth during development	108
4.3.4 Larvae depleted for neuronal Lgr3 activity fail to delay or produce distal growth inhibition following damage	110
4.4 Discussion	112

Chapter 5: Discussion

5.1 Summary	152
5.1.1 Is this model applicable outside of <i>Drosophila</i> regeneration?	154
5.1.2 What is the mechanism of NOS regulation of ecdysone biosynthesis?	155
5.1.3 What is the signaling pathway of Lgr3-NOS production?	159
5.1.4 What is the mechanism of neuronal Lgr3 regulation of growth?	161
5.1.5 How does regenerative growth continue during ecdysone restriction?	164
5.2 Conclusions	167

List of Abbreviations

1H-[1,2,4]oxadiazolo[4,3-a]quinoxalin-1-one	ODQ
4,5-diaminofluorescein diacetate	DAF2-DA
After egg deposition	AED
Central nervous system	CNS
cGMP-dependent protein kinase	PKG
Cyclic adenosine 3', 5'-monophosphate	cAMP
Cyclic guanosine 3', 5'-monophosphate	cGMP
Cytochrome P450	CYP
<i>disembodied</i>	<i>dib</i>
<i>Drosophila</i> insulin like peptides	Dilps
<i>Drosophila</i> insulin-like peptide 8	Dilp8
Ecdysone receptor	EcR
Epidermal growth factor receptor	EGFR
Forkhead box Class O	FoxO
Formaldehyde dehydrogenase	Fdh
Guanosine 5'-triphosphate	GTP
Hypothalamic-pituitary-adrenal	HPA
Insulin growth factor	IGF
Insulin receptor	InR
Insulin/IGF signaling	IIS

Juvenile hormone	JH
Leucine-rich repeat-containing G-protein coupled receptor	Lgr
Methoprene-tolerant	Met
Mitogen-activated protein kinase	MAPK
Nitric oxide	NO
Nitric oxide synthase	NOS
Nuclear hormone receptor	NHR
<i>phantom</i>	<i>phm</i>
Phosphatase and tensin homolog	PTEN
Phosphatidylinositol 3-kinase	PI3K
Prothoracic gland	PG
Prothoracicotropic hormone	PTTH
S-nitrosoglutathione	GSNO
Serine-threonine protein kinase	Akt
<i>shade</i>	<i>shd</i>
<i>shadow</i>	<i>sad</i>
Soluble guanylate cyclase	sGC
<i>spookier</i>	<i>spok</i>
Ultraspiracle	Usp
Untranslated region	UTR

List of Figures

Figure 1: The allometric relationship of brain and heart growth relative to body growth.	26
Figure 2: The relationships of allometric growth.	28
Figure 3: Reciprocal regulation of IIS and ecdysone.	30
Figure 3-1. Imaginal disc growth inhibition during either Eiger-induced damage or targeted irradiation is dependent on Dilp8.	63
Figure 3-2. <i>NOS</i> is required for imaginal disc growth coordination during the regeneration checkpoint.	65
Figure 3-3. <i>NOS</i> is required in the prothoracic gland (PG) to coordinate imaginal tissue growth during the regeneration checkpoint.	67
Figure 3-4. <i>NOS</i> non-autonomously regulates imaginal disc growth.	69
Figure 3-5. DAF2-DA assay for detection of NO production.	71
Figure 3-6. <i>NOS</i> is not required for regulation of developmental time during the regeneration checkpoint.	73
Figure 3-7. The regeneration checkpoint selectively restricts imaginal tissue growth.	75
Figure 3-8. <i>NOS</i> overexpression during larval feeding inhibits ecdysone biosynthesis.	77
Figure 3-9. <i>NOS</i> inhibits ecdysone synthesis during the feeding period, and promotes ecdysone production post-feeding.	79

Figure 3-10. Imaginal disc growth restriction during the regeneration checkpoint is the result of reduced ecdysone signaling.	81
Figure 3-11. Ecdysone regulates larval growth and developmental time.	83
Figure 3-12. Model for allometric growth regulation during the regeneration checkpoint.	85
Figure A1-1. L-NAME feeding inhibits imaginal disc growth.	88
Figure A1-2. The allele <i>NOSΔ</i> reduces growth restriction during targeted damage.	90
Figure A1-3. Expression of the cell gene reaper in the wing imaginal disc delays development and inhibits growth.	92
Figure A1-4. <i>NOS</i> overexpression in the PG does not delay E74A transcription.	94
Figure A1-5. FoxO and NOS in the PG regulate growth in parallel.	96
Figure A1-8. FoxO is not necessary for developmental delay induced by <i>Bx>eiger</i> or <i>phm>NOS</i> .	98
Figure 4-1: The <i>Drosophila</i> relaxin receptor homolog Lgr3 regulates Dilp8 mediated growth coordination and developmental delay during the regeneration checkpoint.	114
Figure 4-2: LGR1 and LGR2 do not regulate growth coordination.	116
Figure 4-3: Enhancer elements of Lgr3 express in the larval CNS and PG.	118
Figure 4-4: Lgr3 in the PG regulates growth coordination and NOS activity.	120

Figure 4-5: Lgr3 in neurons regulates imaginal disc growth and ecdysone signaling during larval development.	122
Figure 4-6: Lgr3 depletion systemically increases imaginal disc growth.	124
Figure 4-7: Lgr3 in neurons regulates developmental delay and growth coordination during the regeneration checkpoint.	126
Figure 4-8: Lgr3 in neurons indirectly regulates PTTH signaling through a NOS-independent mechanism.	128
Figure A2-1. Symmetry assay of adult wings.	131
Figure A2-2. Lgr3-RNAi does not significantly change growth of the larval tissues.	133
Figure A2-3. Lgr3 enhancer fragment expression increase in the CNS after irradiation.	135
Figure A2-4. Expression of Lgr3-RNAi with the enhancer line 18A01 increases imaginal disc growth.	139
Figure A2-5. Expression of Gαq-RNAi in the PG does not rescue growth restriction after targeted irradiation.	141
Figure A2-6. Irradiation increases calcium basal calcium levels and inhibits calcium pulsing and propagation.	143
Figure A2-7. Expression of Lgr3-RNAi in neurons misregulates <i>sgs3</i> expression.	145

- Figure A2-8. Lgr3-RNAi with Dilp8 overexpression in neurons does
not rescue growth but does rescue delay. 147
- Figure A2-9. Lgr3-RNAi expression in neurons increases pupal death
after development irradiation. 149

Chapter 1

Introduction

1.1 Developmental regulation of allometry

“The most obvious differences between different animals are differences of size, but for some reason the zoologists have paid singularly little attention to them”

(J.B.S. Haldane. *On being the right size*. 1926).

1.1.1 The importance of size and proportion

Allometry is broadly defined as the relative growth rate between organs and the body as a whole. Diversity within taxa is largely the result of changes in the allometry of body plans. For instance, most mammals have seven neck vertebrae, but one of the most striking differences between a giraffe and an antelope is their difference allometry. Allometry has a profound impact on life history. Caste membership of *Atta sexdens* ants is determined by developmental polymorphisms of size as each ant's role within the colony is assigned by body size and proportion (Hölldobler and Wilson 1990). Variation in organ allometry also impacts human health. Growth deviations from the optimal allometry of the heart can increase susceptibility for cardiovascular disease (Hill and Olson 2008). Development of extreme proportions in allometry can even result in extinction, evidenced in the forces of sexual selection driving unsustainable growth of the fabled antlers of the Irish elk (Moen, Pastor, and Cohen 1999).

In each of these examples, multiple mechanisms control allometric growth during development. Whether genetic, endocrine, or ecological, these mechanisms contribute to an animal's development and "be[coming] the right size". Some of these mechanisms have been better defined since J.B.S. Haldane pondered the problem of size. Systemic signals, such as growth factors and steroid hormones, are important for integrating environmental and nutrient status with growth rate (Edgar 2006; Callier and Nijhout 2013). Cell and organ autonomous pathways, which include cell division, morphogen signaling, and cell-cell contacts, also regulate growth (Conlon and Raff 1999; Irvine and Harvey 2015).

However, these systemic and autonomous pathways of growth regulation do not fully explain how allometric growth is maintained during development. In this introduction, I will discuss the developmental factors that contribute to allometry. This discussion will include examining our current understanding of growth coordination during development, the evidence for inter-organ communication during development, and how the endocrine system functions to regulate developmental allometry.

1.1.2 Allometry is determined through growth rate and time

The determination of final size and allometry of animals is a combination of two factors: 1) the rate at which growth occurs, and 2) the total time during which

growth occurs. The importance of these two factors is observed in the allometry of brain and heart growth during human development (Figure 1). After birth, the brain grows hypoallometrically (slower rate) to body size, ultimately reaching final size early in development. In contrast, the heart grows nearly isometrically (same rate) throughout development (Figure 2). If development were stopped early the final relative size of the head would be larger than the proportions achieved later in development. For example, the effects of disrupting developmental time are observed in the characteristically large head-to-body ratio observed in patients with the genetic disease progeria. Mutations in the structural protein lamin (*LMNA*) cause an early end to development by inducing premature aging (Pollex and Hegele 2004). This reduces developmental time and ends growth while the head is proportionally larger than the body. This example demonstrates the importance of the regulation of growth rate and developmental time. As I will discuss below, the regulation of growth rate and time during development can be regulated by interconnected mechanisms.

1.1.3 Allometry requires coordination of autonomous and systemic growth

The importance of growth coordination is observed in transplantation and ablation experiments. In mammals, multiple fetal spleens transplanted into a single host stop growing at the total equivalent mass of a control spleen (Metcalf 1964). This experiment suggests that growth is not only regulated by systemic

signals from the host, but also by inter-organ communication, because the organs coordinate to reach a uniform accumulative size. In insects, regenerating imaginal discs demonstrate that growth coordination also occurs through inter-organ communication. Regeneration of insect imaginal discs can be induced by surgical fragmentation, x-ray irradiation, or by transgene expression of cell death inducing genes (Maghavan and Schneiderman 1969, Bryant 1971, Halme, Cheng, and Hariharan 2010). Regenerating imaginal discs slow the growth of the distal undamaged discs (Maghavan and Schneiderman 1969; Nijhout and Emlen 1998; Simmons and Emlen 2006; Parker and Shingleton 2011) by producing a secreted peptide *Drosophila* insulin-like peptide 8 (Dilp8). (Colombani, Andersen, and Leopold 2012; Garelli et al. 2012). Together, these experiments suggest that organs not only read the systemic signals of the host, but also contribute their own signals that communicate their relative growth to other organs.

Based on these observations, Stern and Emlen (1999) proposed that growth coordination pathways would involve methods for organs to translate systemic growth signals individually, either directly or indirectly through a centralized endocrine source. Recent evidence and my work presented in this dissertation suggest that communication between organs and the endocrine system regulates growth coordination and developmental allometry.

1.1.4 Studying of growth coordination in *Drosophila*

The model organism *Drosophila melanogaster* has emerged as a tractable system for studying the coordination between autonomous and systemic growth regulation. As a holometabolous insect, the final size of the adult (imago) is determined by growth during the larval phases of development. Two classes of tissues are present during larval development. The diploid imaginal tissues, which grow by mitosis, are the primary tissues that contribute to the fixed size of the adult structures during metamorphosis. In contrast, tissues that make up most of the size of the larvae (such as the larval epidermis, fat body, and salivary glands) are polyploid and grow by endoreplication (Oldham et al. 2000). The larval tissues make up most of the initial weight of the pupae, but are histolysed during metamorphosis and do not contribute significantly to the final size of the adult. Therefore, regulation of imaginal disc growth produces adult structures with specific size and proportion (Mirth and Shingleton 2012; Callier and Nijhout 2013; Oliveira, Shingleton, and Mirth 2014).

Imaginal disc damage also alters growth rate and time. *Drosophila* imaginal discs have a remarkable capacity to regenerate while maintaining their proper size and allometry following damage (Bryant 1971; Bryant 1975; Schubiger 1971). Surgical or genetic damage to an imaginal disc both activate a regeneration checkpoint (Halme, Cheng, and Hariharan 2010) that extends the larval period of development (Rahn 1972; Dewes 1975; Simpson, Berreur, and

Berreuer-Bonnenfant 1980; Poodry and Woods 1990; Halme, Cheng, and Hariharan 2010) and reduces the growth rate of undamaged imaginal tissues (Madhavan and Schneiderman 1969; Stern and Emlen 1999; Martín and Morata 2006; Parker and Shingleton 2011). Disruption of the regeneration checkpoint results in impaired regeneration (Halme, Cheng, and Hariharan 2010). In this way, the regeneration checkpoint allows repair of damaged tissues to remain coordinated with the rest of development.

The delay of development in response to damage is activated through transcriptional repression of the neuropeptide prothoracicotropic hormone (PTTH) (Halme, Cheng, and Hariharan 2010; Colombani, Andersen, and Leopold 2012; Garelli et al. 2012). PTTH regulates developmental time by integrating circadian cycles with hormonal pulses that initiate developmental transitions. The mechanism of PTTH repression is still largely unknown, but the mechanism of this repression is dependent on expression of Dilp8 in damaged tissues (Colombani, Andersen, and Leopold 2012; Garelli et al. 2012), as well as retinoid signaling (Halme, Cheng, and Hariharan 2010).

Growth coordination during the regeneration checkpoint is also dependent on the expression of Dilp8 (Colombani, Andersen, and Leopold 2012; Garelli et al. 2012). Dilp8 is a secreted protein that shares structural features with the insulin/relaxin protein family, but does not appear to function as an antagonist to insulin signaling (Garelli et al. 2012). Several questions remain about Dilp8

growth regulation. Whether Dilp8 functions directly or indirectly to coordinate growth between tissues remains unclear. Additionally, Dilp8 may regulate growth rate and time by distinct mechanisms, or the regulation of growth and developmental delay maybe mechanistically linked, as growth restriction may lead to developmental delay (Poodry and Woods 1990; Stieper et al. 2008).

1.2 Endocrine regulation of allometry

1.2.1 Nutrient signaling regulates growth and time

Growth rate and developmental time are systemically regulated through endocrine signaling. Growth depends on nutrient availability and hormones convey this information across the animal. In *Drosophila*, nutrient status is regulated by several coordinated components, which include: amino acid and ATP sensing by the TOR pathway (Zoncu, Efeyan, and Sabatini 2011), adipokinetic hormone with glucagon-like functions (Hartenstein 2006), and a family of *Drosophila* insulin like peptides (Dilps). The Dilp family of peptides is structurally related to human insulin/IGF (insulin growth factor)/relaxin by a characteristic motif of three disulfide bonds. Insulin producing cells (IPCs) in the brain secrete Dilp 2, 3, 5, and 7, while the fat body secretes Dilp6. Low levels of *dilp2* expression are detected in the imaginal discs (Nässel, Liu, and Luo 2015).

Mutation or increased expression of Dilp 1, 2 or 6 alters growth (Gronke et al. 2010). Dilps function analogously to mammalian insulin/IGF signaling (IIS) by

activating the insulin receptor (InR), a receptor tyrosine kinase which signals through a conserved downstream kinase cascade that includes phosphatidylinositol 3-kinase (PI3K) activation of serine-threonine protein kinase (Akt). The lipid phosphatase PTEN negatively regulates Akt activity. Akt activity promotes growth by increasing nutrient uptake and storage, increasing biosynthesis, and promoting proliferation and by suppressing activity of the transcription factor Forkhead box Class O (FoxO) (Edgar 2006).

IIS also coordinates nutrient status with developmental time through regulation of the steroid hormone ecdysone. Pulses of ecdysone produced by the prothoracic gland (PG) regulate the transitions between developmental stages, such as larval molting, attainment of critical weight, and pupation. Critical weight is a developmental checkpoint that occurs at the beginning of the last instar of larval development. This checkpoint is thought to determine the minimal amount of growth necessary for development to progress, even when larvae are starved. (Nijhout 2003). The timing of the critical weight checkpoint can be altered by either 1) increasing or decreasing IIS in the PG or by 2) increasing ecdysone titer (Mirth, Truman, and Riddiford 2005; Koyama et al. 2014), demonstrating that both IIS and ecdysone regulate this developmental transition.

Regulation of FoxO is one of the links between IIS and ecdysone. As larvae grow, FoxO activity in the PG decreases in conjunction with increased systemic IIS. FoxO negatively regulates ecdysone production by binding

Ultraspiracle (Usp), inhibiting Usp activation of the ecdysone receptor (EcR) and production of ecdysone (Koyama et al. 2014). This demonstrates a direct mechanism by which IIS regulates ecdysone to ensure that growth remains coordinated with nutrient status and developmental time.

1.2.2 Steroid hormones regulate growth and time

Ecdysone itself is a regulator of growth, functioning as a mitogenic factor and negative regulator of IIS (Colombani et al. 2005; Mirth, Truman, and Riddiford 2005; Nijhout et al. 2007; Nijhout and Grunert 2010; Parker and Shingleton 2011; Boulan, Martín, and Milán 2013).

Ecdysone is produced in the PG from dietary cholesterol. Arthropods do not have the ability to synthesize cholesterol from simple precursors, and rearing larvae on laboratory media provides the precursor ergosterol from yeast for ecdysone biosynthesis. Ecdysone biosynthesis occurs through a series of reactions mediated by a family of cytochrome P450 (CYP) enzymes, collectively named the Halloween genes. Four CYPs, *spookier (spok)*, *phantom (phm)*, *disembodied (dib)*, and *shadow (sad)*, are known to function in the PG to produce ecdysone during the larval period of development. The CYP *shade (shd)* functions in peripheral tissues to convert ecdysone to 20-hydroxyecdysone (20E), an active form of the hormone that can bind EcR (Gilbert and Rewitz 2009).

Ecdysone promotes cell proliferation in imaginal discs through the EcR (Delanoue, Slaidina, and Léopold 2010). The growth promoting effects are concentration dependent. *Manduca sexta* imaginal discs grow the most when cultured in low or moderate levels of ecdysone-supplemented media, while high ecdysone levels inhibit imaginal disc growth (Nijhout and Grunert 2010). *Drosophila* and *Galleria melonella* imaginal disc growth is also promoted by moderate levels of ecdysone, and high levels of ecdysone inhibit imaginal disc growth by reducing developmental time, inducing differentiation, and triggering apoptosis (Postlethwait and Schneiderman 1970; Hodgetts 1977; Champlin and Truman 1998). In contrast, ecdysone inhibits larval tissue growth. Ecdysone signaling through EcR in the fat body inhibits growth by inhibiting dMyc, a positive regulator of fat body cell growth (Delanoue, Slaidina, and Léopold 2010).

Juvenile hormone (JH) is a sesquiterpenoid hormone that regulates developmental time and growth. JH regulates developmental time by functioning as an antagonist to ecdysone. When ecdysone production spikes while JH is high, the larvae will molt into another larval phase. When ecdysone production spikes while JH is low, the end of larval development is initiated and pupation begins (Jindra, Palli, and Riddiford 2011).

JH also regulates growth through regulation of ecdysone and IIS. Loss of JH production increases ecdysone levels and decreases IIS signaling, leading to slowed larval tissue growth. The mechanism of this regulation is unknown, but

loss of the JH receptor (methoprene-tolerant [Met]) in the PG also slows larval tissue growth. Loss of JH does not appear to reduce imaginal disc growth. The reduction of larval growth in JH-deficient larvae is rescued in FoxO mutants, suggesting that JH either antagonizes IIS or functions in parallel to inhibit FoxO activity (Mirth et al. 2014). Several questions remain about the role of JH in growth regulation. JH is epistatic to FoxO, but whether FoxO is a target of JH in the PG or the larval tissues remains to be determined. Also unknown is whether JH regulates ecdysone directly through Met in the PG or indirectly through IIS signaling, and whether JH production is itself regulated by IIS.

The regulation of growth by JH bears similarity to the regulation that the microRNAi *bantam* has on larval growth and ecdysone production. *bantam* activity in the PG decreases as the larvae near pupation. When *bantam* is overexpressed in the PG, ecdysone production is reduced and larval growth is increased, suggesting that *bantam* negatively regulates ecdysone production. Increased IIS activity in the PG, either by active InR or reduction of FoxO, also suppresses *bantam* activity (Boulant, Martín, and Milán 2013). These data suggest that *bantam* in the PG inhibits ecdysone production and that IIS negatively regulates *bantam* to promote ecdysone production. Because JH requires FoxO to regulate growth, JH regulation of ecdysone may be through promotion of *bantam* activity. Further studies should examine the connection of

JH and IIS regulation of ecdysone production, and whether they converge on regulation of *bantam* activity (Figure 3).

1.2.3 Reciprocal regulation of IIS and ecdysone

The roles of IIS and ecdysone in developmental growth regulation have been difficult to dissect due to their contrasting tissue dependent effects, as well as the interaction of IIS and ecdysone in regulating both growth rate and developmental time. Experiments that manipulate the IIS pathway directly in the PG have shown conflicting effects on growth and time.

Inhibiting IIS by overexpressing PTEN or a dominant negative form of PI3K in the PG has been found to increase larval tissue growth; this increase in larval tissue growth was accompanied by a decrease in ecdysone titer and ecdysone signaling (Mirth, Truman, and Riddiford 2005; Colombani et al. 2005). However, one report found that most of these larvae were significantly delayed in development and also fail to transition past the L2/L3 molt. The few larvae that did molt delayed pupation and grew to be became larger adults than controls (Mirth, Truman, and Riddiford 2005). Another report found no significant change in developmental time but did report larger adults (Colombani et al. 2005). Conversely, increasing IIS by expressing PI3K in the PG decreased larval tissue growth and final adult size; these changes were accompanied by slightly increased ecdysone titers. Increased IIS was found to either cause the larvae to

pupariate early, which decreased growth time (Mirth, Truman, and Riddiford 2005), or to have no effect on developmental time (Colombani et al. 2005). These conflicting results may reflect the strength of the Gal4-lines used, or the differences in transgenic IIS reagents. The differences may also be a reflection of the nutrient and photoperiod conditions in which the larvae were raised, as Mirth et al. 2005 found that altering either factor alters the severity of the growth inhibition phenotypes.

Taken together, the interactions between IIS and ecdysone signaling currently understood are: 1) IIS in the PG promotes ecdysone production, and one target of this regulation is the microRNA *bantam*; 2) in imaginal discs, ecdysone and IIS both promote imaginal tissue growth; and 3) in the fat body, ecdysone antagonizes IIS by suppressing dMyc and Dilp production (Figure 3). These distinct networks of regulation suggest that the outcome of total growth and allometry is based on the interaction of IIS and ecdysone in different tissues at different times in development. Further studies focusing on the distinctions between imaginal and larval tissue growth at specific times in development will help bring better clarity to understanding the regulation of developmental allometry.

1.2.4 Coordination of endocrine and autonomous growth regulation

As discussed above, endocrine factors can act directly on organs to regulate growth (e.g. insulin through InR or ecdysone through EcR). In addition to these direct mechanisms, evidence is emerging that endocrine signaling can modulate autonomous regulators of growth through the Hippo pathway. In *Drosophila*, two protein kinases (Hippo and Warts) form the core regulatory cassette of the Hippo pathway. Hippo and Warts function in a kinase cascade to restrict activity of the transcription factor Yorkie by inhibitory phosphorylation. Yorkie activates genes that promote proliferation and cell survival through binding with other transcription factor partners. The Hippo pathway is conserved in mammals, with duplicated components corresponding to each *Drosophila* homologue: Mst1 and 2 for Hippo, Lats1 and 2 for Warts, and YAP and TAZ for Yorkie. The Hippo pathway coordinates organ-autonomous information important for sensing growth and size, including: growth factors, morphogen gradients, cell-cell adhesion, cell junction integrity, cell polarity mechanisms, and tension forces (Irvine and Harvey 2015).

Recent work suggests that IIS and the Hippo pathway both regulate each other. In *Drosophila*, activation of IIS by increased expression of Akt increases Yorkie transcriptional activity. (Straßburger et al. 2012). This interaction between IIS/TOR is also present in mammalian cells, where inhibition of IIS increases YAP phosphorylation. Additionally, increased Yorkie activity also activates insulin

signaling, suggesting that the Hippo pathway also enhances IIS pathway growth regulation (Straßburger et al. 2012). YAP also positively regulates mTOR signaling through activating miR-29, which increases mTOR signaling by inhibiting PTEN translation (Tumaneng et al. 2012). This suggests that coordination between endocrine signals and autonomous pathways is regulated by reciprocal regulation of the IIS/TOR and Hippo pathways.

What remains to be resolved is whether other systemic cues also interact with the Hippo pathway. As expanded on in the Discussion section, the transcription factor Taiman may possibly connect growth regulation between the Hippo pathway and ecdysone signaling (Zhang et al. 2015). More work examining the communication between the Hippo pathway and endocrine signaling will provide valuable insight into the mechanisms that coordinate autonomous and systemic growth regulation.

1.3 Nitric oxide regulation of growth

1.3.1 Nitric oxide synthase

The model of allometric regulation by inter-organ communication suggests growth is coordinated through regulation of endocrine factors. Work has recently emerged to suggest that nitric oxide (NO) functions as a ligand for nuclear hormone receptors (NHRs) to regulate hormone signaling.

The diatomic molecule nitric oxide (NO) is produced in almost all tissues and regulates a vast array of cellular and physiological processes. Famous for its role in vasodilation, NO also regulates immunity, neural development, and growth. NO is generated by nitric oxide synthase (NOS) (an enzyme that functions as a dimer), which converts L-arginine into NO and L-citrulline in association with the co-factors heme, calmodulin, FAD, FMN and NADPH (reviewed by Nathan and Xie 1994; Alderton, Cooper, and Knowles 2001; Tennyson and Lippard 2011). NO is a reactive oxygen species with a lifetime too short for long range signaling in the aerobic-biological environment (Liu et al. 1998; Thomas et al. 2001). To achieve long range signaling or storage, NO reacts to form longer-lived nitrogen oxide complexes such as NO₂, N₂O₃, S-nitrosothiols, or metal-nitrosyl complexes. Ultimately, NO and its derivatives exert physiological or pathophysiological functions by interaction with redox-active metals, redox-active ligands, or metal-free organic species, including peptides containing cysteine, tryptophan, and/or tyrosine (Tennyson and Lippard 2011). The mechanisms important for regulation of growth will be discussed below.

1.3.2 Mammalian NOS

Mammals have three *NOS* genes that encode three distinct isoforms. While the isoforms were originally named for their first defined patterns of expression or activation, all isoforms are now known to have overlapping expression patterns.

Type 1, or nNOS, was first identified in neurons. Type 2, iNOS, was first discovered to be inducible in macrophages. Type 3, or eNOS, was first identified in vascular endothelial cells. NOS isoforms are also distinguished based on their expression and calcium dependence. eNOS and nNOS are constitutively expressed and depend on pulses of calcium for enzymatic activity, while iNOS functions primarily independently of calcium pulses and is regulated by expression. All three isoforms have splice variants. Some isoforms act as dominant-negatives, but their biological function is not clear (Alderton, Cooper, and Knowles 2001; Lorenz et al. 2007). Mice either individually or triply mutant for the NOS isoforms are viable and exhibit obesity, diabetes, cardiovascular, and neurological pathologies (Tsutsui et al. 2006).

1.3.4 *Drosophila* NOS

A single *NOS* gene has been identified in *Drosophila* (dNOS). This locus produces multiple splice variants, but only one known full-length enzyme with catalytic activity (Stasiv et al. 2001). Like the mammalian isoforms, dNOS functions as a dimer with binding sites for heme, calmodulin, FAD, FMN and NADPH. dNOS is dependent on calcium for catalysis. The amino acid sequence of dNOS shares greater homology with the constitutive mammalian eNOS and nNOS isoforms than the inducible iNOS isoform (Regulski and Tully 1995).

The phenotype and viability of *dNOS* mutants have been difficult to characterize. The first mutant, *NOS^C*, contains a residue mutation of Gly to Glu at position 585 near the oxygenase domain and was reported to be lethal (Regulski et al. 2004). This lethality was later attributed to a closely associated mutation in a nearby open reading frame (ORF) (Yakubovich, Silva, and O'Farrell 2010). When the *NOS^C* lesion was isolated by directed recombination, the lethality was rescued. The viability of *NOS^C* is consistent with another mutant, *NOS^{Δ15}*, which lacks the entire oxygenase domain but maintains the reductase domain as well as the 3' and 5' UTRs of the gene. When measured in whole adults or adult head extracts, both the *NOS^C* and *NOS^{Δ15}* alleles have no detectable nitric oxide activity (Regulski et al. 2004; Yakubovich, Silva, and O'Farrell 2010). An additional viable mutant, *NOS¹*, has a stop codon inserted early in the oxygenase domain. This allele appears to be amporhic, as no protein expression has been detected by immunofluorescence in the *Drosophila* CNS (Roof et al. 2012). *NOS¹* and *NOS^{Δ15}* alleles do not complement one another in a fly mobility assay (a measure of neural development), suggesting they both effectively reduce NOS function in adult neurons. Nitric oxide production has not yet been measured for the *NOS¹* allele.

The full-length *dNOS* protein is 152kD; however, an additional 100kD isoform has been observed in the adult and larval CNS (Cáceres et al. 2011). The *NOS^{Δ15}* allele removes the 152kD isoform while retaining the presence of the

100kD isoform. Two RNAi lines (VDRC and TRiP) expressed in the PG only reduced the presence of 152kD isoform; only one RNAi line (IRX) reduces both isoforms (Cáceres et al. 2011).

Production of NO is observed by DAF2-DA fluorescence in the PG at the very end of larval development, when high levels of ecdysone are produced to initiate pupariation. The *NOS*^{Δ15} mutant was observed to retain NO activity in larval PGs when measured with the fluorescent reporter DAF2-DA. NO activity was blocked when the IRX-RNAi was expressed in the PG (Cáceres et al. 2011).

Reconciling the phenotypes of *dNOS* has been difficult when considering all the different assays, alleles, and RNAi lines. However, similar to what is observed in triply *NOS* mutant mice, a completely function NOS enzyme does not seem to be necessary for *Drosophila* development. The observation of an additional protein isoform demonstrates that even though *Drosophila* has one *NOS* gene, the locus is complex; there is still much to be learned about *NOS* regulation. Whether the truncated 100kD isoform possesses NO-enzymatic activity or functions in other catalytic processes remains unclear.

1.3.4 Mechanisms of NO growth regulation

While NO and NOS can both enhance and inhibit growth (reviewed in Villalobo 2006), the majority of observed effects are inhibitory. NOS suppresses DNA synthesis and cell proliferation in *Drosophila* embryos and imaginal discs (Kuzin

et al. 1996; Wingrove and O'Farrell 1999), in *Xenopus* neuroblasts (Peunova et al. 2001), and in many mouse and human tissues (Garg and Hassid 1989; Villalobo 2006). In mammals, the general mechanisms of NO growth regulation can be divided into cGMP-dependent, cGMP-independent, or s-nitrosylation.

NO regulates the cyclic guanosine 3', 5'-monophosphate (cGMP) pathway by reacting with the heme in the heterodimeric subunits of soluble guanylate cyclase (sGC). This activates the sGCs, increasing the conversion of guanosine 5'-triphosphate (GTP) to cGMP and resulting in activation of cGMP-dependent protein kinase (PKG) (Derbyshire and Marletta 2012).

NO regulates the cell cycle transcription of the cyclin-dependant kinase inhibitor *p21* in both the cGMP-dependent and independent pathways. In fibroblasts NO regulates proliferation through cGMP, as addition of cGMP inhibitors rescues NO-inhibition of proliferation (Gu and Brecher 2000). In vascular smooth muscle cells, the addition of NO-donors increases *p21*, thereby reducing cell proliferation. However, cGMP inhibitors do not rescue proliferation or block induction of *p21* demonstrating a NO regulation of proliferation through a cGMP-independent pathway (Bauer, Buga, and Ignarro 2001). Similarly, cGMP inhibitors added to microglial cells do not rescue NO-inhibition of proliferation (Kawahara et al. 2001).

NO also regulates growth by s-nitrosylation of free thiol groups on cysteine residues. In fibroblasts, NO regulates growth by inhibiting the tyrosine kinase

activity of epidermal growth factor receptor (EGFR). This inhibition is not rescued by cGMP inhibitors but is reversed by dithiothreitol (Estrada et al. 1997), suggesting that s-nitrosylation directly inhibits EGFR.

In *Drosophila*, NOS also regulates growth and patterning but the mechanisms are not as well defined as in mammals. During embryogenesis, increased NO or sGC signaling induces cell cycle arrest (Wingrove and O'Farrell 1999; DiGregorio, Ubersax 2001). Addition of the NOS inhibitor L-NAME or the sGC inhibitor 1H-[1,2,4]oxadiazolo[4,3-a]quinoxalin-1-one (ODQ) during metamorphosis disorganized retinal development and growth (Gibbs and Truman 1998). This suggests that NOS promotes synaptic organization of the eye through a cyclic GMP pathway. Systemically increasing NO through the donor SNAP or systemically expressing NOS inhibits imaginal disc growth by reducing cell division in imaginal discs. Conversely, injecting L-NAME into third instar larvae results in over grown imaginal discs (Kuzin et al. 1996). While manipulation of NOS has a clear effect of growth, whether this is due to autonomous or systemic mechanisms has remained unclear.

1.3.5 NO regulation of nuclear hormone receptors

Heme has recently been identified to function as a ligand for some NHR by reacting with heme-moieties. The vertebrate NHR family Rev-Erb and the homologue *Drosophila* E75 both contain a heme prosthetic group that is

regulated by NO (Reinking et al. 2005; Marvin et al. 2009). The isoforms E75A and E75B regulate larval development and pupation, while E75C predominantly regulates late stages of metamorphosis (Bialecki et al. 2002). In the PG, NO and heme regulate the interaction of E75B and *Drosophila hormone receptor 3* (DHR3). In the presence of NO, heme-activation of E75B is inhibited and this prohibits the binding of E75B and DHR3 (Cáceres et al. 2011). In the salivary gland, NO inhibits E75A association with the co-repressor SMRTER, reducing the repression of EcR target genes (D. M. Johnston et al. 2011). These mechanisms demonstrate that NO is a dynamic regulator of NHR activity.

Since NHRs regulate both growth rate and time through endocrine signaling, the ability of NO to directly regulate NHRs makes this pathway a candidate for regulation of allometry. NO regulation of E75 controls ecdysone signaling in the prothoracic gland during the larval to pupal transition. During this transition, a large peak of ecdysone initiates the signaling cascade that starts metamorphosis (Yamanaka, Rewitz, and O'Connor 2013). NHRs in the PG regulate the feed-forward loop that shapes the rate of the ecdysone peak (Moeller et al. 2013). During this process, E75B functions to inhibit DHR3 activation of the downstream target gene *Ftz-F1*. When NO is increased by NOS overexpression or by a pharmacological donor, the inhibitory binding of E75B with DHR3 is blocked; this frees DHR3 to activate transcription of *Ftz-F1* (Cáceres et al. 2011). This model predicts that premature activation of NOS in

the PG drives the animals to precociously begin pupation. However, this has not been observed, as both overexpression of NOS and loss of NOS in the PG delay pupation. Overexpression of NOS in the PG results in smaller larvae and appears to disrupt molting between larval transitions. These phenotypes suggest NO-regulated NHR activity may play several roles throughout larval development.

In humans, mutations in NHRs contribute to the pathologies of obesity, inflammation, cancer, and cardiovascular disease (Chawla et al. 2001; Francis et al. 2003). The vertebrate hypothalamus-pituitary axis regulates growth rate and the onset of puberty through cycles of thyroid hormone produced by the thyroid gland and through steroid hormones produced by the gonads (Sisk and Foster 2004). Puberty, like metamorphosis, is the developmental transition from growth to reproductive maturity. Heme and NO also regulate through Rev-Erb (Reinking et al. 2005; Marvin et al. 2009), the NHR homologue to *Drosophila* E75. Rev-Erb controls circadian rhythms and metabolism in mammals (Burriss 2008), and therefore NO action through Rev-Erb may regulate developmental time and growth. Based on these data, the NO-NHR-endocrine pathway may be a conserved mechanism of developmental allometry.

1.4 Summary

In this introduction I have outlined the importance of growth coordination in understanding the regulation of developmental allometry. I have discussed our

current understanding of how the systemic pathways are coordinated with organ autonomous pathways, highlighting the need for a clearer understanding of the reciprocal regulation of between the IIS and ecdysone pathways. I have outlined how the endocrine system functions to regulate developmental allometry, and how NO regulation of endocrine signaling may function as a conserved mechanism for regulation of allometry. This work has revealed novel a mechanism by which the growth of individual tissues are coordinated through regulation of endocrine signaling.

Figure 1: The allometric relationship of brain and heart growth relative to body growth.

The brain and heart grow at different relative rates, producing different scaling relationships relative to body size. Growth of the heart is nearly isometric to body mass, while the brain starts as hypoallometric before growth stops around age 6. This results in the proportions of the brain becoming smaller as development continues, while the proportions of the heart remain relatively the same. Body mass representative of birth, 2, 5, and 20 years of age. (Adapted from Shingleton 2010).

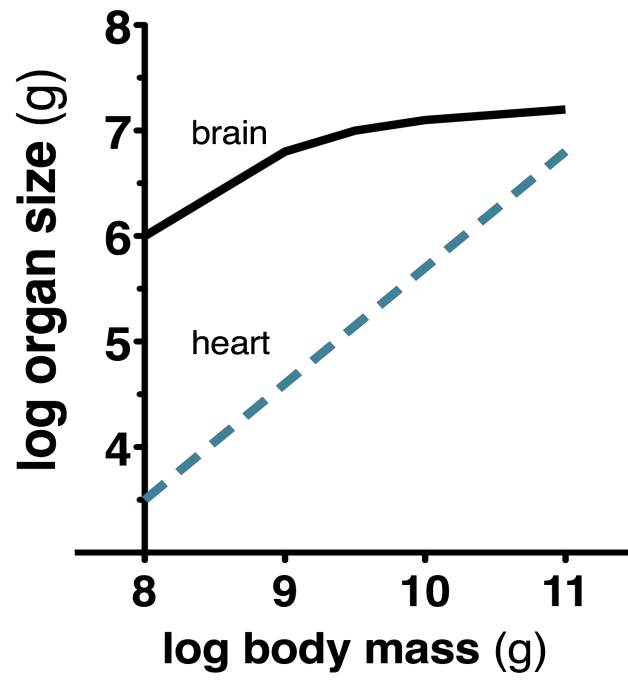


Figure 2: The relationships of allometric growth.

Organs grow isometrically when their size increases at the same relative rate to the body as a whole (solid black line). Hyperallometric growth occurs when organ size increases at a faster rate than body size (dashed line), while hypoallometric growth occurs when the growth rate of an organ is slower than the body rate (dotted line).

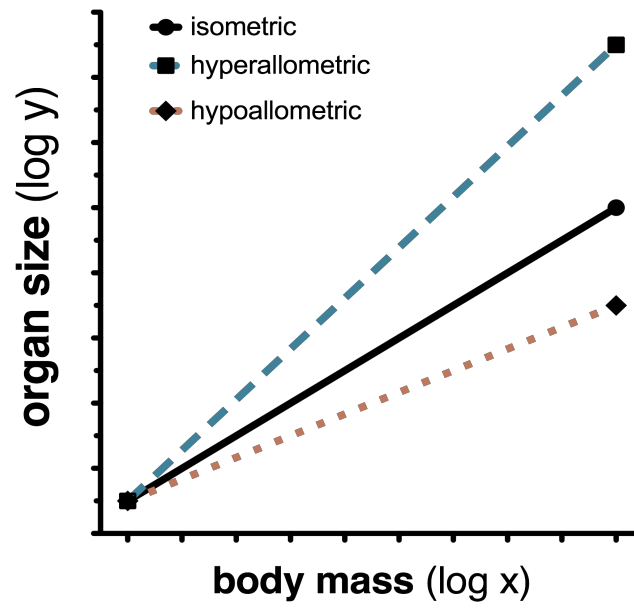
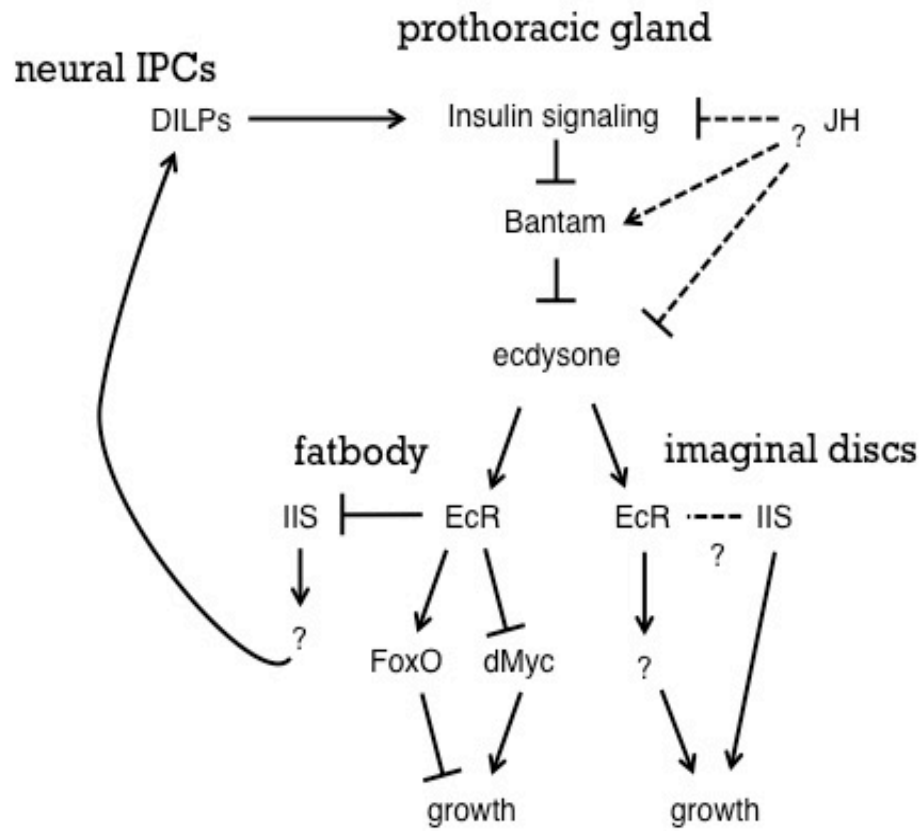


Figure 3: Reciprocal regulation of IIS and ecdysone.

While Dilps promote growth through insulin signaling in all tissues, ecdysone inhibits growth in the fatbody suppressing dMyc and promoting FoxO activity. Ecdysone signaling in the fatbody also inhibits communication between the fatbody and the insulin producing cells (IPCs) in the brain. This contrasts the growth promoting effects of ecdysone in imaginal discs. In the PG, ecdysone production is increased by activation of insulin signaling, which acts at least partially through inhibiting *bantam* activity. New evidence suggests that JH also regulate these pathways, possibly through antagonizing insulin signaling in the PG.



Chapter 2

Methods

2.1 *Drosophila* Stocks

w^* ; P{UAS-Nos.L}2; P{UAS-Nos.L}3 was provided by Pat O'Farrell (Yakubovich, Silva, and O'Farrell 2010). y,w ; phm-GAL4{51A2} was provided by Alexander Shingleton (Mirth, Truman, and Riddiford 2005). UAS-NOS^{mac} and UAS-NOSIR-X was provided by Henry Krause (Cáceres et al. 2011). NOS^1 was provided by James Skeath (Lacin et al. 2014). UAS-eiger and UAS-reaper and $rn-Gal4$, UAS-YFP were provided by Iswar Hariharan (Smith-Bolton et al. 2009). UAS-dilp8::3xFLAG was provided by Maria Dominguez (Garelli et al. 2012). UAS-Avl RNAi was provided by David Bilder (Lu and Bilder 2005). PTTH-GAL4 was provided by Michael O'Connor (Halme, Cheng, and Hariharan 2010; McBrayer et al. 2007). All other stocks were obtained from the Bloomington *Drosophila* Stock Center or the Vienna *Drosophila* RNAi Center. Identifying stock numbers are referenced in the text.

2.2 *Drosophila* culture and media

Unless otherwise specified, larvae were reared at 25°C with a 12hr light cycle on standard cornmeal-yeast-molasses media (Bloomington *Drosophila* Stock Center) supplemented with live bakers yeast granules after developmental synchronization by egg staging. Developmental timing was synchronized through the collection of a 4 hour egg laying interval on grape agar plates. 20 hatched first-instar larvae were transferred to vials containing media 24hrs after egg

deposition (AED). Larvae raised at 21°C were transferred to a 12hr light cycle incubator immediately after staging, and L1 larvae were collected at 48hrs AED. Larvae that were raised at 29°C were transferred to an incubator without a light cycle after L1 collection. Heat shock-mediated expression was induced by 29°C pretreatment and heat shock for 30min at 37°C. Nutrient restriction was initiated at 92hrs AED by transferring larvae to media containing only 1% agarose (Apex) in 1x PBS (pH 7.4 Sigma P4417) for the remainder of larval development.

2.3 Ionizing irradiation damage

Irradiation was performed as previously described (Halme, Cheng, and Hariharan 2010). Briefly, staged larvae were raised in petri dishes on standard media and exposed to 25 Gy X-irradiation generated from a Faxitron RX-650 operating at 130kV and 5.0mA. For targeted irradiation experiments, shielded and control larvae were immobilized by being placed on a chilled glass cover slip, and kept on ice during the duration of the irradiation. Larvae were partially shielded from ionizing irradiation by placing a 0.5 cm² strip of lead tape (Gamma) over the estimated anterior third of their body, covering segments T1-T3. Larvae and control larvae were returned to cornmeal-molasses food at 25°C following irradiation.

2.4 DAF2-DA assay

NO production was detected by 4,5-Diaminofluorescein diacetate (DAF2-DA, Sigma). In Chapter 1, Brain complexes were dissected in PBS and incubated in 10uM DAF2-DA for 1hr at 28°C, rinsed in PBS, stained with DAPI 1:1000, rinsed in PBS, and imaged with by confocal microscopy. In Chapter 2, Brain complexes were dissected in PBS, incubated in 10uM DAF2-DA for 10min at 28°C, rinsed in PBS, fixed with 2-4% paraformaldehyde along with DAPI stain at 1:1000, rinsed in PBS, and finally imaged by confocal microscopy. In both chapters, DAF2-DA fluorescence was quantified in ImageJ (NIH) by measuring the mean gray value of each PG lobe normalized to the background fluorescence of the adjacent brain hemisphere.

2.5 Measurement of growth parameters

Time to pupariation, the time at which half the population had pupated, was calculated by recording the number of pupariated individuals every 12hrs. For measuring imaginal tissue area, tissues were dissected in phosphate-buffered saline (PBS), fixed in 4% paraformaldehyde, mounted in glycerol, imaged by DIC on a Zeiss Axioplan2 microscope, and measured in ImageJ. The area of staged larvae was imaged, after a 10min treatment in PBS at 80o, on an Olympus DP21 microscope digital camera when viewed from the dorsal aspect, and measured in ImageJ.

2.6 Indirect immunofluorescence

Dissected tissues were fixed for 20 minutes in 4% paraformaldehyde, washed in PBS with 0.3% Triton-X100 to permeabilize cells, treated with primary antibodies (overnight at 4°C; rabbit anti-cleaved Caspase-3 (Asp175) 1:100, Cell Signaling Technology, MA; rabbit IGG β -galactosidase, Cappel/ICN), and secondary antibodies (4 hrs at room temperature). Cell death detection by TUNEL with TMR red fluorescent probe (Hoffmann-La Roche, Basel, Switzerland) was performed following manufacturer instructions. Labeling buffers were mixed with secondary antibody stain and incubated for 2hrs at 37°C.

2.7 Ecdysone measurements

Ecdysone levels in third instar larvae were quantified using a competitive enzyme immunoassay (Cayman Chemicals, MI) as described previously (Hackney, Zolali-Meybodi, and Cherbas 2012).

2.8 NADPH-diaphorase assay

NOS enzymatic activity was detected by measuring NADPH-diaphorase activity through an adapted method (Elphick 1997). Tissues were fixed for 1hr in 4% paraformaldehyde and then permeabilized in 0.3% Triton X-100 for 20min. Fixed tissues were suspended in NADPH-diaphorase staining solution in the dark for 15min, then washed in PBS, mounted in 80% glycerol, and imaged by DIC.

2.9 Polymerase chain reaction (PCR)

RNA was isolated from staged larvae using TRIzol reagent treatment (Invitrogen-Life Technologies, CA) followed by RNeasy cleanup (Qiagen, Limburg, Netherlands) and DNase treatment with the Turbo DNase-kit (Ambion-Life Technologies, CA). RNA yield was quantified by using UV spectroscopy to measure A260. cDNA template for RT-PCR was generated using 1 µg sample RNA as a substrate for Roche Transcriptor first strand cDNA synthesis using poly dT primers. Except for Fig. 3-7, and Fig 4-5, which used ReliaPrep™ RNA Cell and Tissue Miniprep Systems (Promega) with poly dT primers and random hexamer primers.

2.10 Semi-quantitative PCR

PCR was performed with TaKaRa Ex Taq DNA Polymerase (Takara, Otsu, Japan) in a MJ research PTC-200 DNA Engine Cyclor. Conditions for amplification were as follows: 94°C for 2 minutes, then 94°C for 15 seconds, 60°C for 15 seconds, and 72°C for 15 seconds for 23 cycles with Tubulin primers or 31 cycles with E75B primers. Amplified products were then identified by electrophoresis on a 3% agarose gel and visualized with SYBR Green (Life Technologies, CA) through epifluorescent analyzer (Fujifilm Intelligent Lightbox LAS-3000). Relative expression differences were measured in ImageJ in relation to tubulin expression. Primers: *E75B* (Moeller et al. 2015),

sgs3 (L-CGCCCTAGCGAGCATCCTG)(R- GGGCTTAGATGTTCGTGCATGG) ,
tubulin (L-CTCATAGCCGGCAGTTTCG)(R-
 GATAGAGATAACATTCACGCATATTGAG).

2.11 Quantitative RT-PCR

PCR was performed with a Mastercycle EP Replex real-time PCR system (Eppendorf). Fold change was calculated relative to tubulin expression by the $\Delta\Delta C_t$ method (Livak and Schmittgen 2001). Isolates were taken from at least three sets of larval stagings to calculate the mean fold change. Two to three independent RNA isolations were assayed within each staging and used to calculate standard error of the mean across stagings. Primers: E74B (Colombani et al. 2005), spookier (*spo*-L CGGTGATCGAAACAACACTCACTGG, *spo*-R GGATGATTCCCGAGGAGAGCAG), disembodied (*dib*-L AGGCTGCTGCGTGAATACG, *dib*-R TCGATCAGCACTGGAGCATC).

2.12 Ecdysone media

Exogenous application of ecdysteroid was performed as previously described (Halme, Cheng, and Hariharan 2010). Briefly, larvae were transferred at 80hrs AED (*Bx>eiger*, *Tub>dilp8*, *Bx>dilp8*, *hs>NOS^{mac}*) or 124hrs AED (*phm>NOS*) to either 0.6 mg 20- hydroxyecdysone (Sigma) dissolved in 90% ethanol/ml of media, or an equivalent volume of ethanol alone. For ecdysone restriction

assays, a defined yeast media was prepared with the *erg-6* mutant yeast strain, sucrose, and agar (Bos et al. 1976; Parkin and Burnet 1986), and larvae were transferred from standard media to *erg6*^{-/-} or *erg6*^{+/-} media at 80hrs AED.

2.13 X-gal staining

Tissues were dissected in PBS and fixed for 15min in 1% gluteraldehyde, incubated at 4°C overnight, rinsed in PBS, and mounted in glycerol.

2.14 Calcium Imaging

Live larvae expressing the calcium sensor GCaMP (BL32236) in the PG (*phm>GCaMP*) were imaged on Nikon Eclipse TE2000-E microscope equipped with a Yokogawa CSU 10 spinning-disk confocal unit with a 20x objective and a 512-by-512 Hamamatsu 9100c-13 EM-BT camera. Larvae were imaged with autofocus at 500ms exposure/500ms frame rate for 5-10min. Larvae were immobilized under a coverslip that was raised on the corners with 4 drops of vasaline and taped on each size to “press” the fatbody tissue away from the PG.

Chapter 3

Nitric oxide synthase regulates growth coordination during *Drosophila melanogaster* imaginal disc regeneration

This chapter is based in part on previously published work: Jaszczak, J.S., Wolpe, J.B., Dao, A.Q., Halme, A. Nitric Oxide Synthase Regulates Growth Coordination During *Drosophila melanogaster* Imaginal Disc Regeneration.

Genetics. Accepted June, 2015. DOI: 10.1534/genetics.115.178053

3.1 Abstract

Mechanisms that coordinate growth during development are essential for producing animals with proper organ proportion. Here we describe a pathway through which tissues communicate to coordinate growth. During *Drosophila melanogaster* larval development, damage to imaginal discs activates a regeneration checkpoint through expression of Dilp8. This produces both a delay in developmental timing and slows the growth of undamaged tissues, coordinating regeneration of the damaged tissue with developmental progression and overall growth. Here we demonstrate that Dilp8-dependent growth coordination between regenerating and undamaged tissues, but not developmental delay, requires the activity of nitric oxide synthase (NOS) in the prothoracic gland. NOS limits the growth of undamaged tissues by reducing ecdysone biosynthesis, a requirement for imaginal disc growth during both the regenerative checkpoint and normal development. Therefore, NOS activity in the prothoracic gland coordinates tissue growth through regulation of endocrine signals.

3.2 Introduction

Allometry, broadly defined as the scaling of organ growth, can have a profound impact on the biological function in animals. For example, in the male dung beetle *Onthophagus netriciventris*, an inverse allometry is observed between horn and testes size, producing distinct reproductive strategies (Simmons and Emlen 2006; Emlen et al. 2012). Allometric growth regulation can also impact human health, where variation from optimal relative heart size can increase susceptibility for cardiovascular disease (Hill and Olson 2008). Despite the fundamental role of growth scaling in biology, no described pathways explain how tissues coordinate growth. Our understanding of growth regulation has been focused on either tissue-autonomous mechanisms – such as how morphogens regulate the activity of cellular growth pathways, or systemic mechanisms – such as how endocrine growth factors control growth in response to environmental change.

These tissue-autonomous and systemic pathways of growth regulation do not explain allometric growth observed during development. Transplantation experiments (Madhavan and Schneiderman 1969) and growth perturbation experiments in *Drosophila* and other insects (Nijhout and Emlen 1998; Simmons and Emlen 2006; Parker and Shingleton 2011) suggest that inter-organ communication may be necessary for allometric growth. Based on these observations, Stern and Emlen (Stern and Emlen 1999) proposed a model for

growth coordination that requires communication between growing organs, either directly or indirectly through an endocrine organ. However, the mechanism of this communication pathway has been unclear.

In *Drosophila* larvae, the growth of the imaginal discs is tightly regulated to produce adult structures with specific size and proportion (Mirth and Shingleton 2012; Callier and Nijhout 2013). Allometry between these tissues is preserved even when developmental growth programs are altered. For instance, *Drosophila* imaginal discs have a remarkable capacity to regenerate and restore proper size and allometry following damage (Bryant 1971; Schubiger 1971). Damage to an imaginal disc activates a regeneration checkpoint (Halme, Cheng, and Hariharan 2010) that extends the larval period of development (Rahn 1972; Dewes 1975; Simpson, Berreur, and Berreur-Bonnenfant 1980; Poodry and Woods 1990; Halme, Cheng, and Hariharan 2010), allowing time for regenerative tissue repair. Regeneration checkpoint activation also slows the growth rate of undamaged tissues (Madhavan and Schneiderman 1969; Stern and Emlen 1999; Martín and Morata 2006; Parker and Shingleton 2011), coordinating regeneration with the growth of undamaged imaginal discs. Developmental delay and growth coordination are both depend on the expression of *Drosophila insulin-like peptide 8* (*Dilp8*) in damaged tissues (Colombani, Andersen, and Leopold 2012; Garelli et al. 2012). Dilp8 is a secreted protein that shares structural features with the insulin/relaxin protein family. Several questions remain about how Dilp8 produces

both growth regulation and developmental delay. It is possible that these two responses might be mechanistically linked - for instance, growth restriction may lead to developmental delay (Poodry and Woods 1990; Stieper et al. 2008).

Alternatively, these two systemic responses may reflect distinct Dilp8-dependent mechanisms. Additionally, it remains unclear whether Dilp8 functions to directly coordinate growth between tissues, or whether Dilp8 mediates growth coordination indirectly through other systemic growth signals.

Nitric oxide synthase (NOS) produces nitric oxide (NO), a potent free radical that regulates many biological processes, including neuronal activity, immunity, and vascular regulation. Altering the activity of the sole NOS protein found in *Drosophila* produces changes in imaginal disc growth (Kuzin et al. 1996) and larval tissue growth (Cáceres et al. 2011). However, the mechanism of this regulation has remained unclear. In the experiments presented here, we outline a pathway through which tissues communicate with each other to produce allometric growth. We demonstrate that NOS activity is required for the Dilp8-dependent coordination of growth between regenerating and undamaged tissues following tissue damage, and that NOS regulates growth in undamaged tissues by reducing ecdysone biosynthesis in the prothoracic gland.

3.3 Results

3.3.1 Nitric oxide synthase (NOS) is necessary for growth regulation during the regeneration checkpoint

During larval development, imaginal disc damage activates a regeneration checkpoint that coordinates the regeneration of damaged imaginal tissues with developmental progression. Activation of the regeneration checkpoint produces both: 1) delayed larval-pupal transition (Rahn 1972; Dewes 1975; Simpson, Berreur, and Berreur-Bonnenfant 1980; Poodry and Woods 1990; Halme, Cheng, and Hariharan 2010), and 2) reduced growth rate of undamaged imaginal tissues (Stern and Emlen 1999; Martín and Morata 2006; Parker and Shingleton 2011). Developmental delay and growth regulation have been shown to be dependent on Dilp8, but it has not been determined how Dilp8 reduces growth of undamaged imaginal tissues (Colombani, Andersen, and Leopold 2012; Garelli et al. 2012). We observe that growth coordination between damaged and undamaged imaginal discs occurs when damage is induced by genetically targeted ablation of wing imaginal discs ($Bx > eiger$) or by exposing the posterior of the larva to X-irradiation (Fig. 3-1A-C and S1B for a description of the targeted irradiation technique). Consistent with earlier work (Colombani, Andersen, and Leopold 2012; Garelli et al. 2012), we find that both of these targeted damage

models depend on the expression of *dilp8* from damaged tissues for growth coordination and developmental delay (Fig. 3-2B and C, Fig. 3-1C and D).

NOS regulates imaginal disc growth during *Drosophila* development (Kuzin et al. 1996), but the mechanism of this regulation is unknown. Therefore, we asked whether NOS is involved in Dilp8-dependent growth coordination. Using targeted irradiation, we observed that the reduced growth of shielded eye discs is rescued when larvae are homozygous for an amorphic allele of NOS (*NOS*¹ (Lacin et al. 2014)) (Fig. 3-2D). Overexpression of *dilp8* is sufficient to reduce imaginal disc growth and produce developmental delay (Figure 3-1E and (Colombani, Andersen, and Leopold 2012; Garelli et al. 2012)). To determine whether Dilp8-induced growth restriction is dependent on NOS, we measured growth of eye imaginal discs in *NOS* mutant larvae overexpressing *dilp8* in the wing imaginal discs (*Bx>dilp8;NOS*¹*-/-*). We observe that Dilp8-induced growth restriction is rescued in *NOS*¹*-/-* mutant larvae (Fig. 3-2E). Therefore NOS is required for growth coordination during the regeneration checkpoint, and Dilp8 is dependent on NOS for imaginal disc growth restriction.

3.3.2 Nitric oxide synthase activity in the prothoracic gland regulates imaginal disc growth

Consistent with previous observations (Kuzin et al. 1996), we find that a transient pulse of NOS expression (*hs>NOS*) early in the third larval instar (76hrs after egg

deposition (AED)) reduces imaginal disc growth. (Fig. 3-3A, 3-4A). However, overexpression of *NOS* within imaginal discs produces no observable effect on imaginal disc growth (Fig. 3-4B), suggesting that *NOS* regulates growth via a non-autonomous pathway. Additionally, we observed that *NOS* induction following heat shock produces a developmental delay (Fig. 3-3A, 3-4A) without producing damage or apoptosis within the imaginal discs (Fig. 3-4C).

The timing of developmental transitions in *Drosophila* larvae is regulated by the prothoracic gland (PG) through pulsed production of the steroid hormone ecdysone (Warren et al. 2006). *NOS* expression in the PG has been demonstrated to regulate the larval to pupal transition by promoting ecdysone production in post-feeding larvae (Cáceres et al. 2011). However, when Cáceres et al. constitutively overexpressed *NOS* in the PG at 25°C throughout larval development, they observed a delayed developmental progression and decreased larval size. Therefore, we examined whether *NOS* regulates growth through activity in the PG during the larval growth prior to the post-feeding phase of larval development. Using the phantom-Gal4 driver, which specifically targets Gal4-mediated expression to the PG throughout larval development (Mirth, Truman, and Riddiford 2005), we observed that most *phm>NOS* larvae raised at 25°C died prior to the third larval instar. To determine if larval lethality could be rescued by reducing the expression of *NOS* in the PG, we raised *phm>NOS* and control larvae at 21°C, which reduces GAL4 activity and slows developmental

time (Fig. 3-4D). The majority of *phm>NOS* larvae raised at 21°C progressed through the 3rd instar to pupation (Fig. 3-4E). We observed that in these *phm>NOS* larvae, the growth rate of the eye imaginal tissues is reduced relative to control larvae raised at 21°C (Fig. 3-3B). The pupation of these larvae is also delayed in comparison to control larvae (Fig. 3-3C). Therefore, *NOS* overexpression in the PG is sufficient to reduce the growth of imaginal discs during the third larval instar and can delay the exit from larval development.

NOS catalyzes the production of the free radical nitric oxide (NO), an important cellular signaling molecule, from L-arginine. To determine whether *NOS* activity is increased in the PG during the regeneration checkpoint, we used the fluorescent reporter molecule 4,5-diaminofluorescein diacetate (DAF2-DA) to measure NO production, as can be observed in the PG of *phm>NOS* larvae (Fig. 3-5). Larva with genetically targeted wing ablation (*Bx>eiger*) or systemic *dilp8* misexpression, both produce increased levels of NO signaling in the PG compared to control larvae (Fig. 3-3C), demonstrating that the regeneration checkpoint acts through Dilp8 to increase *NOS* activity in the PG. To examine whether this activation of *NOS* in the PG is required for the regeneration checkpoint growth coordination, we expressed a *NOS*-targeted RNAi to disrupt *NOS* function specifically in the PG using the *phm*-GAL4 driver (*phm>NOS^{IR-X}* (Cáceres et al. 2011) or *phm>NOS^{Ri}* (Bloomington #28792)). Using the targeted irradiation technique, we observed that depletion of *NOS* in the PG by RNAi

restored eye imaginal disc growth in shielded larvae to the rate observed in unirradiated larvae (Fig. 3-3D). Therefore, nitric oxide production is increased in the PG during the regeneration checkpoint, and NOS activation in the PG is necessary to regulate imaginal tissue growth during the regeneration checkpoint.

Growth regulation during the regeneration checkpoint is dependent on NOS. However, we observed no effect on the delay of development induced by irradiation in NOS-RNAi knockdown or in the NOS mutant larvae (Fig. 3-6A and B). These data suggest that overexpression of *NOS* (Fig 3-3A and B) delays development through a mechanism distinct from the regeneration checkpoint. Together, these data demonstrate that localized imaginal disc damage produces two effects: 1) growth inhibition in undamaged imaginal tissues, which is dependent on NOS function in the PG, and 2) a delay in developmental timing, which occurs through a NOS-independent pathway.

3.3.4 The growth of imaginal tissues is selectively regulated during the regeneration checkpoint

Larval size is determined by the growth of polyploid larval tissues such as the larval epidermis, fat body, and salivary glands (Oldham et al. 2000). Unlike the diploid imaginal tissues, which will become much of the adult fly following metamorphosis, most larval tissues are histolysed during metamorphosis and do not contribute significantly to the adult. To determine whether imaginal tissues

are selectively targeted for growth regulation during the regeneration checkpoint, we compared the effects of regeneration checkpoint activation on the growth of both imaginal tissues and total larval size, which correlates with the growth of the polyploid larval epidermis (Halme, Cheng, and Hariharan 2010). Consistent with our earlier observations, targeted irradiation or genetically targeted ablation of wing imaginal discs (*Bx>eiger*) is sufficient to activate the regeneration checkpoint and produce growth inhibition of undamaged eye imaginal discs (Fig. 3-7A, B). Both damage models depend on Dilp8 for growth inhibition and developmental delay (Fig. 3-1 and 3-2). Consistent with a role for NOS and Dilp8 in growth regulation during the regeneration checkpoint, we observe growth inhibition of undamaged eye imaginal tissues by expression of *NOS* in the PG (*phm>NOS*, Fig. 3-7B) and *dilp8* expression in the wing pouch, the region of the imaginal disc that will become the adult wing blade (*rn>dilp8*, Fig. 3-7B).

In stark contrast, we found that checkpoint activation does not reduce overall larval growth (Fig. 3-7C, D). In our two damage models, larval growth continued at the same rate or even slightly faster than the growth observed in control larvae. Similarly, we observed a slight but not statistically significant increase in the rate of larval tissue growth in larvae with *phm>NOS* and wing-targeted expression of Dilp8 (*rn>dilp8*), as compared with control larvae (Fig. 3-7D). Additionally, we examined other disruptions of wing imaginal disc growth

and found that induction of neoplastic tumors in the wing imaginal tissues using knockdown of the *Drosophila* syntaxin protein Avalanche (*Bx>avl^{RNAi}*, (Lu and Bilder 2005)) also produces slower growth in the eye imaginal discs without altering larval tissue growth (Fig. 3-7B, D). This is consistent with the observed activation of Dilp8 during tumorigenesis (Colombani, Andersen, and Leopold 2012; Garelli et al. 2012). This pattern of growth regulation observed during the regeneration checkpoint – reduced growth of imaginal discs and sustained or even increased growth of larval tissues – contrasts with the growth pattern observed in larvae with reduced insulin signaling in response to nutrient restriction, where growth of both imaginal and larval tissues are reduced (Fig. 3-7B, D). Therefore, we sought to test a growth regulatory pathway other than insulin that would explain how regenerative checkpoint activation and NOS activity could specifically reduce imaginal disc growth.

3.3.5 NOS in the PG inhibits ecdysone biosynthesis during the larval growth phase

The PG produces pulses of ecdysone synthesis during the larval growth phase that determine the timing of developmental transitions such as larval molts, the mid-third instar transition (Andres and Cherbas 1992), critical weight (Koyama et al. 2014), and the exit from larval development. Experiments support roles for ecdysone in both promoting (Nijhout et al. 2007; Delanoue, Slaidina, and Léopold

2010; Nijhout and Grunert 2010; Parker and Shingleton 2011) and restricting (Mirth, Truman, and Riddiford 2005; Colombani et al. 2005; Delanoue, Slaidina, and Léopold 2010; Nijhout and Grunert 2010; Boulan, Martín, and Milán 2013) growth of imaginal discs. Activation of the regeneration checkpoint slows the progression of the morphogenetic furrow in undamaged eye discs (see Fig. 3-7A). The furrow progression is dependent on ecdysone (Brennan, Ashburner, and Moses 1998), therefore its slowed progression is consistent with the regeneration checkpoint reducing ecdysone signaling during larval development. Since the overexpression of *NOS* in the PG influences both developmental timing and imaginal disc growth, we examined whether *NOS* activity in the PG alters ecdysone signaling during the regeneration checkpoint.

Regeneration checkpoint activation has been shown to reduce ecdysone biosynthesis (Hackney, Zolali-Meybodi, and Cherbas 2012). To examine whether *NOS* activity in the PG reduces ecdysone production, we measured ecdysteroid levels using a competitive enzyme immunoassay (Porcheron et al. 1989). In larvae overexpressing *NOS* in the PG (*phm>NOS*), we observed a strong reduction in ecdysteroid levels during the mid 3rd instar when imaginal disc growth is rate reduced (Fig. 3-8A). To determine whether ecdysone signaling is reduced during this period, we measured transcription of the ecdysone target gene *E74B* (Colombani et al. 2005; Parker and Shingleton 2011; Hackney, Zolali-Meybodi, and Cherbas 2012). In *phm>NOS* expressing larvae we observed that

the expression of *E74B* is lower than in control larvae during the mid and late 3rd instar (Fig. 3-8B), suggesting that ecdysone titers are reduced during this period. Consistent with previous studies (Hackney, Zolali-Meybodi, and Cherbas 2012), we observed that transcription of *E74B* is reduced following activation of the regeneration checkpoint in *Bx>eiger* larvae (Fig. 3-9A). Together, these results demonstrate that ecdysone production is reduced when NOS is active in the PG during the 3rd instar larval growth period.

To better understand how NOS reduces ecdysone production in larvae, we examined whether NOS regulates the expression of ecdysone biosynthetic genes. Ecdysone is synthesized in the PG from sterol precursors by the consecutive actions of the P450 enzymes collectively referred to as the Halloween enzymes (Gilbert and Rewitz 2009). Previous work has demonstrated that the expression of Halloween genes is reduced during activation of the regeneration checkpoint (Hackney, Zolali-Meybodi, and Cherbas 2012). To determine whether NOS regulates ecdysone synthesis by limiting Halloween gene expression, we examined the transcription of the Halloween genes *spookier* (*spok*) (ONO et al. 2006) and *disembodied* (*dib*) during either targeted tissue damage or *NOS* overexpression in the PG (Chávez et al. 2000). Transcription of both *spok* and *dib* are reduced in *phm>NOS* larvae in comparison to control larvae (Fig. 3-8C), consistent with the reductions observed during regeneration checkpoint activation (Fig. 3-9A). Therefore, upon activation of the regeneration

checkpoint, NOS functions in the PG to reduce ecdysone signaling through the transcriptional repression of ecdysone biosynthesis genes.

This model contrasts with a model arising from previous work demonstrating that NOS activity in the PG of post-feeding larvae enhances ecdysone signaling by inhibiting the nuclear hormone receptor E75, an antagonist of ecdysone biosynthesis (Cáceres et al. 2011). To reconcile these two distinct descriptions of NOS activity in the PG, we first sought to determine whether this post-feeding E75-dependent pathway could be active during the earlier growth phase of larval development. We observed that the *E75B* expression, which is normally upregulated during the post-feeding period of larval development, is completely suppressed in larvae with targeted wing damage (Fig. 3-9B). Therefore, we conclude the pathway by which NOS promotes ecdysone signaling in post-feeding larvae is not likely to be active during the growth phase of larval development and is delayed following activation of the regeneration checkpoint. Consistent with this, the ability of transient *NOS* misexpression (*hs>NOS*) to delay pupation is most robust when expressed during larval feeding (76hrs or 80hrs). This delay is significantly decreased when *NOS* was misexpressed later in the 3rd instar as the larvae entered the post-feeding phase (96hrs or 104hrs) (Fig. 3-8D). These results suggests that the ecdysone-inhibiting and ecdysone-promoting mechanisms of NOS are temporally separated during the larval growth and post-feeding phases of development.

To further test whether NOS activity is dependent on developmental stage of the larvae, we examined whether the reduction of imaginal disc growth induced by transient misexpression of *NOS* (*hs>NOS*) is dependent on the stage of development. We observed that misexpressing *NOS* early in the 3rd instar during the larval feeding period (76hrs AED) produces a robust restriction of imaginal disc growth (Fig. 3-8E – 76hrs). However, we found that misexpression of *NOS* late in the 3rd instar, at the time that larvae stop feeding (104hrs AED), produces minimal effect on imaginal disc growth and developmental time (Fig. 3-8E and D – 104hrs). In fact, a slight increase in growth was measurable. Consistent with this, we also observed decreases in *E74B* and *dib* transcription after early *NOS* misexpression, and an increase in *spok* transcription in late *NOS* misexpression (Fig. 3-9C and D). These results suggest that as development progresses, the regulatory effect of NOS in the PG has two distinct states. During the feeding phase of larval development, NOS inhibits ecdysone production as we describe here. Later in post-feeding larvae, as described in Cáceres et al., NOS functions to promote ecdysone signaling by inhibiting E75 activity (Cáceres et al. 2011).

3.3.6 The regeneration checkpoint reduces growth of undamaged tissues by limiting ecdysone signaling

We then determined whether the reduced growth of undamaged discs during regeneration checkpoint activation is the result of reduced ecdysone production. Feeding larvae food supplemented with ecdysone (0.6mg/ml) increases ecdysone titer in larvae (Colombani et al. 2005). Using this approach, we tested whether we could bypass NOS-dependent growth inhibition by ecdysone feeding. We observed that ecdysone feeding can bypass the imaginal disc growth restriction produced by: 1) imaginal tissue damage (*Bx>eiger*, Fig. 3-10A), 2) regeneration checkpoint signaling (*Tub>dilp8*, Fig. 5B), or 3) transient misexpression of *NOS* (*hs>NOS*, Fig. 5C and S6A), and *NOS* activity in the PG (*phm>NOS*, Fig. 3-10D). Ecdysone feeding did not significantly alter the growth of larval tissues during damage or *NOS* overexpression, but strongly reduced larval tissue growth in *dilp8* misexpressing larvae, as reflected in the overall larval size (Fig. 3-11C).

To determine whether ecdysone promotes imaginal disc growth during normal development, we reduced ecdysone levels in third instar larvae by transferring larvae to yeast-sucrose food prepared using *erg6*^{-/-} mutant yeast, which lacks the necessary steroid precursors for ecdysone synthesis (Bos et al. 1976; Parkin and Burnet 1986) (see Experimental Procedures). This resulted in a marked decrease in imaginal tissue growth (Fig. 3-11D), an extended

developmental time to pupation (Fig. 3-11E), and a slight, but significant increase in larval tissue growth (Fig. 3-11F), as compared with control larvae. Therefore, ecdysone is required for a normal rate of imaginal disc growth during the 3rd instar even in the absence of imaginal disc damage. Furthermore, we observed that ecdysone limitation by growth on *erg6*^{-/-} food produces only a minor effect on the growth of imaginal tissues in *Bx>eiger* larvae (Fig. 3-11D). This epistatic interaction supports a model in which the regeneration checkpoint and ecdysone regulate imaginal tissue growth via convergent mechanisms. Together, these results demonstrate that the regeneration checkpoint limits undamaged imaginal disc growth through NOS-dependent reduction of ecdysone synthesis.

3.4 Discussion

During *Drosophila* development, damage to larval imaginal discs elicits a regeneration checkpoint that has two effects: 1) it delays the exit from the larval phase in development to extend the regenerative period, and 2) it coordinates regenerative growth with the growth of undamaged tissues by slowing the growth rate of distal, undamaged tissues. How regenerating tissues communicate with undamaged tissues to coordinate growth has been an open question. Damaged

tissues may produce signals that directly influence the growth of undamaged tissues or may indirectly influence the growth of undamaged tissues by producing signals that alter the levels of limiting growth factors. Consistent with the latter model, we describe an indirect-communication pathway for growth coordination during the regeneration checkpoint (Fig. 3-12).

An essential component of this growth coordination is the secreted peptide Dilp8, which is released by damaged tissues and is both necessary and sufficient to regulate the growth of distal tissues during the regeneration checkpoint (Colombani, Andersen, and Leopold 2012; Garelli et al. 2012). Dilp8 shares structural similarity to insulin-like peptides, which function to stimulate growth by activating the insulin receptor. However, in contrast to insulin-like peptides, Dilp8 acts to limit growth. A simple model explaining Dilp8 function would be that Dilp8 acts directly as an antagonist to insulin receptor activity, thus reducing growth in undamaged tissues. However, we show that the growth response to checkpoint activation of polyploid larval tissues differs from imaginal discs (Fig. 3-7). The growth of polyploid larval tissues are very sensitive to changes in insulin signaling, therefore these results are inconsistent with Dilp8 regulating imaginal disc growth by antagonizing systemic insulin signaling.

We show here that NOS functions in the PG to regulate the growth of imaginal discs during the developmental checkpoint. We demonstrate that growth coordination during the regeneration checkpoint increases NO production in the

PG, and is dependent on *NOS* gene function in the PG. Although constitutive expression of *NOS* in the PG might produce effects earlier in development that might alter our interpretations, we also demonstrate that transient pulses of *NOS* during the third instar and targeted *NOS* activation in the PG both produce the same effects: inhibition of imaginal disc growth by limiting ecdysone signaling. We show that *NOS* activity in the PG reduces ecdysone production through the transcriptional inhibition of the P450 enzymes *disembodied* and *spookier*, which are necessary for ecdysone biosynthesis. Although it has been known that *NOS* activity is capable of regulating growth of imaginal discs (Kuzin et al. 1996), the experiments we describe here elucidate the mechanism of this growth regulation.

The activity of *NOS* we describe here contrasts with published experiments demonstrating that NO signaling in the PG promotes ecdysone signaling during the larval-to-pupal transition, following the larval feeding period (Cáceres et al. 2011). However, experiments from Cáceres et al. demonstrate that earlier *NOS* expression in the PG during larval development produces small larvae that arrest at second larval instar stage of development. This arrest can be partially rescued by either ecdysone feeding (Cáceres et al. 2011), or by reducing the level of GAL4-UAS driven *NOS* expression by raising larvae at a lower temperature (Fig. 3-4E). Additionally, pharmacological increase of NO levels in larvae can produce larval developmental delays (Lozinsky et al. 2012; Lozinsky et al. 2013). Together, these observations suggest that *NOS* activity earlier in

larval development might inhibit rather than promote ecdysone signaling during the larval growth period. Finally, we observe that *E75B* is not expressed in larvae that have activated the regenerative checkpoint (Fig. 3-9B), suggesting that the NOS dependent pathway that has been described by Caceres et al. for is not active during the regeneration checkpoint.

We have focused on the role of NOS during the growth phase of the third larval instar (76-104h AED) and have found that heat-shock mediated pulses of NOS activity during this period of development inhibit growth and ecdysone signaling, while pulses of *NOS* activity at the end of larval development do not inhibit growth or ecdysone signaling (Fig. 3-8). Based on these results, we conclude that there are distinct roles for NOS in the PG during different phases in development; NOS activity post-larval feeding promotes ecdysone signaling through inhibition of *E75*, whereas NOS activity during the larval growth phase limits ecdysone synthesis and signaling by reducing the expression of ecdysone biosynthesis genes through a yet-to-be defined mechanism. Some intriguing possible mechanisms are through regulation of the growth of the PG or the cGMP pathway.

Furthermore, we demonstrate that ecdysone is essential for imaginal disc growth. Most studies have supported a model in which ecdysone acts as negative regulator of growth based on two observations: 1) the final pulse of ecdysone at the end of the third larval instar shortens developmental time and

therefore reduces final organ size, and 2) increased ecdysone signaling can antagonize Dilp synthesis in the fat body (Mirth, Truman, and Riddiford 2005; Colombani et al. 2005; Delanoue, Slaidina, and Léopold 2010; Nijhout and Grunert 2010; Boulan, Martín, and Milán 2013). However, when measuring the effects of ecdysone on growth, many previous studies have focused on measuring either the growth of the larvae (which as we observe does not always reflect the growth of the imaginal tissues) or measuring the final size of adults (which is a function of both growth rate and time). When one either examines clones expressing mutant alleles of ecdysone receptor (Géminard et al. 2006) or measures the growth of entire imaginal discs directly following ecdysone feeding as we have done here, ecdysone signaling can be shown to promote imaginal disc growth.

During the regeneration checkpoint, both growth coordination and the delay in developmental timing are dependent on reduced ecdysone levels. Therefore, we might expect both delay and growth inhibition to be dependent on the same pathways. However, we clearly demonstrate that the genetic requirements for these two systemic responses to damage are distinct. NOS is necessary for growth regulation following tissue damage, but is not necessary for the developmental delay. While we do observe that overexpression of *NOS* in the PG produces developmental delay, our results suggest that this is through a different mechanism than delays produced during the regeneration checkpoint.

Therefore, Dilp8 secretion from damaged imaginal discs produces developmental delay and growth restriction through distinct mechanisms.

Finally, our observations suggest that regenerative growth, which is able to proceed despite reduced ecdysone signaling, may have different growth requirements than undamaged tissues. Understanding these differences in growth regulation could provide valuable insights into the mechanistic distinctions between regenerative and developmental growth.

Figure 3-1. Imaginal disc growth inhibition during either Eiger-induced damage or targeted irradiation is dependent on Dilp8.

(A) *Dilp8* expression is increased in *eiger*-misexpressing wing imaginal discs. *Dilp8* expression is visualized in control (*dilp8-GFP*) and Eiger-misexpressing (*Bx>eiger;dilp8-GFP*) wing discs (outlined) using the *dilp8-GFP* enhancer trap (BL33079). Scale bars = 100 μ m. (B) Illustration of the targeted irradiation method that produces damage in the posterior tissues while protecting anterior tissues from ionizing radiation. Lead shielding protects eye imaginal discs from X-irradiation induced apoptosis. Levels of apoptosis measured by TUNEL staining (red) in eye imaginal discs (outline) isolated from larvae either completely exposed to X-rays, or partially shielded with lead tape to protect anterior tissues from direct damage. Scale bars = 100 μ m. (C and D) Developmental delay resulting from targeted wing damage (*Bx>eiger*) or targeted irradiation is dependent on *dilp8*. Measurement of pupariation timing for larvae with targeted wing expression of *eiger* (*Bx>eiger*) or targeted irradiation (shielded) damage, in larvae homozygous for *dilp8-GFP*^{-/-}, or in WT control larvae is shown. (E) Eye imaginal disc size measured at 104hr AED following systemic misexpression of *dilp8* (*Tub>dilp8*) or in control larvae (*Tub>GFP*) is shown. Measurement of pupariation timing for larvae with systemic (*Tub>dilp8*) misexpression of *dilp8* is shown. Statistical analysis: Time in C, D and E, triplicates \pm SEM. E, growth mean \pm SD. * $p < 0.05$, ** $p < 0.01$, **** $p < 0.001$ calculated by two-tailed Student's t-test, except for shielding experiments in D, calculated by one-way ANOVA with Tukey's post-test.

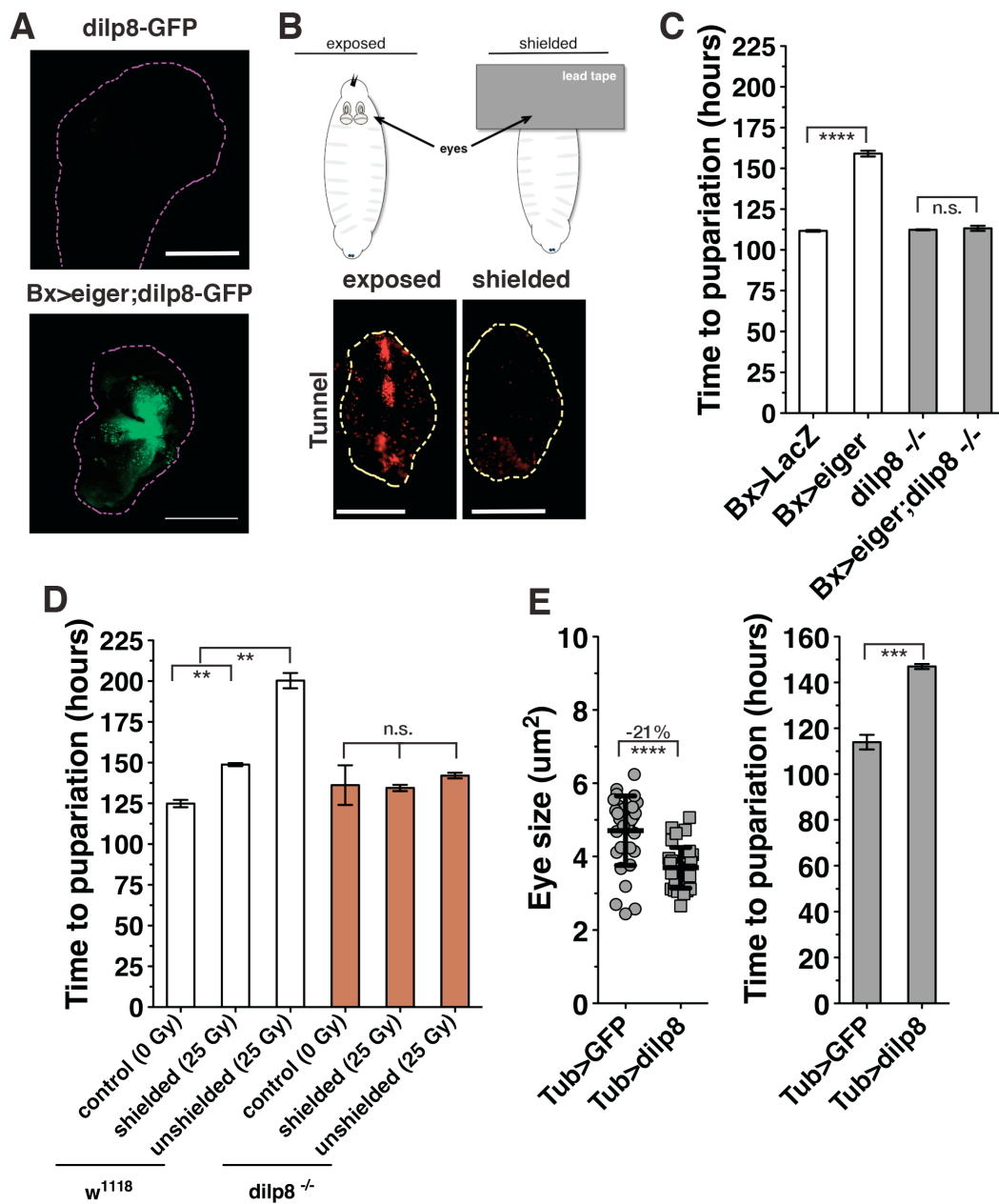


Figure 3-2. NOS is required for imaginal disc growth coordination during the regeneration checkpoint.

(A) Growth reduction of undamaged eye imaginal discs in larvae with targeted tissue damage in the wings (*Bx>eiger*) and control larvae (*Bx>GFP*). Eyes were isolated at 104hr AED and stained with rhodamine-labeled phalloidin. Scale bar = 100 μ m. (B) Dilp8 is required for coordinating imaginal tissue growth during targeted wing damage. Eye imaginal disc size measured at 104hr AED following targeted wing expression of *eiger* (*Bx>eiger*) or control (*Bx>LacZ*) in larvae wildtype for *dilp8* or homozygous for *dilp8*^{-/-}. (C) Dilp8 is required for coordinating imaginal tissue growth during irradiation damage. Measurement of undamaged eye imaginal disc size following targeted irradiation (shielded, 25 Gy) compared to unirradiated control (0 Gy) in wildtype (*w*¹¹¹⁸) and larva homozygous for *dilp8*^{-/-}. Posterior tissues were exposed to 25 Gy ionizing irradiation at 80hr AED while anterior tissues were shielded using lead tape (see methods and figure S1B for more detail). Eye imaginal disc size measured at 104hr AED. (D) NOS is required for coordinating imaginal tissue growth during the regeneration checkpoint. Coordination of growth during targeted irradiation is lost in larvae mutant for *NOS*. Measurement of undamaged eye imaginal disc size following targeted irradiation compared to unirradiated control in wildtype (*w*¹¹¹⁸) and larva heterozygous or homozygous for *NOS* mutant (*NOS*¹). Posterior tissues were exposed to irradiation at 80hr AED and eye imaginal disc size was measured at 104hr AED. (E) Dilp8 growth restriction requires NOS. Eye imaginal disc growth restriction during *dilp8* overexpression in the wing (*Bx>dilp8*) is lost in larvae mutant for *NOS* (*NOS*¹ *-/-*). Larvae were raised at 29°C and eye imaginal disc size was measured at 100hr AED. Statistical analysis: mean \pm SD. * $p < 0.05$, **** $p < 0.001$ calculated by two-tailed Student's t-test.

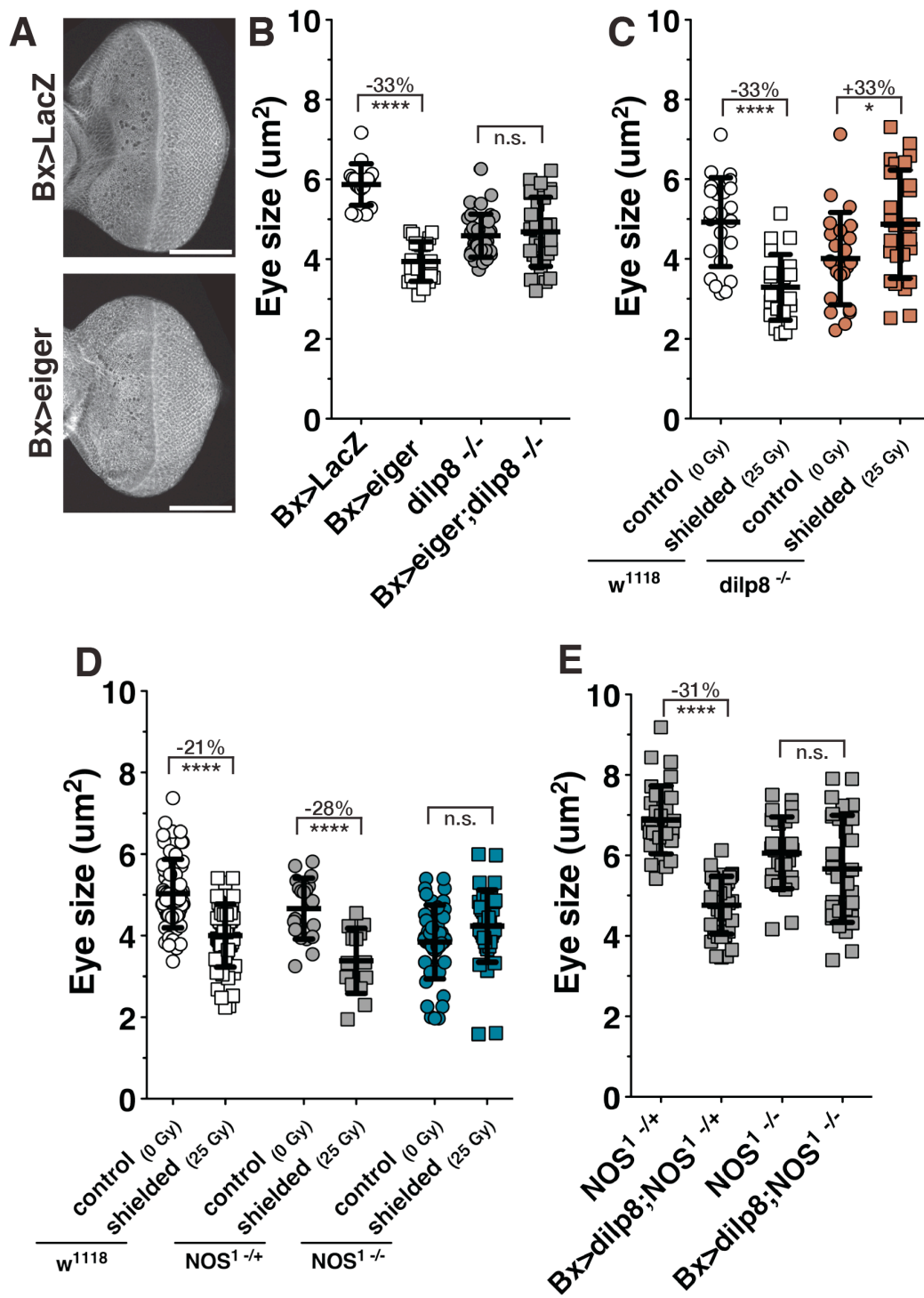


Figure 3-3. NOS is required in the prothoracic gland (PG) to coordinate imaginal tissue growth during the regeneration checkpoint.

(A) A systemic pulse of *NOS* expression early during the larval feeding period restricts imaginal disc growth throughout the rest of larval development. *NOS* was systemically expressed by heatshock (Δ) at 76hr AED and eye imaginal disc size was measured in populations of larva at subsequent time points. *NOS* overexpression at 76hr AED extends larval development. Measurement of pupariation timing (marked by eversion of anterior spiracles) following systemic expression of *NOS* (*hs>NOS*) is depicted on the right. (B) *NOS* overexpression in the PG (*phm>NOS*) restricts imaginal disc growth and extends larval development. *phm>GFP* and *phm>NOS* expressing larvae were raised at 21°C (see Fig. S2D). (C) Targeted tissue damage (*Bx>eiger*) and systemic *dilp8* expression (*Tub>dilp8*) both increase nitric oxide (NO) production in the PG. Measurement of NO production by the fluorescent reporter DAF2-DA. Brain complexes with the PG attached were isolated and stained with DAPI and DAF2-DA at 93hr AED. N: *Bx>LacZ* = 36, *Bx>eiger* = 23, *Tub>LacZ* = 20, *Tub>dilp8* = 23. (D) *NOS* is required in the PG for regeneration checkpoint growth coordination. Measurement of undamaged eye imaginal disc size following shielded irradiation (25 Gy) compared to unirradiated control (0 Gy) in control (*phm>LacZ*) or *NOS*-targeted RNAi expressed in the PG (*phm>NOS^{IR-X}* or *phm>NOS^{Ri}* BL28792). Posterior tissues were exposed to 25 Gy ionizing irradiation at 80hr AED and anterior tissues, including the eye discs, were shielded using lead tape. Eye imaginal disc size was measured at 104hr AED. Statistical analysis: A, Differing letters denote statistical significance calculated by one-way ANOVA with Tukey's post-test. B, mean \pm SD. Time in A and B, mean of triplicate experiments \pm SEM. C, mean of triplicate experiments. D, mean \pm SD. * $p < 0.05$, ** $p < 0.01$, *** $p < 0.005$, **** $p < 0.001$ calculated by two-tailed Student's t-test.

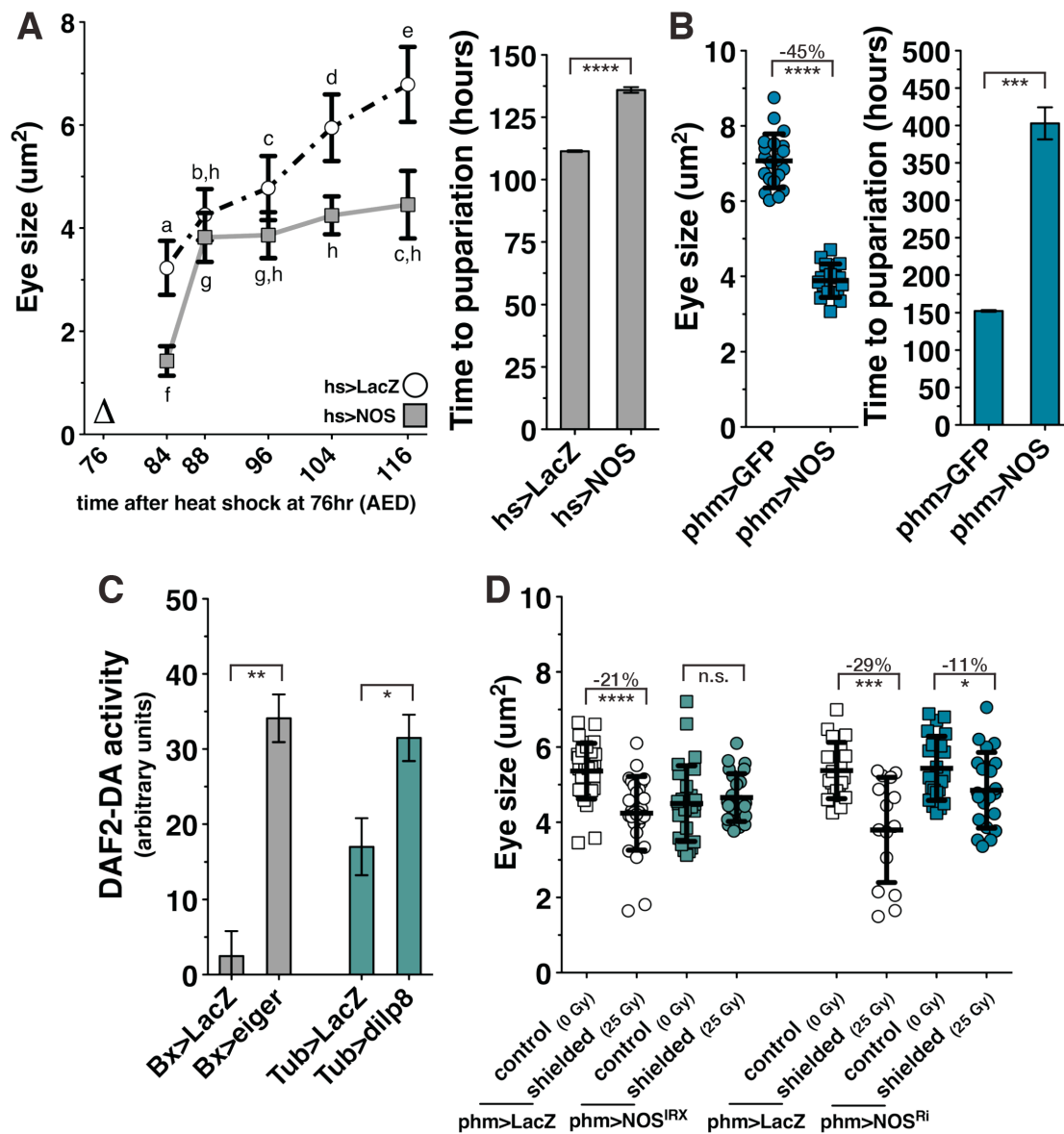


Figure 3-4. NOS non-autonomously regulates imaginal disc growth.

(A) Systemic misexpression of mouse macrophage *NOS* (*NOS^{mac}*) reduces imaginal disc growth and delays developmental timing. Control (*hs>LacZ*) and *hs>NOS^{mac}* expressing larvae were raised at 25°C and eye imaginal disc sizes were measured at 104hr AED. (B) *NOS* overexpression in the wing disc does not reduce growth. Targeted misexpression of *NOS* to the pouch of the wing imaginal tissue (*Bx>NOS*) is not sufficient to reduce growth of the wing pouch, nor wing area (data not shown). Wing imaginal discs measured at 104hr AED from larvae with targeted expression of *NOS* in the wing (*Bx>NOS*) and control (*Bx>LacZ*) larvae. (C) Systemic *NOS* misexpression does not induce cell death. Systemic *NOS* misexpression (*hs>NOS*) does not induce cell death in the wing discs. Cleaved caspase staining (CC3) in wing discs (outlines) isolated at 104hr AED. Control (*hs>GFP*) and *NOS* misexpression larvae (*hs>NOS*) that had been heat shock treated at 76hr AED, or larvae irradiated with 25 Gy as positive control for cell death (irradiation). Scale bars = 100µm. (D) Rearing larvae at 21°C slows developmental time by approximately a factor of 1.5x that of developmental time at 25°C. Instar transitions estimated from time to pupation and observations of larval size. (E) *NOS* overexpression in the PG at 21°C increases larval survival into the 3rd instar (L3). *phm>NOS* larvae raised at 25°C die before the third instar. Rearing *phm>NOS* larvae at 21°C increased the number of larvae that progress to the third instar. Percent viable L3 *phm>NOS* and control (*phm>LacZ*) larvae raised at 25°C and 21°C. Statistical analysis: A and C, mean +/- SD. Time, mean of triplicate experiments +/- SEM. D, mean +/- SEM of three replicates. * p<0.05, ****p<0.001 calculated by two-tailed Student's t-test.

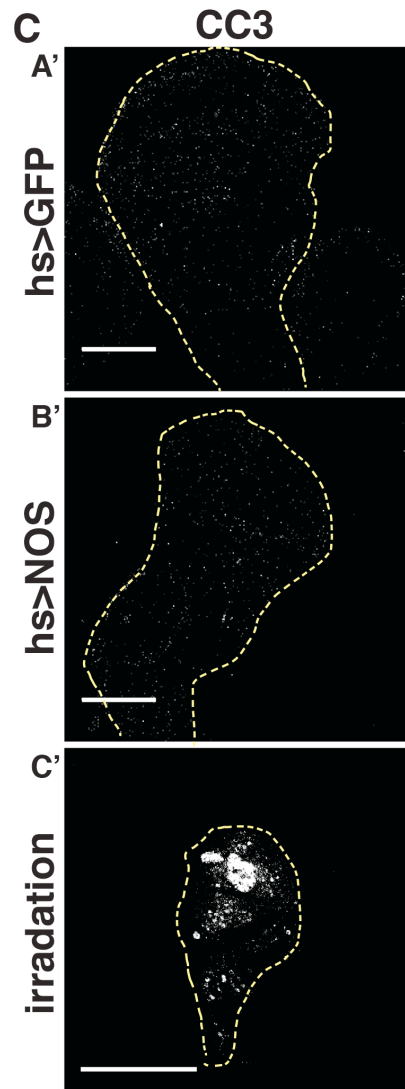
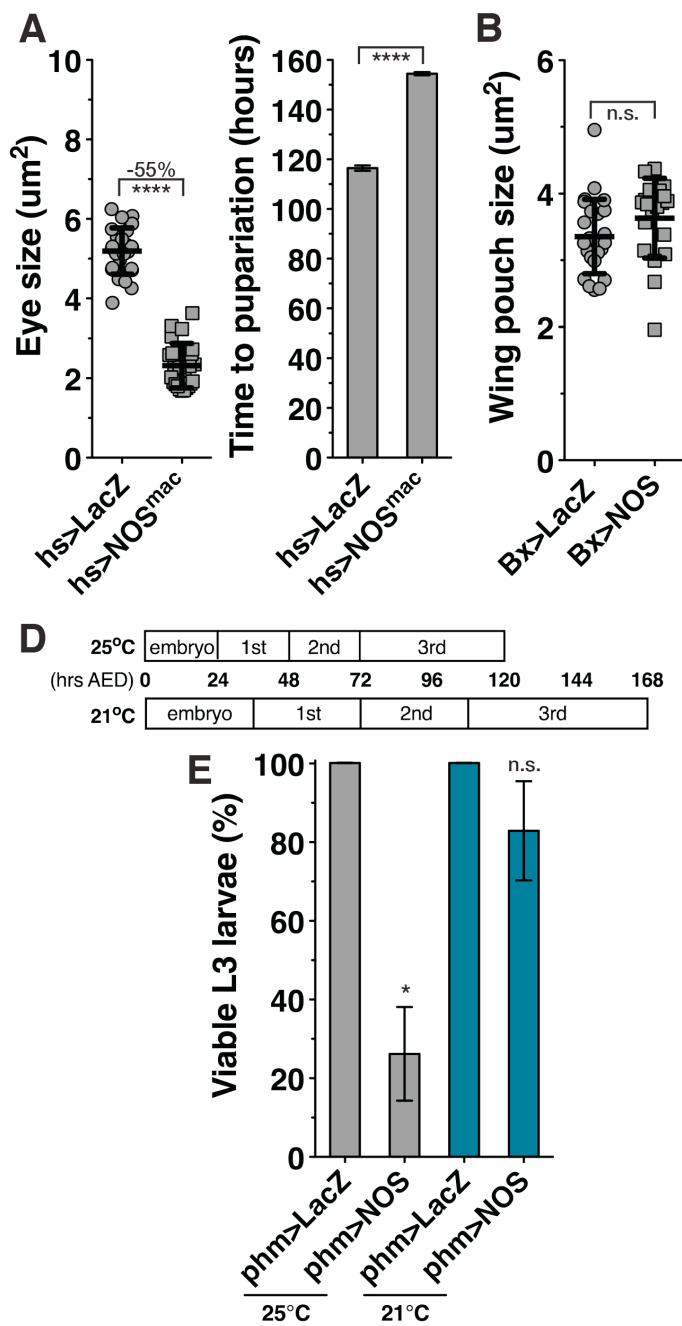


Figure 3-5. DAF2-DA assay for detection of NO production.

(A) NOS enzymatic activity visualized by NADPH-diaphorase staining in targeted overexpression of *NOS* to the PG cells (outlined) (*phm>NOS*) and control (*phm>LacZ*). Larvae were raised at 21°C and brain complexes were dissected from wandering larvae. Scale bars = 200µm. (B) *NOS* overexpression in the PG (*phm>NOS*) increases NO production in the PG cells (outlined). Measurement of nitric oxide (NO) production by the fluorescent reporter DAF2-DA. Larvae were raised at 21°C and brain complexes with the PG were isolated and stained at 117hr AED. Scale bar = 100µm. n: *phm>LacZ* = 29, *phm>NOS* = 30. Statistical analysis: mean +/- SEM. ** $p < 0.01$ calculated by two-tailed Student's t-test.

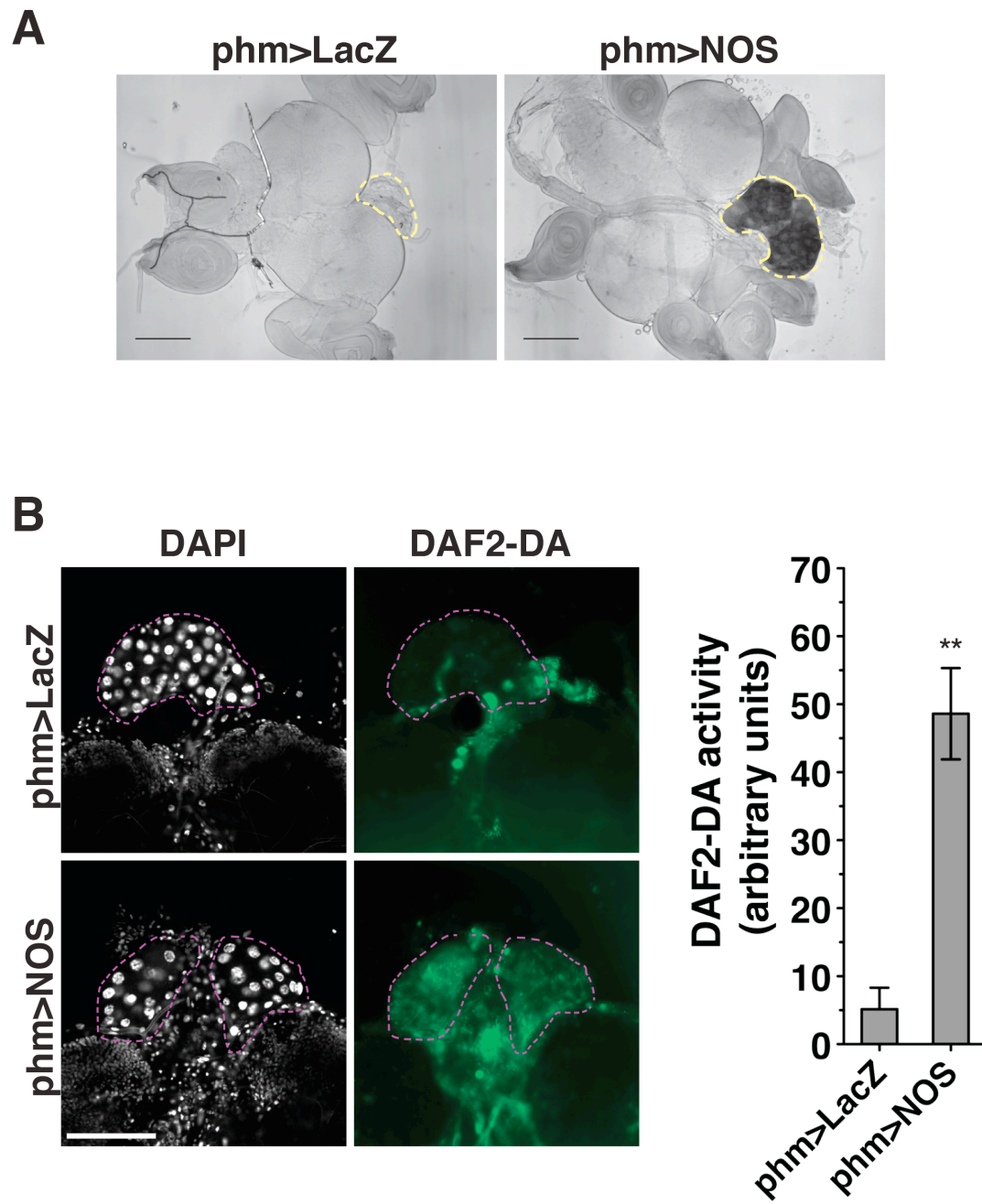


Figure 3-6. NOS is not required for regulation of developmental time during the regeneration checkpoint.

Loss of *NOS* function either by (A) knockdown of *NOS* in the PG (*phm>NOS^{Ri}*) or (B) *NOS* mutant (*NOS¹*) does not alter developmental delay. Measurement of pupariation timing for larvae with irradiation damage (25 Gy) and control larvae (0 Gy). Mean of triplicates +/- SEM. * $p < 0.05$ calculated by one-way ANOVA with Tukey's post-test.

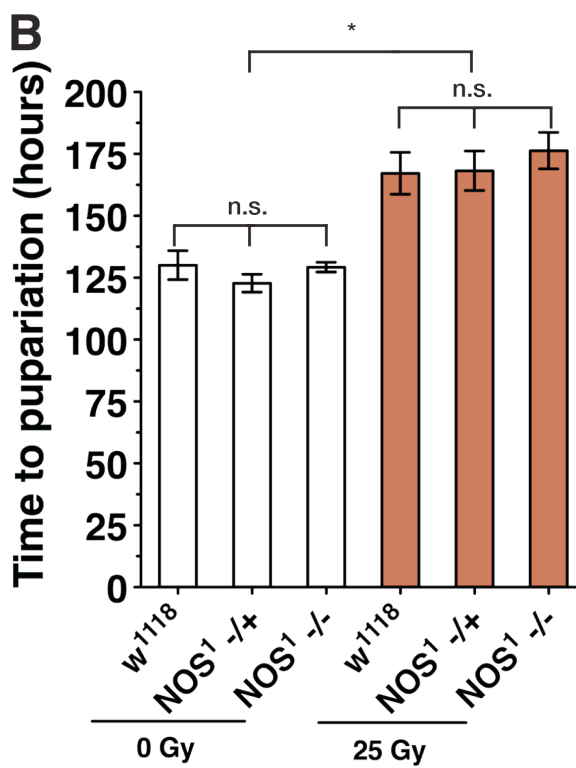
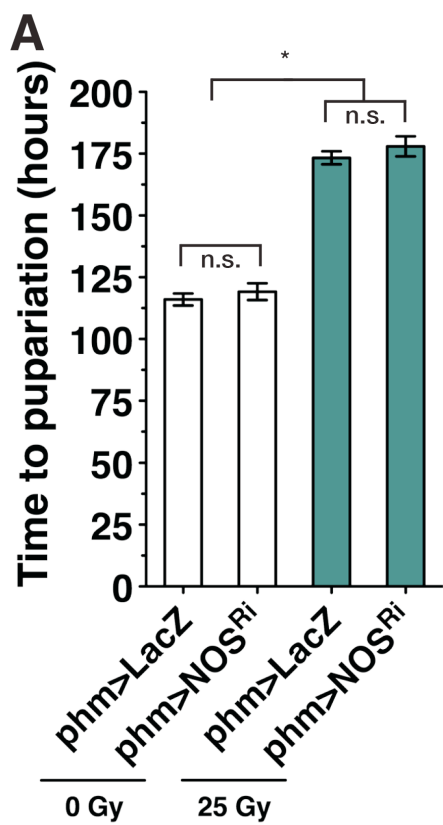


Figure 3-7. The regeneration checkpoint selectively restricts imaginal tissue growth.

(A) Growth reduction and developmental delay of undamaged eye imaginal discs in larvae with targeted tissue damage in the wings (*Bx>eiger*) and control larvae (*Bx>GFP*). Eyes were isolated at 104hr AED and stained with rhodamine-labeled phalloidin. Brackets highlight the progression of the morphogenetic furrow in each disc. Scale bar = 100 μ m. (B) Measurement of eye imaginal disc size following nutrient restriction (NR) or multiple distinct activators of the regeneration checkpoint including: targeted irradiation with 25 Gy (shielded), expression of pro-inflammatory signal (*Bx>eiger*), expression of *NOS* in the PG (*phm>NOS*), wing-targeted expression of *dilp8* (*rn>dilp8*), and wing-targeted neoplastic transformation (*Bx>av^{RNAi}*). Larvae were raised at 25°C and eye imaginal discs were isolated at 104hr AED for measurement of all experiments except for the following: *rn>GFP* and *rn>dilp8*, raised at 29°C and eye discs were dissected and measured at 80hr AED to maximize *dilp8* overexpression and the systemic growth phenotype. *phm>LacZ* and *phm>NOS* larvae were raised at 21°C and eye discs were dissected and measured at 142hr AED to reduce *NOS* overexpression and permit analysis of third instar growth phenotypes. (C) The regeneration checkpoint does not restrict larval growth. *Bx>eiger* and control larvae isolated at 104hr AED. Scale bar = 1 mm. (D) Measurement of larval growth. Larvae were raised and isolated for measurement as the same conditions in B. Statistical analysis: B and D, mean +/- SD. * $p < 0.05$, ** $p < 0.01$, **** $p < 0.001$ calculated by two-tailed Student's t-test.

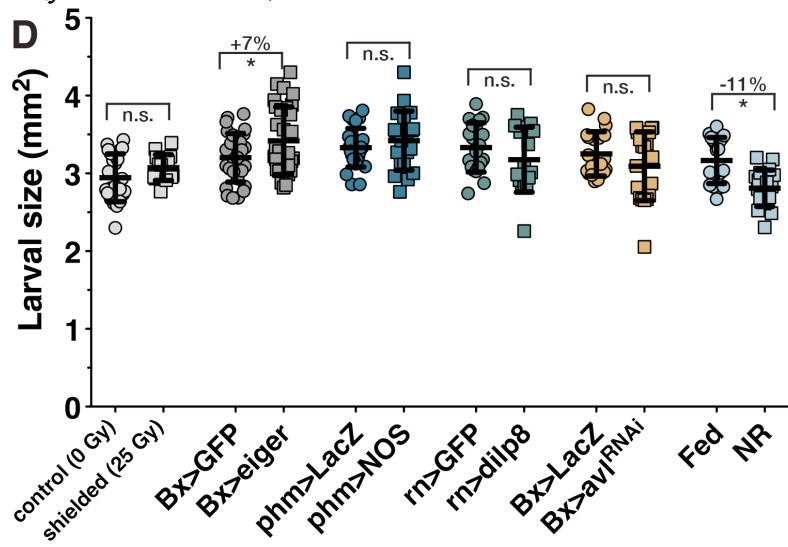
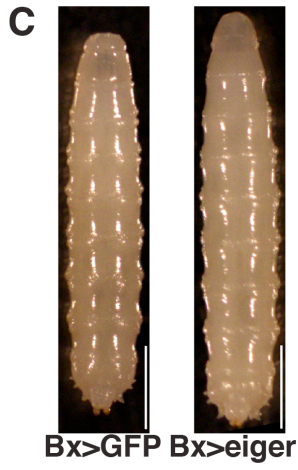
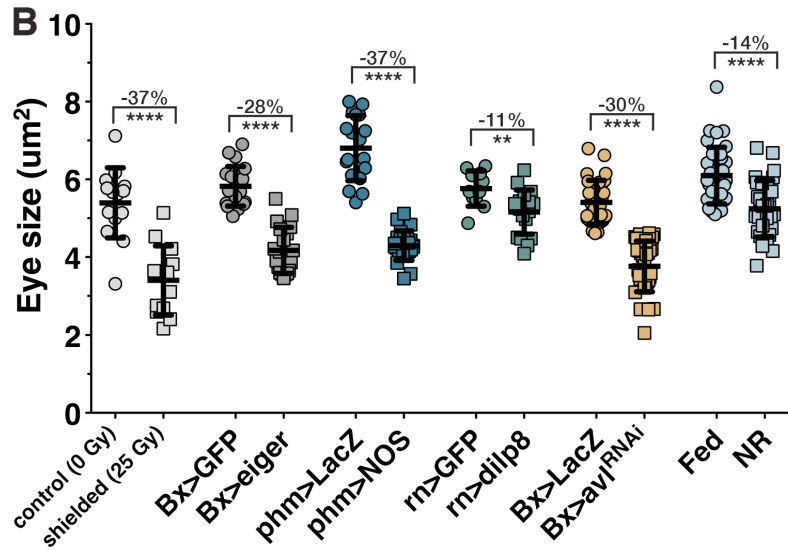
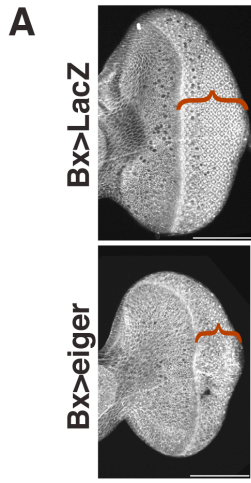


Figure 3-8. NOS overexpression during larval feeding inhibits ecdysone biosynthesis.

(A) NOS activity in the PG reduces ecdysteroid production. The presence of ecdysteroids are reduced in larvae with *NOS* overexpression in the PG (*phm>NOS*) compared to control (*phm>LacZ*) larvae. Ecdysone levels were measured by ELISA assay for independent isolation triplicates. (B) *NOS* expression in the PG reduces ecdysone signaling. Transcription of *E74B* is reduced in larvae with *NOS* overexpression in the PG (*phm>NOS*) compared to control (*phm>LacZ*) larvae. Transcription levels measured by qRT-PCR in triplicate, normalized to control expression levels at 116hr AED. (C) *NOS* activity in the PG reduces Halloween gene transcription. Relative expression of *spok* and *dib* in control (*phm>LacZ*) larvae and larvae with *NOS* overexpression in the PG (*phm>NOS*) are depicted. Transcription levels were measured by qRT-PCR in triplicate, normalized to control transcription levels. (D) Expression of *NOS* early during the larval feeding period (76hr and 80hr AED) substantially delays larval development, while *NOS* expression late during around the wandering period (96hr and 104hr AED) does not delay development. *NOS* was systemically expressed by heatshock (*hs>NOS*) once at either 76hr, 80hr, 96hr, or 104hr AED and time to pupariation was measured. (E) Expression of *NOS* early during the larval feeding period restricts imaginal disc growth, while *NOS* expression late during the wandering period does not inhibit growth. *NOS* was systemically expressed by heatshock (*hs>NOS*) at either 76hr or 104hr AED and eye imaginal disc size was measured at 116hr AED. All *phm>LacZ* and *phm>NOS* expressing larvae were raised at 21°C. Statistical analysis: A and E, mean of triplicates +/- SD calculated by two-tailed Student's t-test. B and C, mean of triplicates +/- SEM., calculated by paired one-tailed t-test. D, mean of triplicates +/- SEM. * p<0.05, ** p<0.01. ****p<0.001

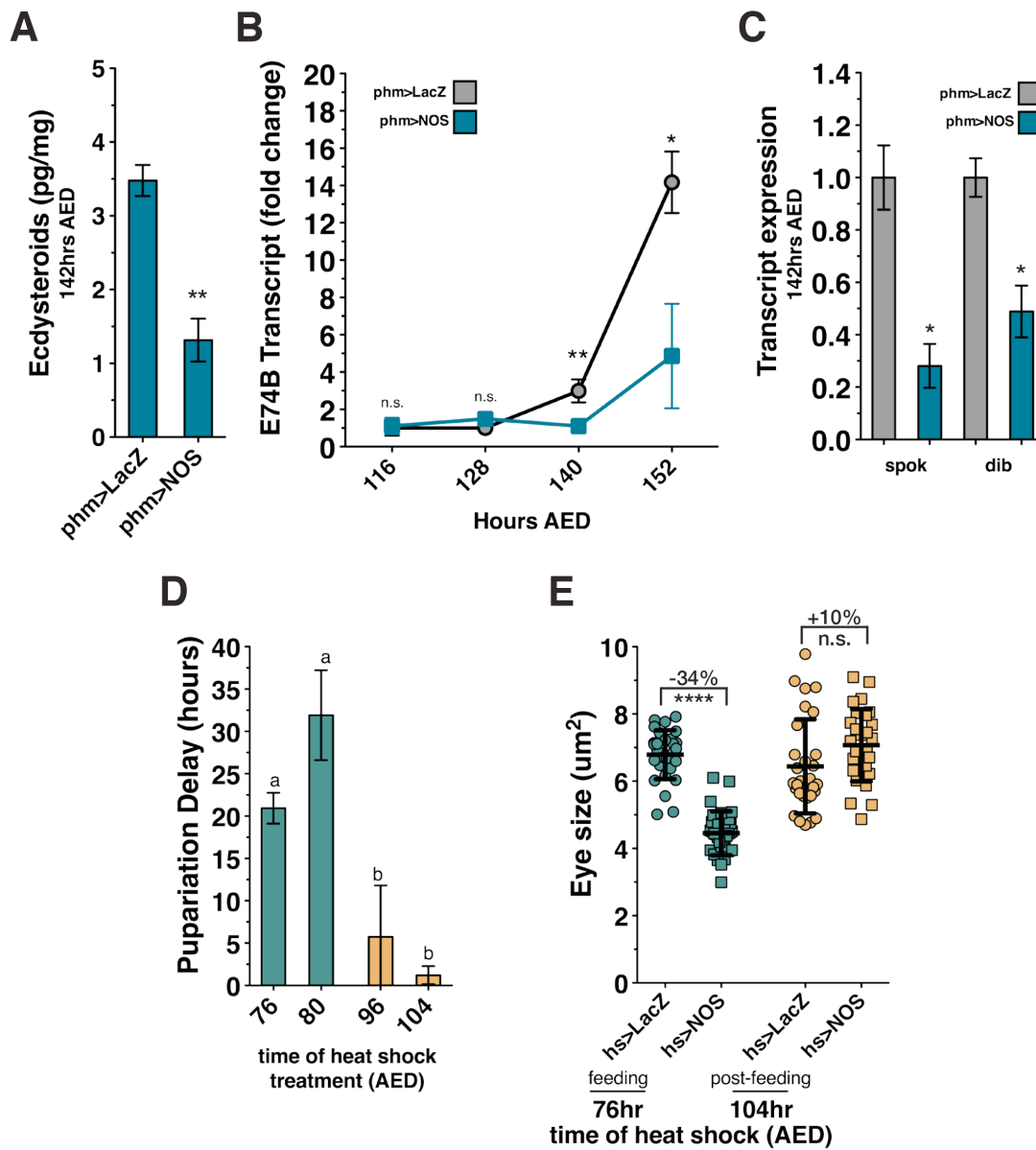


Figure 3-9. NOS inhibits ecdysone synthesis during the feeding period, and promotes ecdysone production post-feeding.

(A) Regeneration checkpoint activation reduces ecdysone signaling and Halloween gene transcription. Transcription of ecdysone-induced E74B, a reporter for early ecdysone levels during the third larval instar, in control larvae (Bx>LacZ) and larvae with targeted tissue damage (Bx>eiger). Transcription of spok and dib, ecdysone biosynthesis genes, in control larvae (Bx>LacZ) and larvae with targeted tissue damage (Bx>eiger). (B) Targeted tissue damage (Bx>eiger) suppresses transcription of the nuclear hormone receptor (E75B) involved in the initiation of pupariation. Transcript levels of E75B and tubulin measured by semi-quantitative PCR in Bx>LacZ and Bx>eiger larvae from 92h AED until the end of the larval growth period are shown. (C) Expression of NOS early, during the larval feeding period, restricts ecdysone biosynthesis genes and signaling. NOS was systemically expressed by heat shock (hs>NOS) at 76hr AED and ecdysone signaling (E74B) and Halloween gene (spok and dib) transcription was measured by qRT-PCR at 116hr AED. (D) Expression of NOS late, during the wandering period promotes ecdysone biosynthesis gene transcription. NOS was systemically expressed by heat shock (hs>NOS) at 104hr AED and E74B, spok, and dib transcription was measured by qRT-PCR at 116hr AED. Statistical analysis: A, mean of triplicates +/- SEM. * p<0.05, ** p<0.01, calculated by paired one-tailed student's t-test. B, mean of two isolation replicates +/- SEM. * p<0.05, calculated by two-way ANOVA. C and D, mean of duplicates +/- SEM. * p<0.05, calculated by paired one-tailed student's t-test.

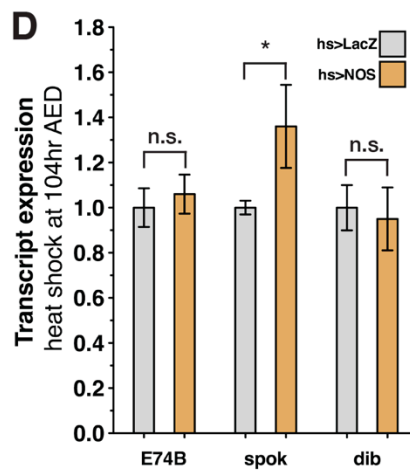
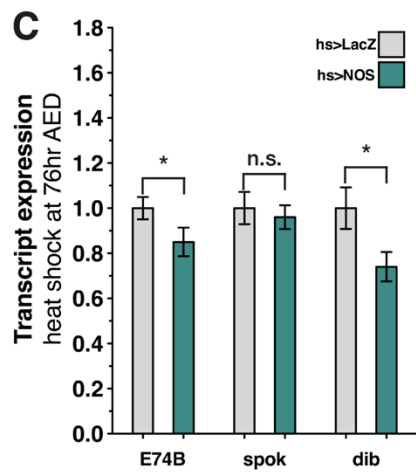
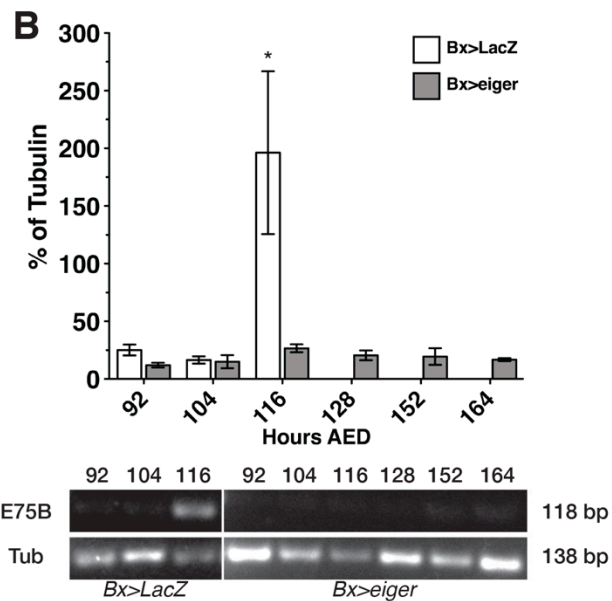
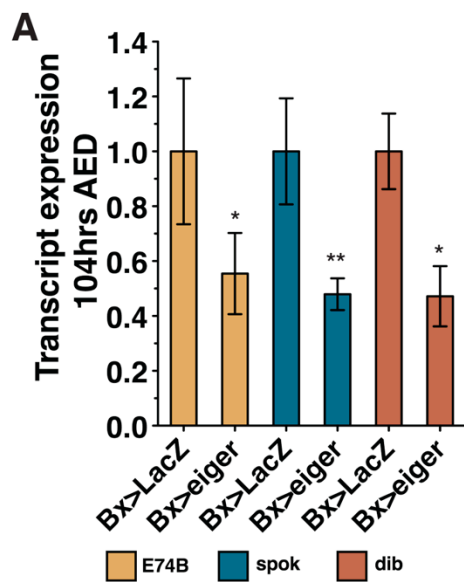


Figure 3-10. Imaginal disc growth restriction during the regeneration checkpoint is the result of reduced ecdysone signaling.

Ecdysone levels are rate-limiting for imaginal disc growth during the regeneration checkpoint. 20-hydroxyecdysone (20E) rescues growth restriction induced by (A) targeted wing damage (*Bx>eiger*), (B) systemic *dilp8* misexpression (*Tub>dilp8*), (C) systemic NOS misexpression (*hs>NOS*), and (D) PG NOS overexpression (*phm>NOS*) compared to control ethanol only fed larvae (EtOH). Statistical analysis: mean +/- SD. * $p < 0.05$, ** $p < 0.01$, **** $p < 0.001$ calculated by two-tailed Student's t-test.

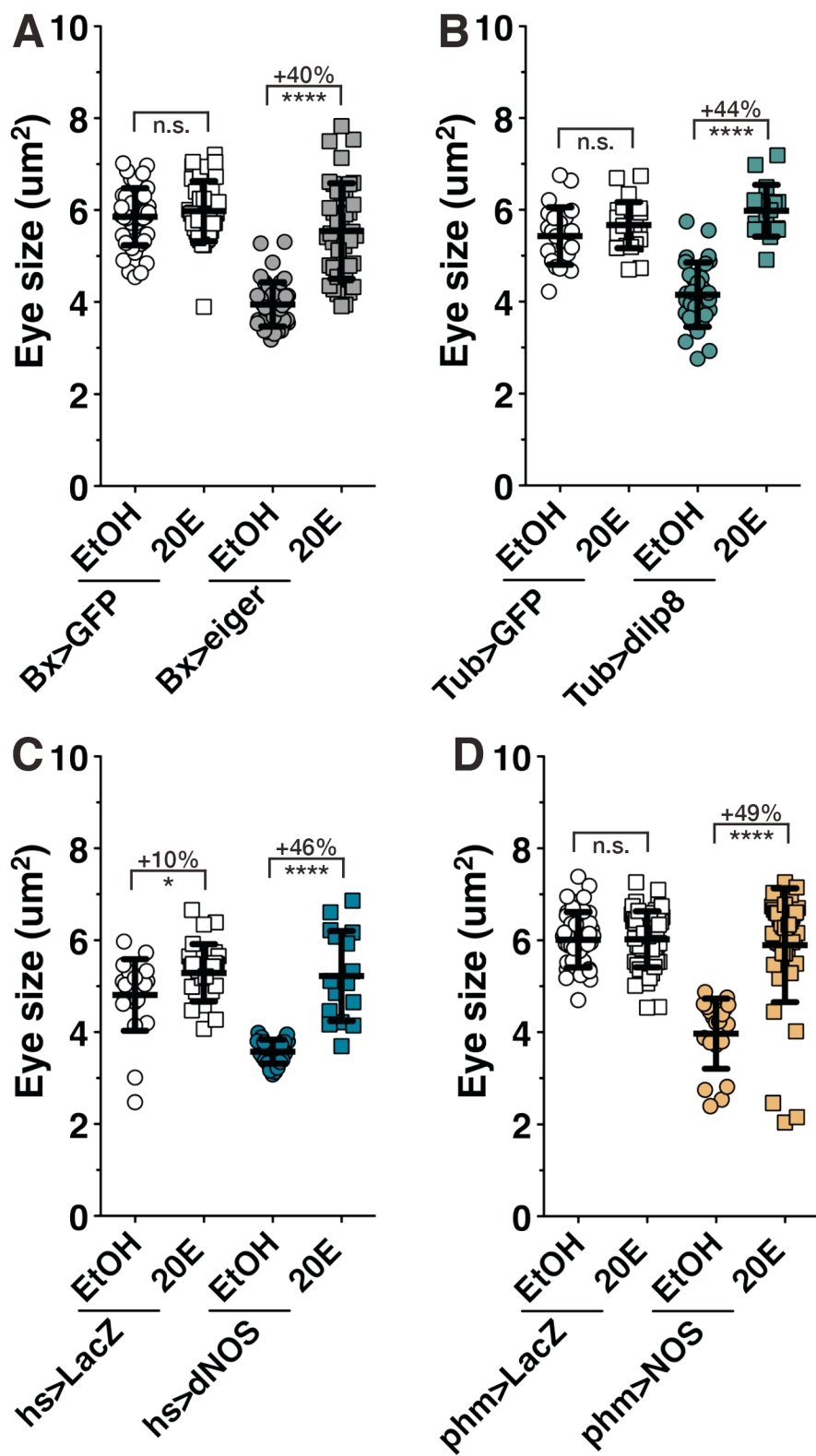


Figure 3-11. Ecdysone regulates larval growth and developmental time.

(A) Ecdysone levels are rate-limiting for imaginal disc growth during the systemic *NOS^{mac}* misexpression. 20E rescues growth restriction induced by *hs>NOS^{mac}* compared to control ethanol only fed larvae (EtOH). Larvae were heat shocked at 76hr and eye discs were measured at 104hs AED. (B) Ecdysone rescues developmental delay induced by *Bx>eiger*, *hs>NOS*, and *phm>NOS*. Measurement of time to pupariation for larvae raised in food with supplemental ecdysone (20E) or control food (EtOH). (C) Supplemented 20E only significantly reduces larval tissue growth in *Tub>dilp8* larvae. Measurement of larval growth at 104hr AED in larvae raised in food with supplemental ecdysone (20E) or control food (EtOH) is shown. (D) Non-additive effects of wing damage and ecdysone reduction on eye imaginal disc growth suggest convergent mechanisms. Measurement of eye imaginal disc size in larvae with targeted wing damage (*Bx>eiger*) and control larvae (*Bx>GFP*). Larvae were transferred at 80hr to food lacking steroid ecdysone precursor (*erg6 -/-*) or control food (*erg6 -/+*). (E) Restriction of ecdysone synthesis (*erg6 -/-*) extends the time to pupation when compared to permissive synthesis conditions (*erg6 -/+*) for both control (*Bx>GFP*) and *Bx>eiger*. (F) *erg6 -/-* inhibition of ecdysone increases the growth rate of larval tissues. Measurements of imaginal disc growth and larval growth were at 104hr AED. Statistical analysis: A, C, D, and F mean +/- SD. B and E, triplicates +/- SEM. * p<0.05, ** p<0.01, ***p<0.0005, ****p<0.001 calculated by two-tailed Student's t-test.

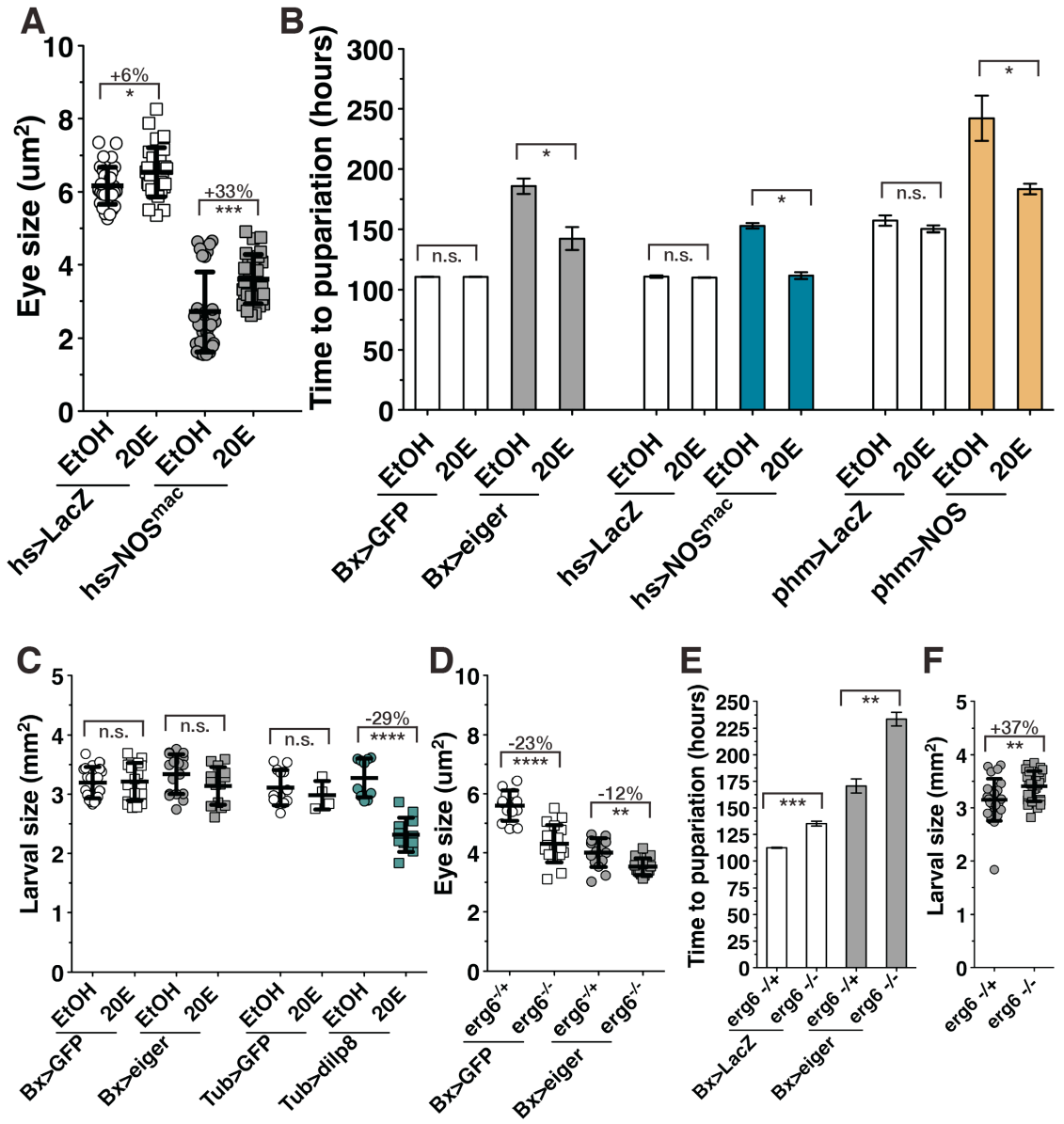
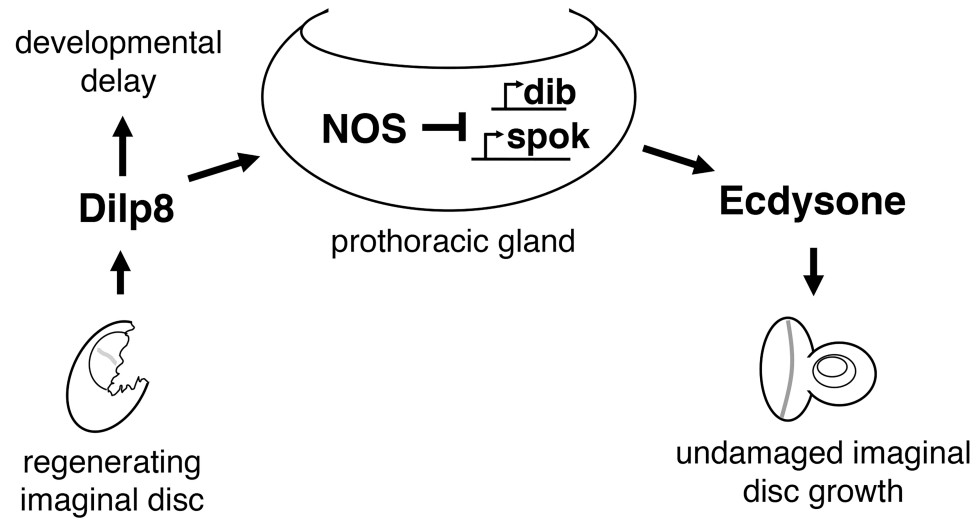


Figure 3-12. Model for allometric growth regulation during the regeneration checkpoint.

Growth is coordinated between regenerating and undamaged imaginal discs through the PG. During the larval growth period, Dilp8 secreted from regenerating imaginal discs activates nitric oxide synthase in the prothoracic gland, inhibiting ecdysone biosynthesis and reducing undamaged imaginal disc growth. Dilp8-dependent developmental delay is produced through a NOS independent-mechanism.



Appendices 1

Figure A1-1. L-NAME feeding inhibits imaginal disc growth.

Feeding larvae the inhibitor of NOS enzymatic activity, L-NAME, during the 3rd larval instar reduces imaginal disc growth. L-NAME was dissolved in H₂O and mixed with cornmeal-molasses food immediately before transferring larvae. L-NAME was fed to larvae at 80hrs AED. Imaginal discs size was measured at 104hrs. ** p<0.01, ***p<0.005 calculated by two-tailed Student's t-test.

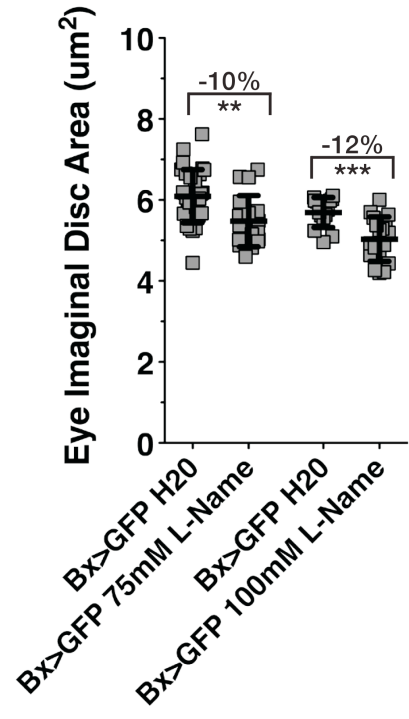


Figure A1-2. The allele *NOSΔ* reduces growth restriction during targeted damage.

Targeted damaged was genetically induced by expression of *eiger* in the wing imaginal disc (*Bx>eiger*). Larvae homozygous for *NOSΔ* (*Bx>eiger;NOSΔ*) did not inhibit undamaged eye imaginal disc growth as much as the control (104hrs), and this difference become greater later in development (144hrs) after the controls had pupariated. * $p < 0.05$, **** $p < 0.001$ calculated by two-tailed Student's t-test.

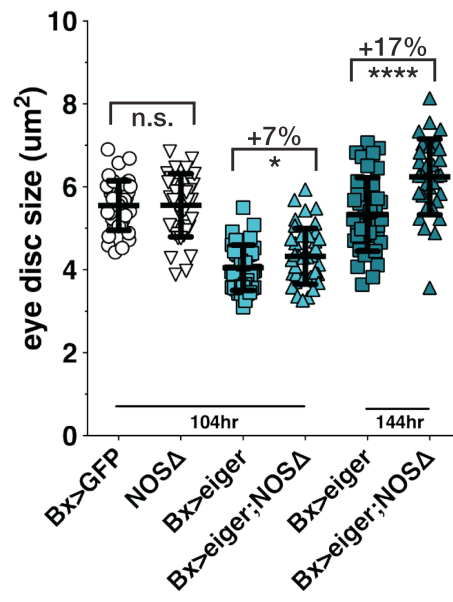


Figure A1-3. Expression of the cell gene reaper in the wing imaginal disc delays development and inhibits growth.

(A) Expression of the cell death gene *reaper* (*Bx>reaper*) delays development longer than induction of death by the JNK pathway (*Bx>eiger* or *Bx>hep^{CA}*) $p = * p < 0.05$. (B) *Reaper* expression in the wing inhibits growth of the eye imaginal discs and (C) growth of the larval tissues. Size was measured at 104hrs AED. * $p < 0.05$, **** $p < 0.001$ calculated by two-tailed Student's t-test.

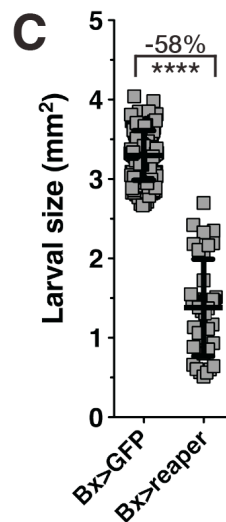
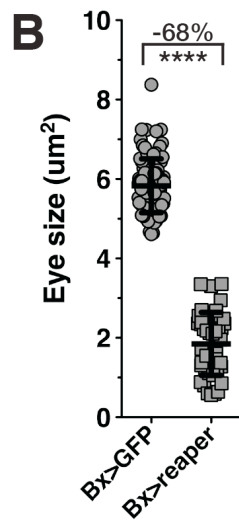
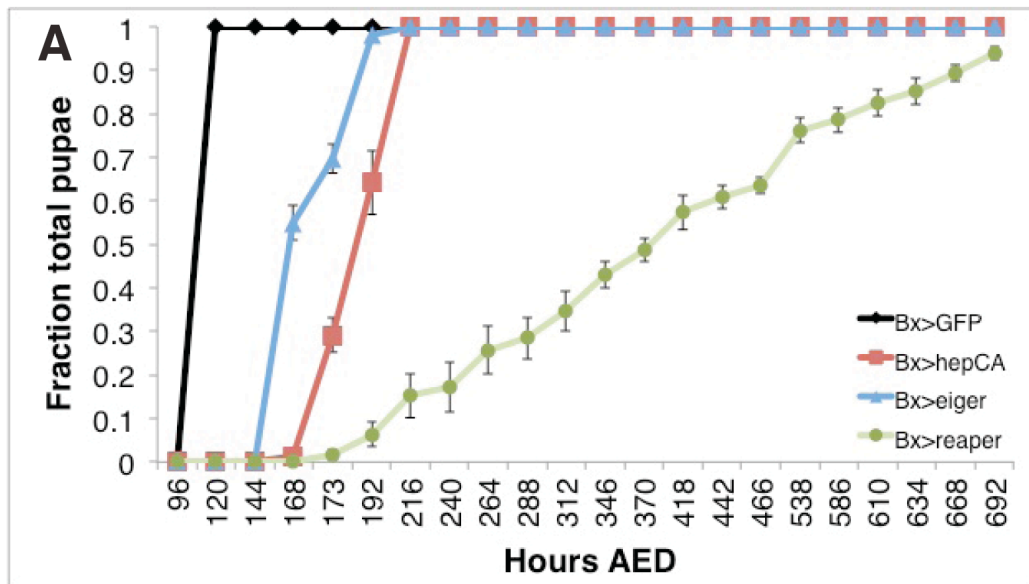


Figure A1-4. NOS overexpression in the PG does not delay E74A transcription.

E74A transcription was measured in larvae overexpressing *NOS* in the PG (*phm>NOS*). Larvae were raised at 21°C. * $p < 0.05$ calculated by two-tailed Student's t-test.

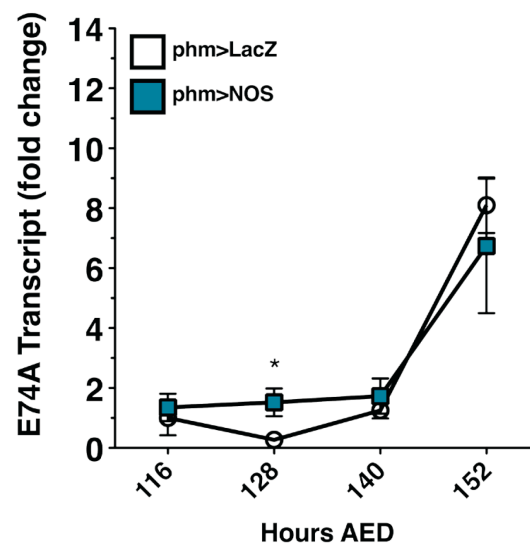


Figure A1-5. FoxO and NOS in the PG regulate growth in parallel.

(A) Overexpression of *FoxO* in the PG (*phm>FoxO*) inhibits imaginal disc growth. (B) Expression of FoxO-RNAi in the PG does not rescue growth coordination during targeted irradiation. (C) Growth inhibition by *NOS* overexpression in the PG (*phm>NOS*) is not rescued by expression of FOXO-RNAi (*phm>NOS;FoxO-RNAi*). (D) Growth restriction by targeted genetic damage (*Bx>eiger*) is reduced in larvae with trans-mutations for *FoxO* (*Bx>eiger;FoxO^{21/25}*). (B) and (D) imaginal discs were measured at 104hrs. (A) and (C) larvae were raised at 21°C and imaginal discs were measured at 142hrs. ****p<0.001 calculated by two-tailed Student's t-test.

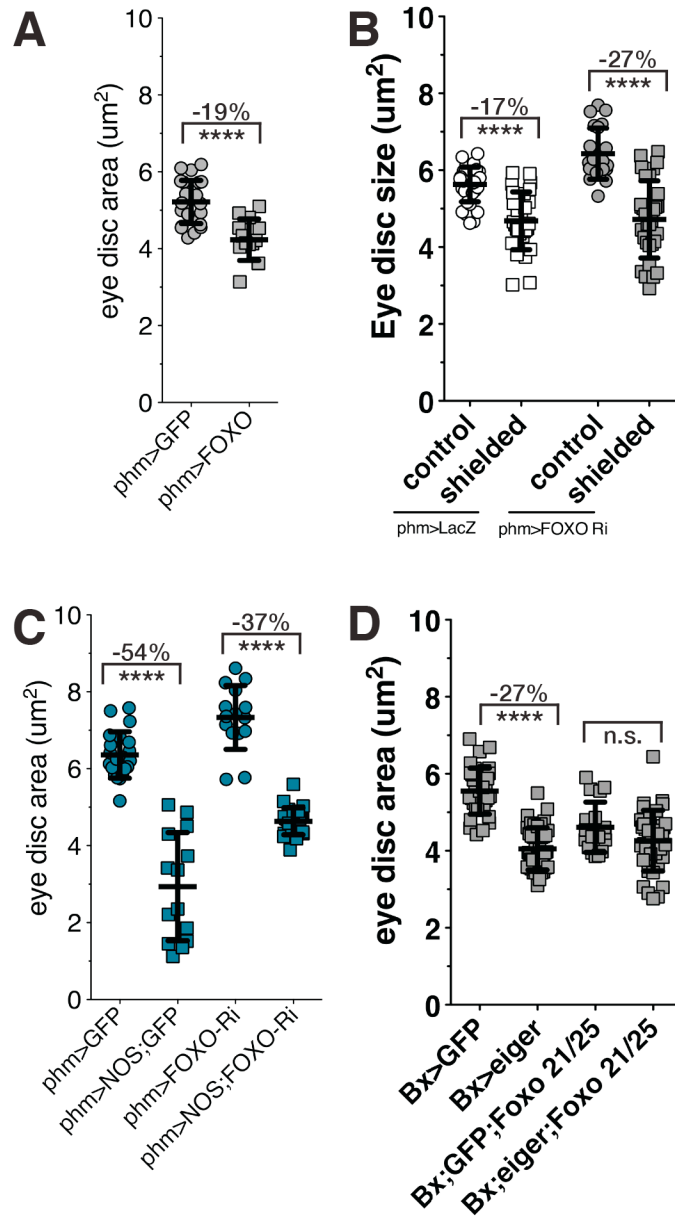
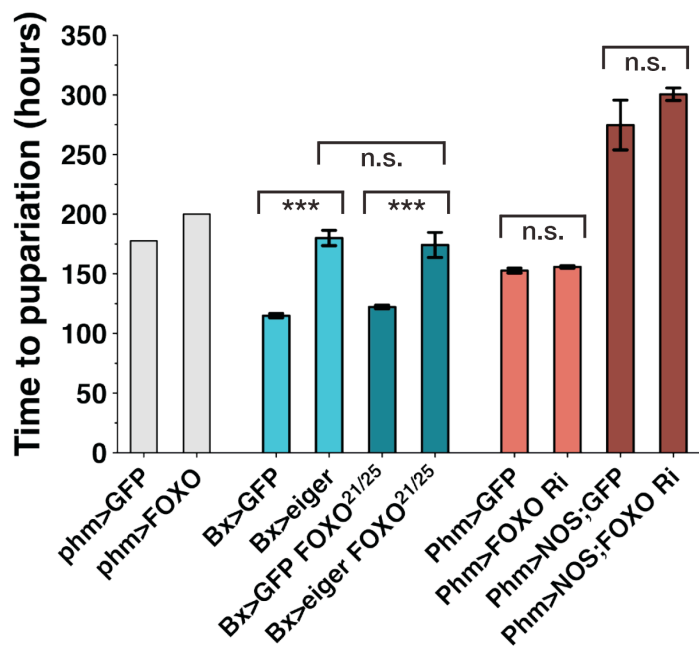


Figure A1-8. FoxO is not necessary for developmental delay induced by Bx>eiger or phm>NOS.

Overexpression of *FoxO* in the PG (*phm>FoxO*) delays puariation. Delay induced by targeted genetic damage (*Bx>eiger*) not changed in larvae with trans-mutations for *FoxO* (*Bx>eiger;FoxO^{21/25}*) Developmental delay induced by NOS overexpression in the PG (*phm>NOS*) is not rescued by expression of FOXO-RNAi (*phm>NOS;FoxO-RNAi*). *phm>FoxO* and *phm>NOS;FoxO-RNAi* larvae were raised at 21oC. ***p<0.01 calculated by two-tailed Student's t-test.



Chapter 4

The leucine-rich repeat-containing G-protein-coupled receptor Lgr3 mediates growth coordination and developmental delay during regeneration

This chapter is based work submitted but not yet accepted for publication:

Jacob S. Jaszczak, Jacob B. Wolpe, Rajan Bhandari, Rebecca G. Jaszczak, and

Adrian Halme

4.1 Abstract

Drosophila melanogaster imaginal discs damage activates a regeneration checkpoint through Dilp8 that extends larval development and coordinates the growth of the damaged and undamaged imaginal discs. Growth coordination slows the growth of undamaged discs through limiting ecdysone synthesis by Dilp8 activation of NOS in the prothoracic gland (PG). Here we demonstrate that the *Drosophila* relaxin receptor homologue Lgr3, a leucine-rich repeat-containing G-protein coupled receptor, is required for the Dilp8-dependent regeneration checkpoint. Lgr3 regulates developmental delay and growth coordination via distinct mechanisms in different tissues. Using tissue-specific RNAi disruption of *Lgr3* expression, we show that Lgr3 functions in the PG upstream of NOS, and is necessary for NOS activation and growth coordination during the regeneration checkpoint. In CNS neurons, we also have identified a NOS-independent activity of Lgr3. In undamaged larvae, RNAi disruption of Lgr3 in neurons significantly increases imaginal disc growth and produces precocious ecdysone signaling, suggesting that Lgr3 in the CNS acts to restrict growth and ecdysone synthesis during normal development. We also demonstrate that when Lgr3 is depleted from neurons, imaginal disc damage no longer produces either developmental delay or growth coordination. Together, these results identify new roles for a

relaxin receptor in mediating damage signaling to regulate growth and developmental timing.

4.2 Introduction

Regulation of the rate of growth and the total time of development are two mechanistically distinct processes that must act in concert to ensure that all organs develop to the right size in a temporally coordinated manner. Lacking in our understanding of growth regulation and developmental time are how these process remain coordinated even when environmental factors change or growth is perturbed.

Following damage to imaginal discs, *Drosophila* larvae delay their development and slow the growth of undamaged imaginal discs in order to coordinate regeneration with the growth and development of undamaged tissues (Halme, Cheng, and Hariharan 2010; Stieper et al. 2008; Garelli et al. 2012; Colombani, Andersen, and Leopold 2012; Jaszczak et al. 2015). Dilp8, a member of the insulin/IGF/relaxin family of peptide hormones, is produced by regenerating imaginal discs and is required for both delay and growth coordination (Garelli et al. 2012; Colombani, Andersen, and Leopold 2012; Jaszczak et al. 2015). Growth coordination between regenerating and undamaged tissues is dependent on

Dilp8 activation of NOS in the prothoracic gland (PG), which slows the growth of undamaged discs by limiting ecdysone synthesis (Halme, Cheng, and Hariharan 2010; Garelli et al. 2012; Colombani, Andersen, and Leopold 2012). Dilp8 also regulates developmental delay, but through a NOS-independent mechanism.

Based on the structural similarities between Dilp8 and relaxin proteins, we sought to determine whether Dilp8 activity is dependent on a *Drosophila* relaxin receptor homolog. Relaxin receptors in mammals belong to a larger family of leucine-rich repeat-containing G-protein coupled receptors (LGRs). LGRs are subdivided into type A vertebrate gonadotropin receptors, type B Wnt agonist R-spondin receptors Lgr4/5/6 (including the *Drosophila* bursicon receptor Lgr2/rickets), and type C relaxin receptors (Barker, Tan, and Clevers 2013). The different classes of LGR receptors are distinguished by different numbers of extracellular leucine rich repeats (LRRs), the presence of a low-density lipoprotein receptor class A domain (LDL_A), and the structure of the hinge region connecting the transmembrane region to the LRR domain. *Drosophila* have four LGR proteins, of which only Lgr3 and Lgr4 share structural homology with the type C relaxin receptors (Fig. 4-1A). Lgr3 and Lgr4 have recently been shown to be expressed in many tissues throughout larval development (Van Hiel et al. 2014).

4.3 Results

4.3.1 The *Drosophila* relaxin receptor homolog, Lgr3, is required for growth coordination and delay during the regeneration checkpoint

Damage to *Drosophila melanogaster* imaginal discs activates a regeneration checkpoint that 1) extends larval development and 2) coordinates the regeneration of the damaged disc with the growth of undamaged tissues (Halme, Cheng, and Hariharan 2010; Poodry and Woods 1990; Simpson, Berreur, and Berreur-Bonnenfant 1980; Stieper et al. 2008; Garelli et al. 2012; Colombani, Andersen, and Leopold 2012). These two systemic responses to damage are both mediated by Dilp8 which is released by regenerating tissues (Garelli et al. 2012; Colombani, Andersen, and Leopold 2012; Jaszczak et al. 2015). Dilp8 has structural similarities to relaxin proteins; therefore, we sought to determine whether Dilp8 activity is dependent on any of the four *Drosophila* relaxin receptor homologs. To test whether these *Drosophila* relaxin homologs are necessary for growth coordination or developmental delay during the regeneration checkpoint, we ubiquitously expressed UAS-driven RNAi transgenes against each of the two receptors throughout the whole animal using tubulin-Gal4. We then activated the regeneration checkpoint in these larvae through targeted irradiation, producing damage in posterior tissues of the larvae while protecting anterior tissues like the eye imaginal discs and the PG (see Experimental Procedures and (Jaszczak et

al. 2015)). Following posterior irradiation, the growth of anterior tissues is normally reduced due to Dilp8-dependent growth coordination (Jaszczak et al. 2015). RNAi targeting of Lgr3 reduces checkpoint growth inhibition, restoring the growth of undamaged tissues in larvae with targeted irradiation (Fig. 4-1B). This observation was confirmed with a second RNAi transgene with a different targeting sequence in Lgr3 (Fig. 4-2A). To examine whether either of the *Drosophila* relaxin homologs are necessary for developmental delay, we irradiated whole larvae and found that only RNAi constructs targeting Lgr3 significantly reduced the regeneration checkpoint delay (Figure 4-1C and Fig. 4-2B). Additionally, we tested RNAi targeted to the other *Drosophila* LGR genes and found that neither Lgr1 nor Lgr2 depletion reduced damage-induced growth inhibition or developmental delay, suggesting that those LGRs do not mediate Dilp8 activity. In contrast, we observed that expression of either Lgr1 or Lgr2 RNAi produced a significantly longer delay following irradiation than in control larvae (Fig. 4-2C and D), suggesting that they function in distinct roles in regulating developmental timing, which could warrant future investigation.

Expression of *dilp8* alone, in the absence of damage, is sufficient to induce growth restriction and developmental delay (Fig 4-1D,E) (Garelli et al. 2012; Colombani, Andersen, and Leopold 2012; Jaszczak et al. 2015). To test whether Dilp8 induction of these systemic responses depends on Lgr3, we systemically co-expressed Dilp8 and an RNAi targeting Lgr3 using the tubulin-

Gal4 driver. In larvae depleted of Lgr3, Dilp8-induced growth inhibition and developmental delay were both rescued (Fig. 4-1D,E). Together, these data demonstrate that of the *Drosophila* LGR proteins, Lgr3 alone is required for Dilp8-dependent coordination of growth and developmental delay during the regeneration checkpoint.

4.3.2 Lgr3 mediates Dilp8 activation of NOS in the PG and is necessary for growth coordination during the regeneration checkpoint

To identify tissues where Lgr3 is expressed and thus may respond to Dilp8 signaling, we used a collection of Lgr3 enhancer-Gal4 transgenes (Pfeiffer et al. 2008) (Fig. 4-3A). These transgenes allow us to express nuclear-localized β -galactosidase in tissues where Lgr3 regulatory regions are transcriptionally active. Following staining, we observed that these enhancer-Gal4 transgenes expressed predominantly in the central nervous system (CNS) (Fig. 4-3B-F). However, the enhancer-Gal4 transgene 18A01 expresses strongly in both the CNS and PG (Fig 4-2A and 4-3E). We have recently reported that Dilp8 coordinates growth through the activation of NOS in the PG (Jaszczak et al. 2015); therefore, we further tested whether Lgr3 is required for growth regulation in the cells that express the 18A01 enhancer-Gal4 transgene. When an Lgr3-targeting RNAi was expressed using the 18A01 enhancer-Gal4, growth inhibition of the undamaged imaginal discs does not occur (Fig. 4-4B), suggesting that the

18A01 enhancer expresses in cells that require *Lgr3* to produce growth coordination following damage. Next, we asked whether *Lgr3* activity in the PG was necessary for growth coordination following damage. In larvae where phantom-Gal4 directs the expression of an *Lgr3*-targeting RNAi to the PG (Mirth, Truman, and Riddiford 2005), we observed that inhibition of undamaged tissue growth following regeneration checkpoint activation is lost (Fig. 4-4C). This result demonstrates that *Lgr3* activity in the PG is necessary for growth coordination following regeneration checkpoint activation. Interestingly, we observed that RNAi depletion of *Lgr3* in the PG has no effect on the developmental delay produced by activation of the regeneration checkpoint (Fig. 4-4D). This observation is consistent with what we have reported for NOS activity, where NOS activation in the PG is necessary for damage and *Dilp8*-mediated growth inhibition, but not developmental delay (Jaszczak et al. 2015). Therefore, we speculated that *Lgr3* might be regulating NOS activity in the PG during the regeneration checkpoint.

To determine whether PG expression of *Lgr3* is required for the activation of NOS, we used the fluorescent reporter molecule 4,5-diaminofluorescein diacetate (DAF2-DA) to measure NO production in the PG. We have previously shown that *dilp8* expression is sufficient to induce NOS activation in the PG (Jaszczak et al. 2015). After posterior irradiation of larvae, NO production increases in the PG in a *Dilp8* dependent manner (Fig. 4-4E and F). When we

express an Lgr3-targeting RNAi in the PG with the phantom-Gal4 driver, activation of NOS is no longer detected in the PG following irradiation (Figure 4-4G). These data demonstrate that Lgr3 activity in the PG is required for NOS activation during the regeneration checkpoint. To establish that NOS functions downstream of Lgr3, we determined whether artificially increasing NOS activity could restrict growth independently of Lgr3 function in the PG. To do this, we overexpressed NOS along with the Lgr3- RNAi in the PG using phantom-Gal4. We found that even when Lgr3 is depleted from the PG, NOS is still able to inhibit imaginal disc growth (Fig.4-4H). Together, these data demonstrate that Lgr3 in the prothoracic gland functions upstream of NOS, is necessary for NOS activation, and is required for Dilp8-mediated growth control through NOS.

4.3.3 Lgr3 functions in neurons to regulate ecdysone production and imaginal tissue growth during development

All the Lgr3 enhancer-Gal4 transgenes analyzed express in the CNS (Fig. 4-3B-F). To examine the function of Lgr3 in neurons, we expressed Lgr3-targeted RNAi in differentiated neurons using the pan-neuronal driver elav-Gal4. We first noticed that Lgr3 depletion in neurons substantially increases the growth of the imaginal discs in undamaged larvae (Fig. 4-5A). This is consistent with the increase observed in growth of the eye imaginal discs when Lgr3-targeting RNAi is ubiquitously expressed using tubulin-Gal4 (Fig. 4-6A). In contrast, depletion of

Lgr3 in the PG only has a modest effect on imaginal tissue growth during normal development (Fig. 4-5B). We also noted that the increase in imaginal disc growth in *tub>Lgr3-RNAi* larvae was not seen in our earlier targeted irradiation experiments (Fig. 4-6B). We suspect that chilling the larvae, which is required for immobilization during targeted irradiation, slows development and reduces the difference in imaginal disc size at 104 hours AED. The increased imaginal tissue growth seen in *elav>Lgr3-RNAi* larvae is not accompanied by faster overall larval development (Fig. 4-5B). Rather, populations of *elav>Lgr3-RNAi* larvae exhibit a very slight developmental delay, with less synchronized pupariation timing (Fig. 4-5C).

Ecdysone levels determine the rate of imaginal disc growth during the third larval instar (Jaszczak et al. 2015; Warren et al. 2006; Delanoue, Slaidina, and Léopold 2010). Thus, the increased growth of imaginal discs we observed in *elav>Lgr3-RNAi* larvae might be due to increased or dysregulated ecdysone signaling. To test this, we examined the expression of the ecdysone target gene *E75* (Segraves and Hogness 1990). Expression of *E75* is normally increased at the very end of larval development, 4-6 hours before pupariation (Karim and Thummel 1992; Andres et al. 1993). In comparison to control larvae, *Lgr3* depletion from neurons substantially increases *E75* expression. Also, *E75* expression occurs much earlier in larval development than is observed in control larvae (Fig. 4-5C). In summary, these results demonstrate that neuronal *Lgr3* is

necessary for limiting ecdysone signaling and imaginal disc growth during the larval third instar.

4.3.4 Larvae depleted for neuronal Lgr3 activity fail to delay or produce distal growth inhibition following damage

Since ecdysone signaling and imaginal tissue growth are dysregulated in *elav>Lgr3-RNAi* larvae, we wanted to determine if Lgr3 activity in neurons is important for regulating systemic responses to damage during the regeneration checkpoint. In particular, Lgr3 function is essential for developmental delay in response to imaginal disc damage (Fig. 4-1C), but not through its activity in the PG (Fig. 4-4D). Therefore, we first examined whether *Lgr3* expression in neuronal cells is necessary for damage-induced developmental delays. In *elav>Lgr3-RNAi* larvae, irradiation damage produced essentially no delay in development (Fig. 4-7A). Unexpectedly, depletion of Lgr3 in neurons also completely eliminated growth coordination following targeted irradiation (Fig. 4-7B). This neuronal dependence on Lgr3 for growth coordination was confirmed with the neuron-specific synaptobrevin-Gal4 expression of Lgr3-targeted RNAi (Pauli et al. 2008), which also eliminated growth coordination following targeted irradiation (Fig. 4-8A). Further confirming that Lgr3 activity in the CNS is specific to neurons, expression of Lgr3-targeted RNAi in glial cells using *repo-Gal4* did not rescue growth inhibition or developmental delay (Fig. 4-8B,C). Therefore, in

addition to regulating both growth and ecdysone signaling during development, *Lgr3* in neuronal cells is also required for both delay and growth inhibition during the regeneration checkpoint.

Because expression of the neuropeptide *PTTH* is delayed following activation of the regeneration checkpoint (Halme, Cheng, and Hariharan 2010), we tested whether *Lgr3* might be acting in the *PTTH*-expressing neurons (McBrayer et al. 2007) to directly regulate delay or growth inhibition. However, neither growth nor delay was affected by *Lgr3*-targeted RNAi expression specifically in the *PTTH*-expressing neurons (Fig. 4-8D). Therefore, other neurons expressing *Lgr3* are likely communicating regeneration checkpoint activation to the *PTTH*-expressing neurons.

Since the *Lgr3*-dependant activation of NOS in the PG is required for growth coordination (Jaszczak et al. 2015), we also tested whether NOS is required in the neurons for regulating *Lgr3*-dependent growth coordination and developmental delay during the regeneration checkpoint. Using a NOS-directed RNAi expressed in neurons (*elav>NOS-RNAi*) during targeted irradiation, we found that neuronal depletion of NOS did not restore growth to undamaged tissues (Fig. 4-8D) or reduce developmental delay (Fig. 4-8E). Therefore, *Lgr3* in neurons regulates growth and delay through a NOS-independent mechanism.

4.4 Discussion

Our observations demonstrate that the *Drosophila* relaxin receptor Lgr3 regulates imaginal disc growth and ecdysone production during larval development; Lgr3 also mediates the effects of Dilp8 on developmental timing and growth coordination during *Drosophila* imaginal disc regeneration (Fig. 4-7C). Previous understanding of the biological activities of relaxins and their receptors have been largely restricted to their roles in sexual development and their function in the reproductive organs (Bathgate et al. 2013). We demonstrate that *Drosophila* relaxin receptor Lgr3 participates in growth regulation during development and is necessary for coordinating growth between tissues during a regeneration checkpoint. We find that Lgr3 regulates growth coordination via multiple, tissue-specific mechanisms. Lgr3 in the PG mediates Dilp8 activation of NOS, whereas Lgr3 in neurons regulates developmental time and growth through a NOS-independent pathway. An important question arises from this model of growth coordination and regulation of developmental time; how does Lgr3 in the neurons regulate developmental time and growth, and how does this neural pathway intersect with the Lgr3-NOS pathway in the PG? This work finds that Lgr3 in the neurons regulates the timing of changes in ecdysone signaling. In previous work we found that the advancement of development inhibits the ability of NOS to restrict growth (Jaszczak et al. 2015). Together, this suggests that

Lgr3 in the neurons may intersect with Lgr3 in the PG to regulate advancement of developmental time, possibly through E75 regulation of ecdysone.

Recently, allele polymorphism at Lgr8/RXFP2 (the mammalian homologue of the *Drosophila* Lgr3) has been demonstrated to be an important genetic determinant of relative horn size within a population of wild Soay sheep (Johnston et al. 2013). This suggests that a role for relaxin receptors in regulating growth and organ allometry is likely to be conserved in mammals.

Figure 4-1: The *Drosophila* relaxin receptor homolog Lgr3 regulates Dilp8 mediated growth coordination and developmental delay during the regeneration checkpoint.

(A) Comparison of the mammalian (black) and *Drosophila melanogaster* (blue) LGR protein types. LRR: Leucine-rich repeat domain – the number above denotes the number of repeats typically found among receptors of that LGR type; LH: long hinge domain; SH: short hinge domain; 7TM: seven transmembrane domain (B) Lgr3 regulates the regeneration checkpoint. Targeted irradiation to the posterior of the larva inhibits growth of the anterior-undamaged eye imaginal discs (*tub>LacZ*, irradiated vs control). Systemic expression of Lgr3-RNAi (*tub>Lgr3-RNAi*: TRiP line GL01056, unless otherwise noted) rescues growth restriction. Systemic expression of Lgr4-RNAi (TRiP JF03070) does not rescue growth restriction. *tub-Gal4* line is derived from Bloomington stock 5138. (C) Full irradiation induces a developmental delay (*tub>LacZ*), which is rescued by systemic expression of Lgr3-RNAi. (D and E) Lgr3 mediates Dilp8 signaling. Systemic expression of *dilp8* inhibits imaginal disc growth and developmental delay (*tub>dilp8*). Systemic expression of Lgr3-RNAi simultaneously with *dilp8* blocks both growth inhibition and Dilp8-induced delay (*tub>dilp8; Lgr3-RNAi*). Growth: mean +/- SD. Time: mean of duplicate or triplicate experiments +/- SEM. ** $p < 0.01$, **** $p < 0.001$ calculated by two-tailed Student's t-test.

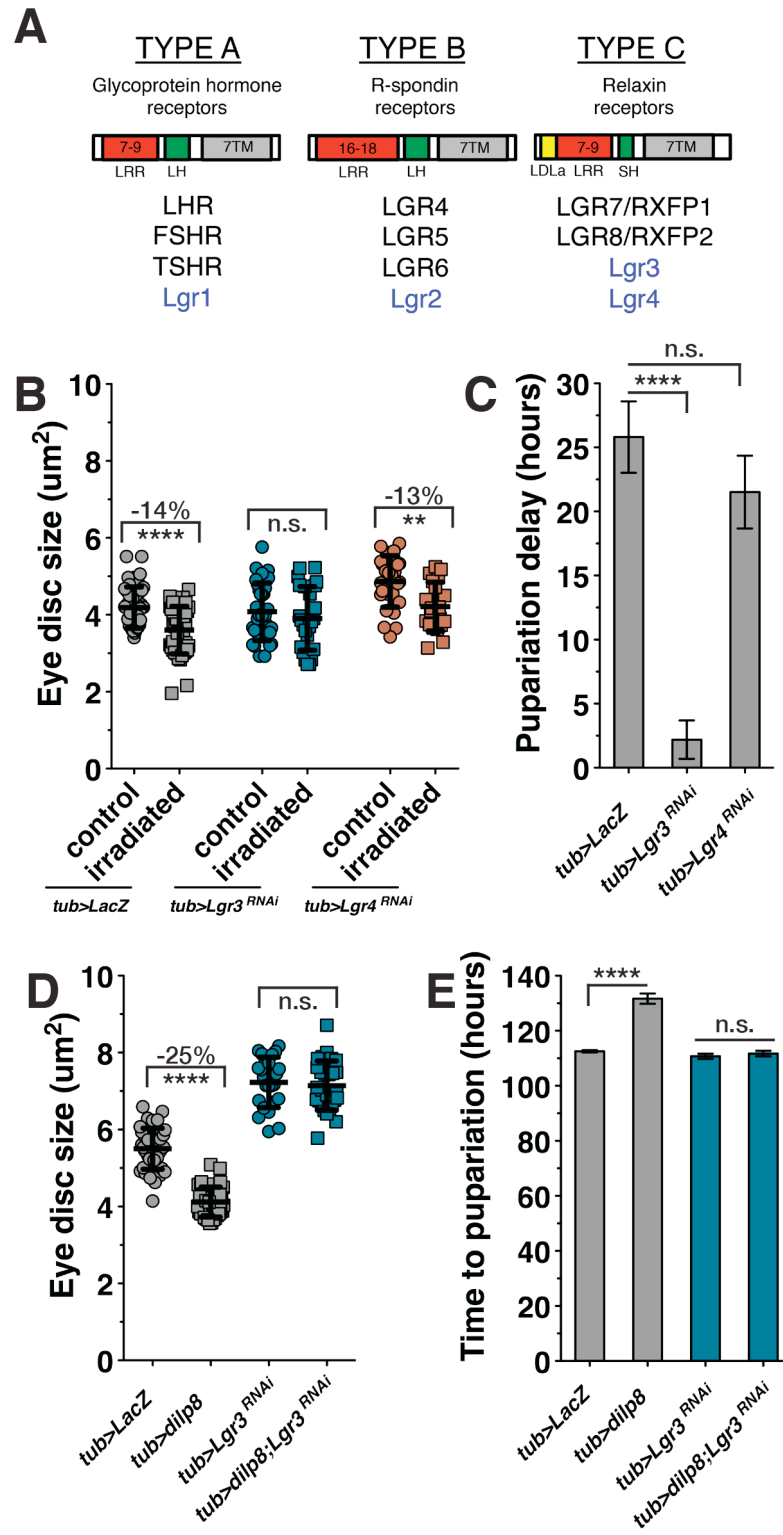


Figure 4-2: LGR1 and LGR2 do not regulate growth coordination.

(A and B) Systemic expression of Lgr3-RNAi (TRiP JF03217) rescues growth restriction induced by targeted irradiation and developmental delay induced by irradiation. (C and D) Systemic expression of Lgr1-RNAi (TRiP JF02659), or Lgr2-RNAi (TRiP JF02678), does not rescue growth restriction induced by targeted irradiation or developmental delay induced by irradiation. Growth: mean \pm SD. Time: mean of duplicate or triplicate experiments \pm SEM. * $p < 0.05$, ** $p < 0.01$, *** $p < 0.001$ calculated by two-tailed Student's t-test.

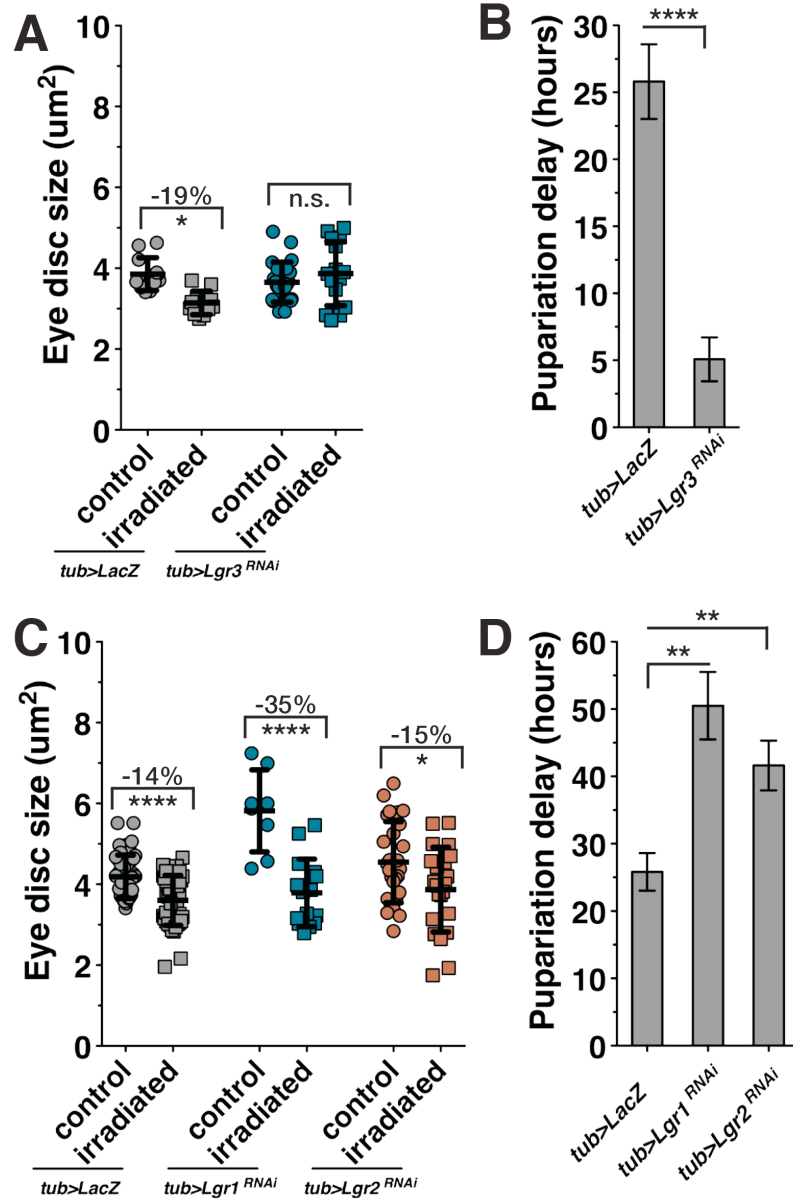


Figure 4-3: Enhancer elements of Lgr3 express in the larval CNS and PG.

(A) Gene map of Lgr3 and corresponding regions of enhancer elements used for enhancer-Gal4 transgenes. Blue boxes: 3' and 5' UTR. Red boxes: coding sequence. (B-F) Expression of nuclear-localized β -galactosidase visualized by X-gal staining in 104hr AED larva. The arrow denotes enhancer activity seen in the PG (E). Arrowheads denote regions with recurring patterns of CNS enhancer activity. Scale bars = 200um.

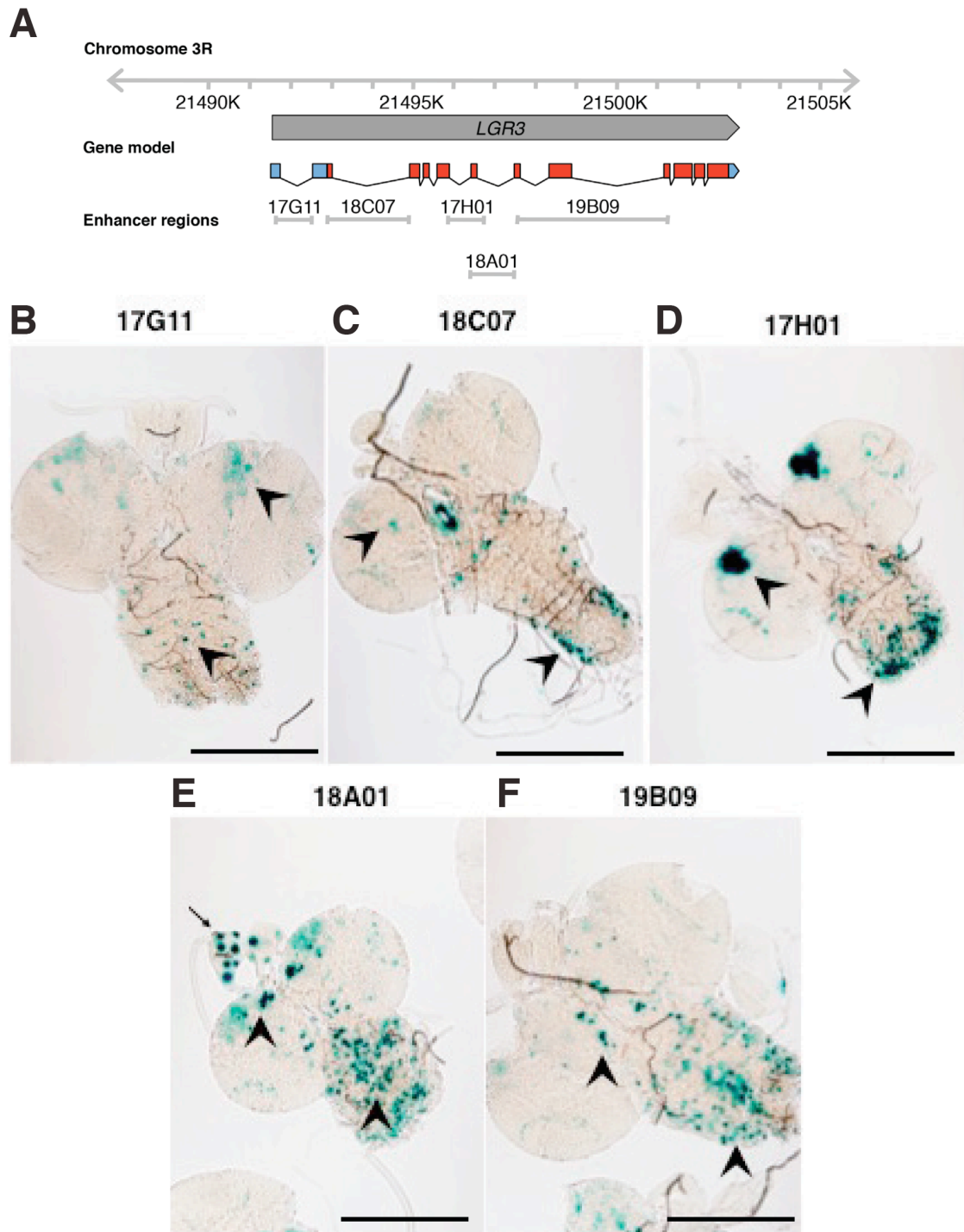


Figure 4-4: Lgr3 in the PG regulates growth coordination and NOS activity.

(A) The Lgr3 enhancer element 18A01 expresses in the PG and CNS. Expression of nuclear-localized β -galactosidase (BL3956) visualized with anti- β -galactosidase in 104hr AED larva driven by enhancer 18A01 (*18A01>LacZ*). cyan: actin, red: anti- β -galactosidase. Arrow denote enhancer activity seen in the PG. Arrowheads denote regions in the CNS of recurring patterns of enhancer activity. Scale bars = 100 μ m. (B) Expression of Lgr3-RNAi with the Lgr3 enhancer-Gal4 (*18A01>Lgr3-RNAi*) reduces growth inhibition induced by targeted irradiation, increasing imaginal disc growth. (C) Lgr3 in the PG regulates growth coordination. Expression of Lgr3-RNAi in the PG (*phm>Lgr3-RNAi*) rescues growth inhibition induced by targeted irradiation. (D) Expression of Lgr3-RNAi in the PG does not affect developmental delay induced by irradiation. (E) Targeted irradiation increases NO production in the PG. (gray: DAPI, green: DAF2-DA). (F) Activation of NO production in the PG after targeted irradiation is lost in larva mutant for Dilp8 (*dilp8*^{-/-} BL33079). (n = 5-10 PGs) (G) Lgr3 in the PG regulates NOS activity. Expression of Lgr3-RNAi in the PG blocks activation of NO production after targeted irradiation. (n = 5-10 PGs) (H) Overexpression of NOS in the PG (*phm>NOS*) inhibits imaginal disc growth even when Lgr3-RNAi is also expressed (*phm>NOS;Lgr3RNAi*). Growth: mean \pm SD. Time: mean of duplicate or triplicate experiments \pm SEM. * $p < 0.05$, *** $p < 0.005$, **** $p < 0.001$ calculated by two-tailed Student's t-test.

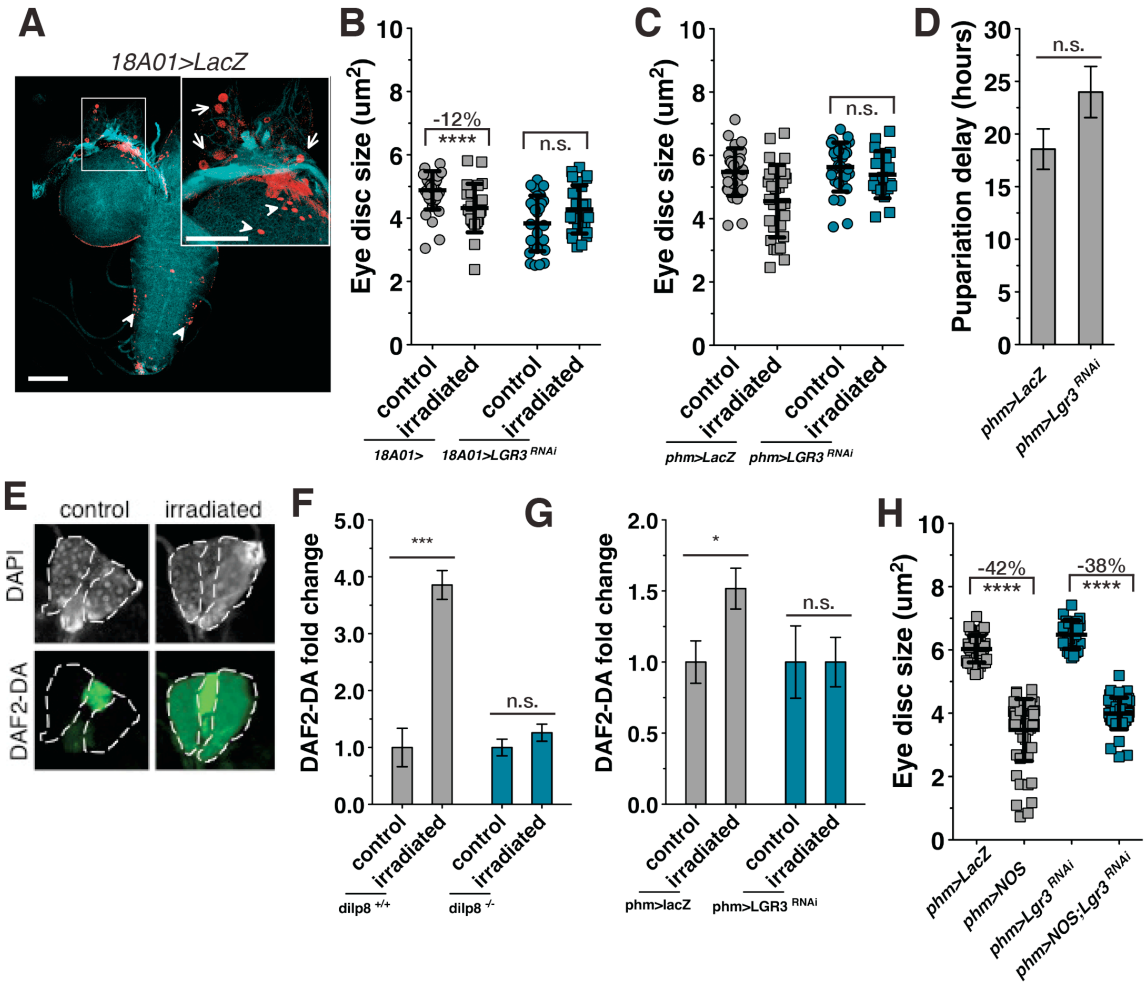


Figure 4-5: Lgr3 in neurons regulates imaginal disc growth and ecdysone signaling during larval development.

(A) Lgr3 in neurons regulates imaginal disc growth. Expression of Lgr3-RNAi with a neuronal driver (*elav>Lgr3-RNAi*, BL8760) increases imaginal disc growth. (B) Expression of Lgr3-RNAi in neurons does not significantly change the length of larval development. (C) Expression of Lgr3-RNAi in neurons causes less synchronized pupariation timing. Time to pupation is only slightly delayed (<10 hr). (D) Lgr3 in neurons regulates ecdysone signaling. The ecdysone target gene *E75* is transcriptionally active at least 12hrs earlier in *elav>Lgr3-RNAi* larvae (104hrs), compared with controls, and is significantly increased later in development (116hrs). Fold change relative to *elav>LacZ* at 92hrs measured by semi-quantitative PCR. Growth: mean +/- SD. Time: mean of duplicate or triplicate experiments +/- SEM. * p<0.05, ** p<0.01, ****p<0.001 calculated by two-tailed Student's t-test.

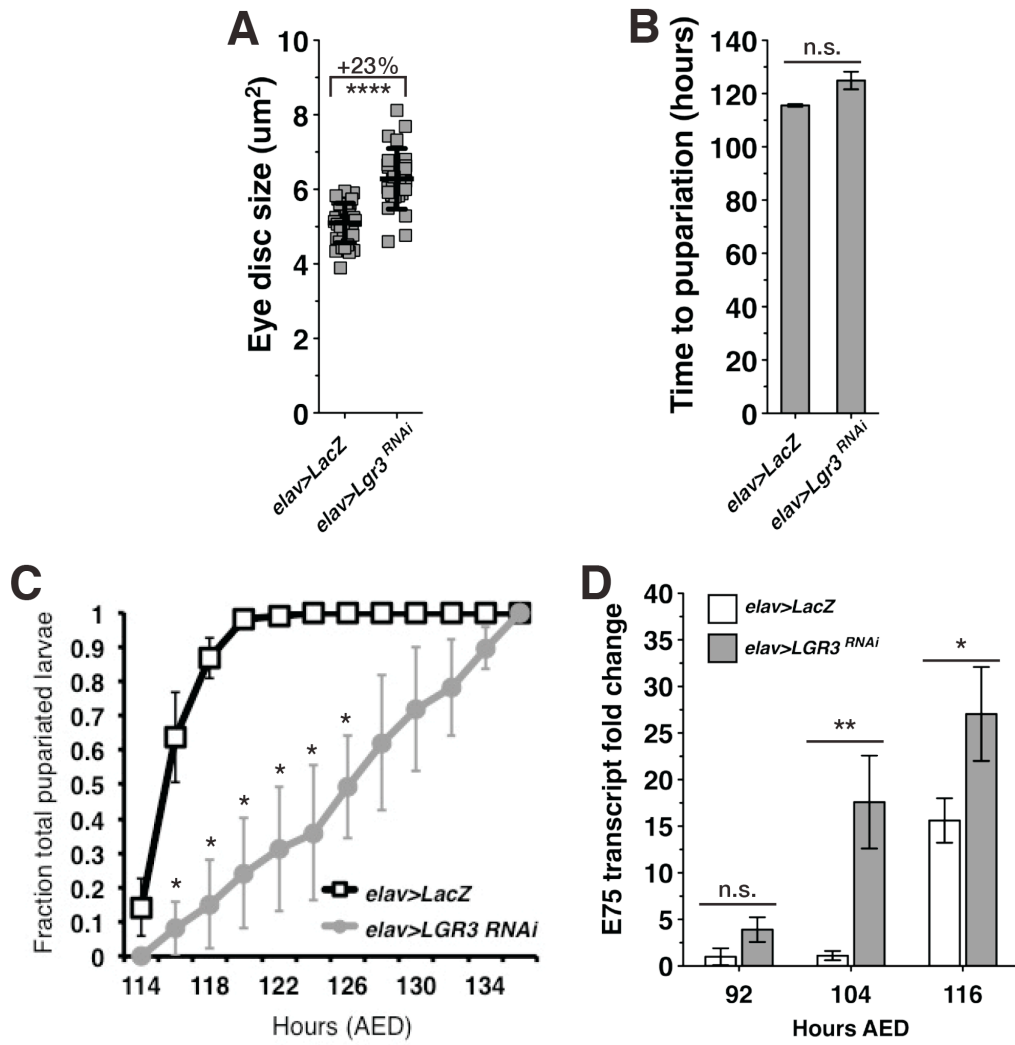


Figure 4-6: Lgr3 depletion systemically increases imaginal disc growth. (A) Systemic expression of Lgr3-RNAi (*tub>Lgr3^{RNAi}*) increases imaginal disc growth. (B) Expression of Lgr3-RNAi in the PG (*phm>Lgr3^{RNAi}*) increases imaginal disc growth. Mean +/- SD. ****p<0.001 calculated by two-tailed Student's t-test.

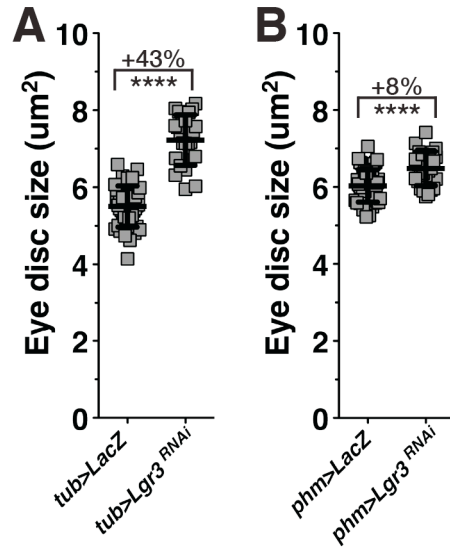


Figure 4-7: Lgr3 in neurons regulates developmental delay and growth coordination during the regeneration checkpoint.

(A) Lgr3 in neurons regulates developmental delay. Expression of Lgr3-RNAi in neurons (*elav>Lgr3-RNAi*) largely abrogates developmental delay induced by irradiation. (B) Lgr3 in neurons regulates growth coordination. Targeted irradiation of larvae expressing Lgr3-RNAi in neurons (*elav>Lgr3-RNAi*) increases imaginal disc growth in contrast to the growth inhibition in the control (*elav>LacZ*). (C) Lgr3 mediates growth coordination and developmental delay during the regeneration checkpoint through distinct tissues. Lgr3 in the PG regulates growth coordination, but not delay, through activation of NOS, which reduces ecdysone production. Lgr3 in the neurons has a constitutive role in regulating imaginal disc growth and ecdysone signaling during development. It is possible that depletion of Lgr3 in neurons may increase imaginal tissue growth through increased ecdysone signaling, or via an ecdysone-independent mechanism. Lgr3 in neurons is also necessary for damage-induced growth coordination and developmental delay. Growth: mean +/- SD. Time: mean of duplicate or triplicate experiments +/- SEM. ** p<0.01, ****p<0.001 calculated by two-tailed Student's t-test.

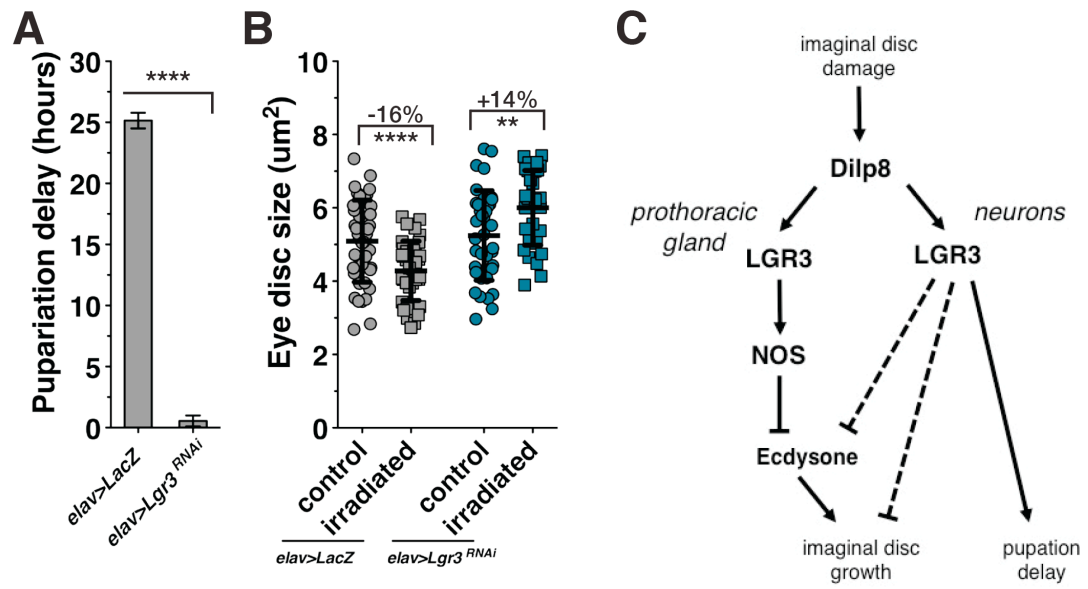
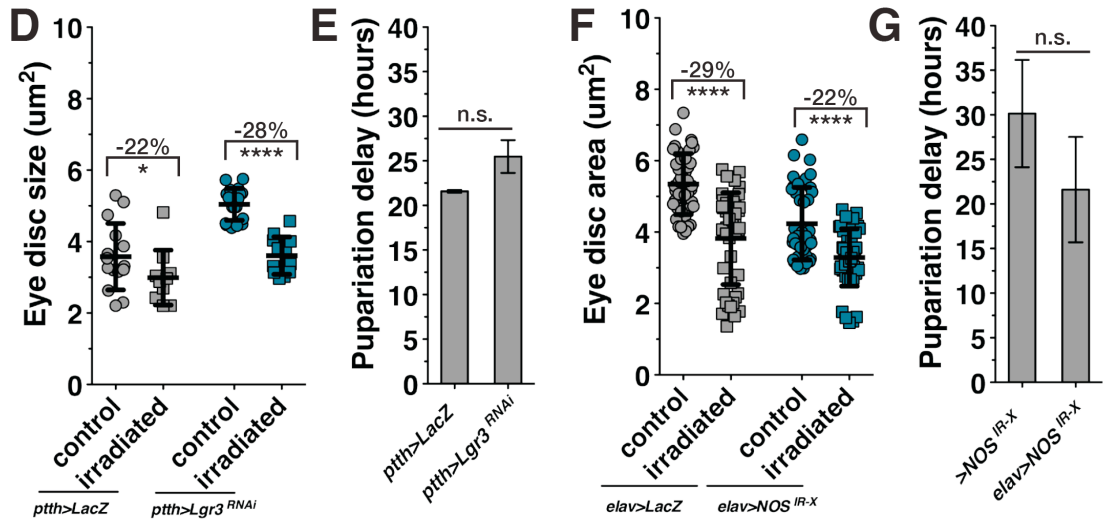
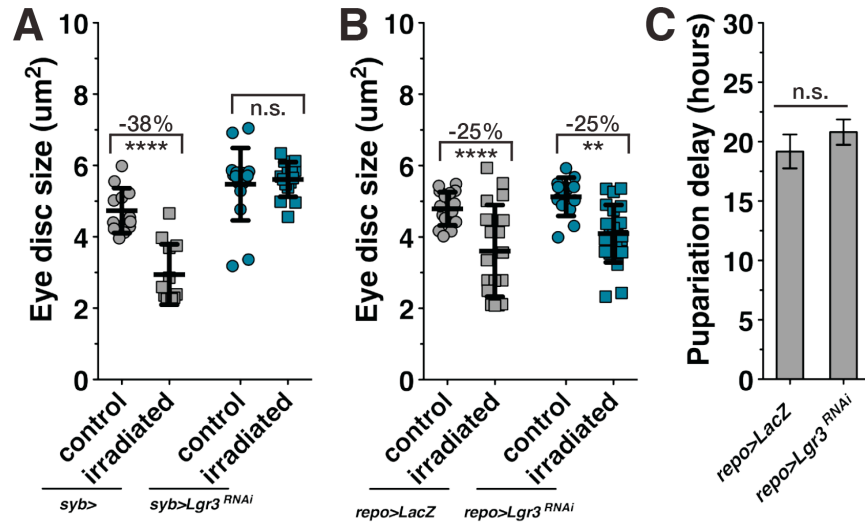


Figure 4-8: Lgr3 in neurons indirectly regulates PTTH signaling through a NOS-independent mechanism.

(A) Expression of Lgr3-RNAi with a neuronal-specific driver BL51635 (*syb>Lgr3-RNAi*) rescues growth inhibition induced by targeted irradiation. (B and C) Lgr3 does not function in glia to regulate growth coordination or developmental delay. Expression of Lgr3-RNAi with a glial-specific driver (*repo>Lgr3-RNAi*) does not rescue growth inhibition induced by targeted irradiation or developmental delay. (D and E) Lgr3 does not function in the PTTH neurons to regulate growth coordination or developmental delay. Expression of Lgr3-RNAi (TRiP JF03217) in the PTTH neurons (*ptth>Lgr3-RNAi*) does not rescue growth inhibition induced by targeted irradiation or developmental delay. (F and G) NOS is not required in the neurons to regulate growth coordination or developmental delay. Expression of NOS-RNAi in neurons does not rescue growth inhibition induced by targeted irradiation or developmental delay. Growth: mean +/- SD. Time: mean of duplicate or triplicate experiments +/- SEM. * p<0.05, ** p<0.01, ****p<0.001 calculated by two-tailed Student's t-test.



Appendices 2

Figure A2-1. Symmetry assay of adult wings.

Symmetry of adult wings was calculated as percent difference from the mean of the left and right wing for each individual *Drosophila*. Using this measurement, the two wings shown in Garelli et al. 2012 have a 19% difference. In this graph, w^{1118} has a mean difference of 1.27% and *dilp8^{-/-}* has a mean difference of 1.46%. These populations are not significantly different by the student's t-test, even when the two w^{1118} outliers are excluded. Larvae were staged and raised at 25°C on standard cornmeal-molasses food.

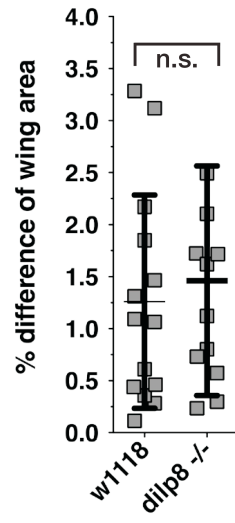


Figure A2-2. Lgr3-RNAi does not significantly change growth of the larval tissues.

- (A) Expression of Lgr-RNAi systemically. Larval area measured at 80hr AED.
- (B) Expression of Lgr-RNAi systemically. Larval area measured at 104hr AED.
- (C) Expression of Lgr-RNAi systemically. Pupal size measured before eclosion.
- (D) Expression of Lgr3-RNAi in neurons. Larval area measured at 104hr AED.
- (E) Expression of Lgr3-RNAi in the PG. Larval area measured at 104hr AED.

** $p < 0.01$, *** $p < 0.005$, **** $p < 0.001$ calculated by two-tailed Student's t-test.

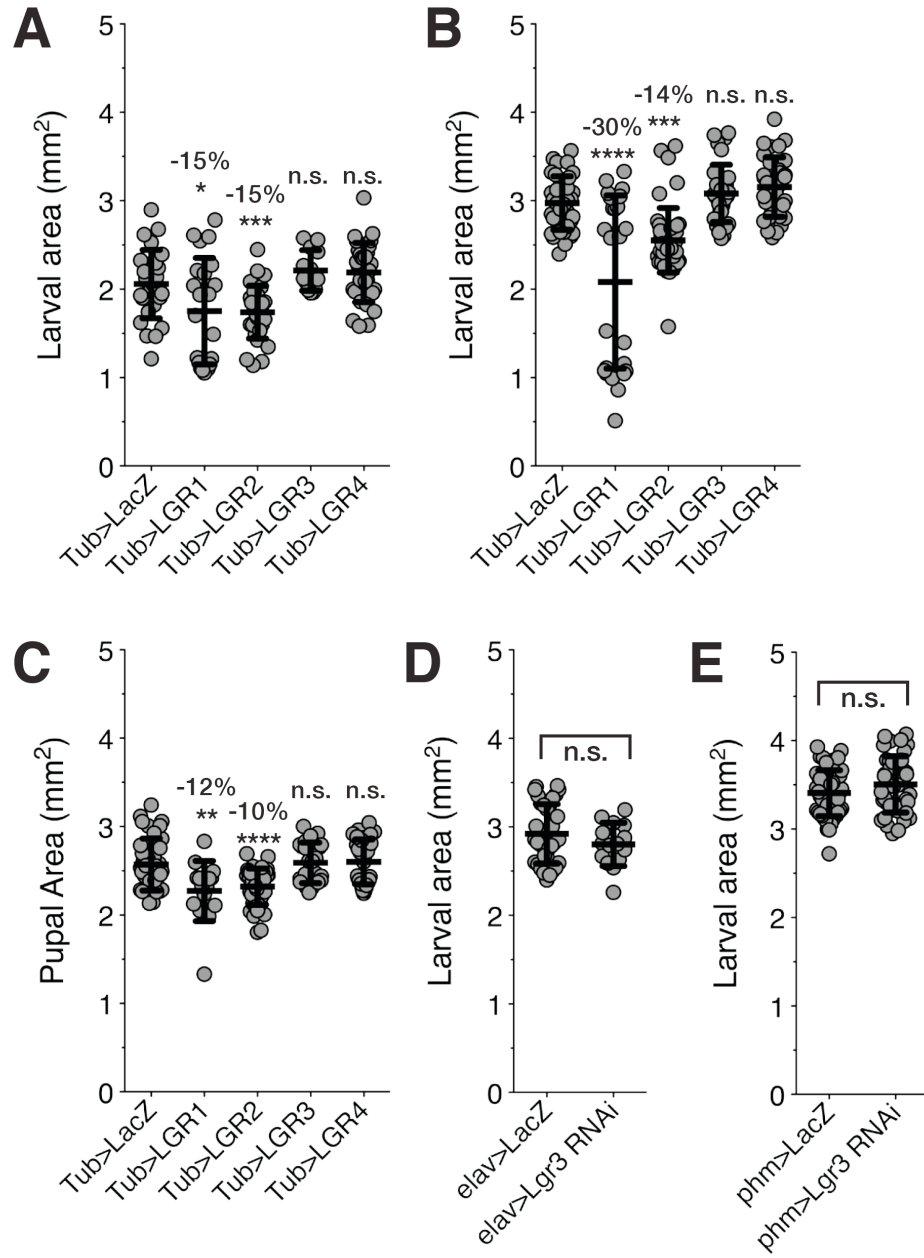
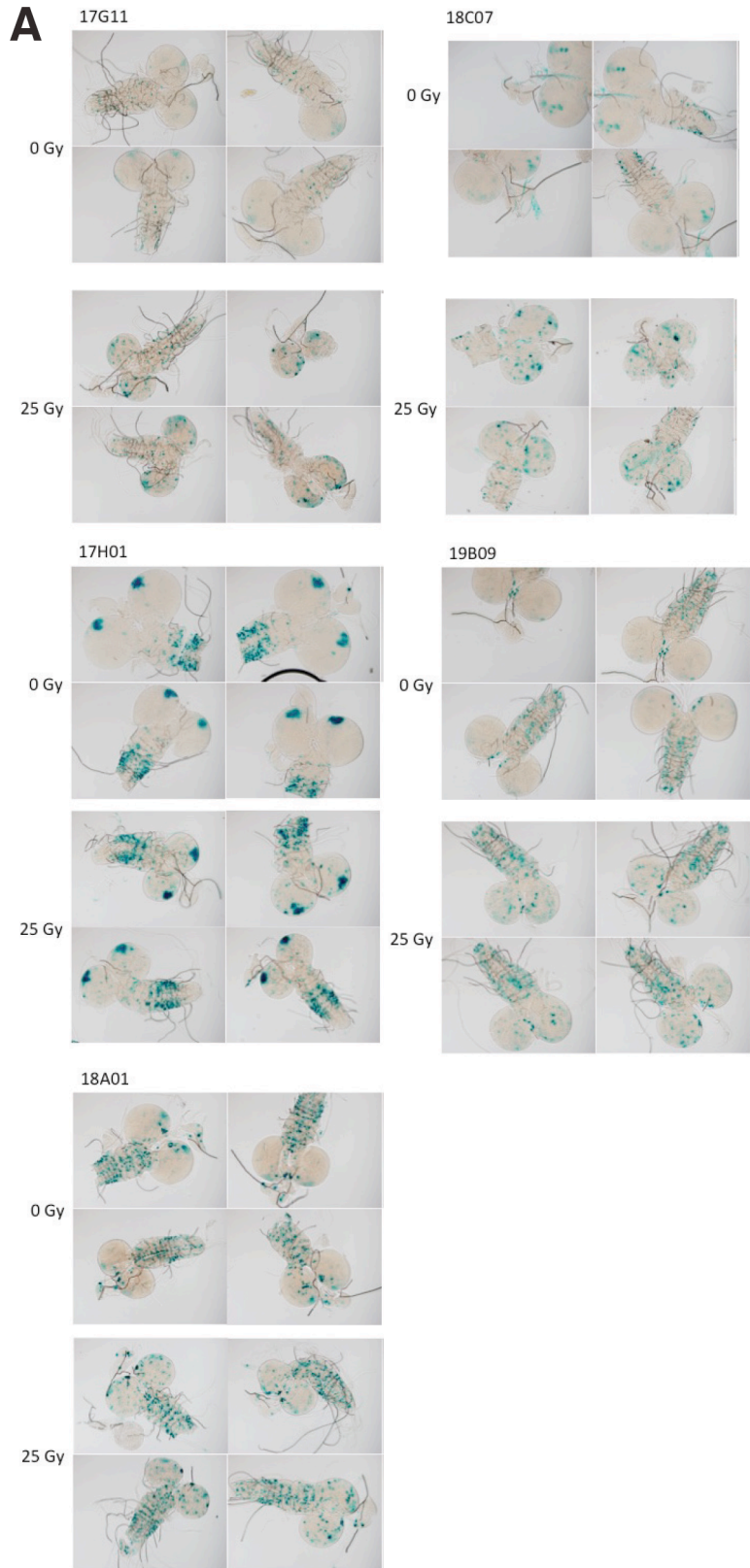
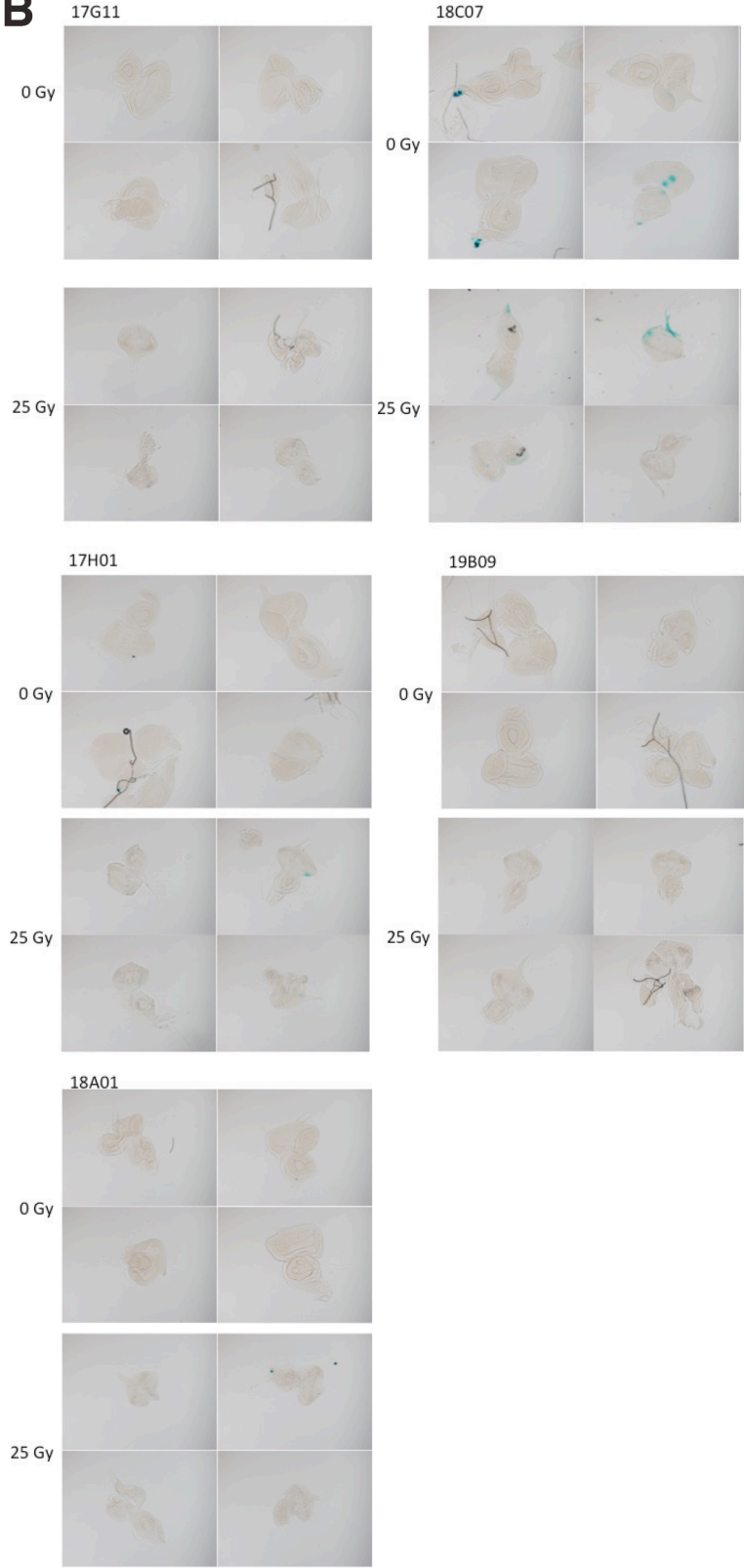


Figure A2-3. Lgr3 enhancer fragment expression increase in the CNS after irradiation.

Staged larvae with Lgr3 enhancer Gal4 lines expressing LacZ (see also Figure 4-3) were irradiated at 80hrs with 25 Gy (not shielded) and dissected at 104hrs. Expression patterns were measured by X-gal staining with an overnight 4°C incubation. (A) Irradiation increases expression in the CNS, but not the PG. (B) Irradiation does not change expression in eye imaginal discs. (C) Irradiation does not change expression in wing imaginal discs.



B



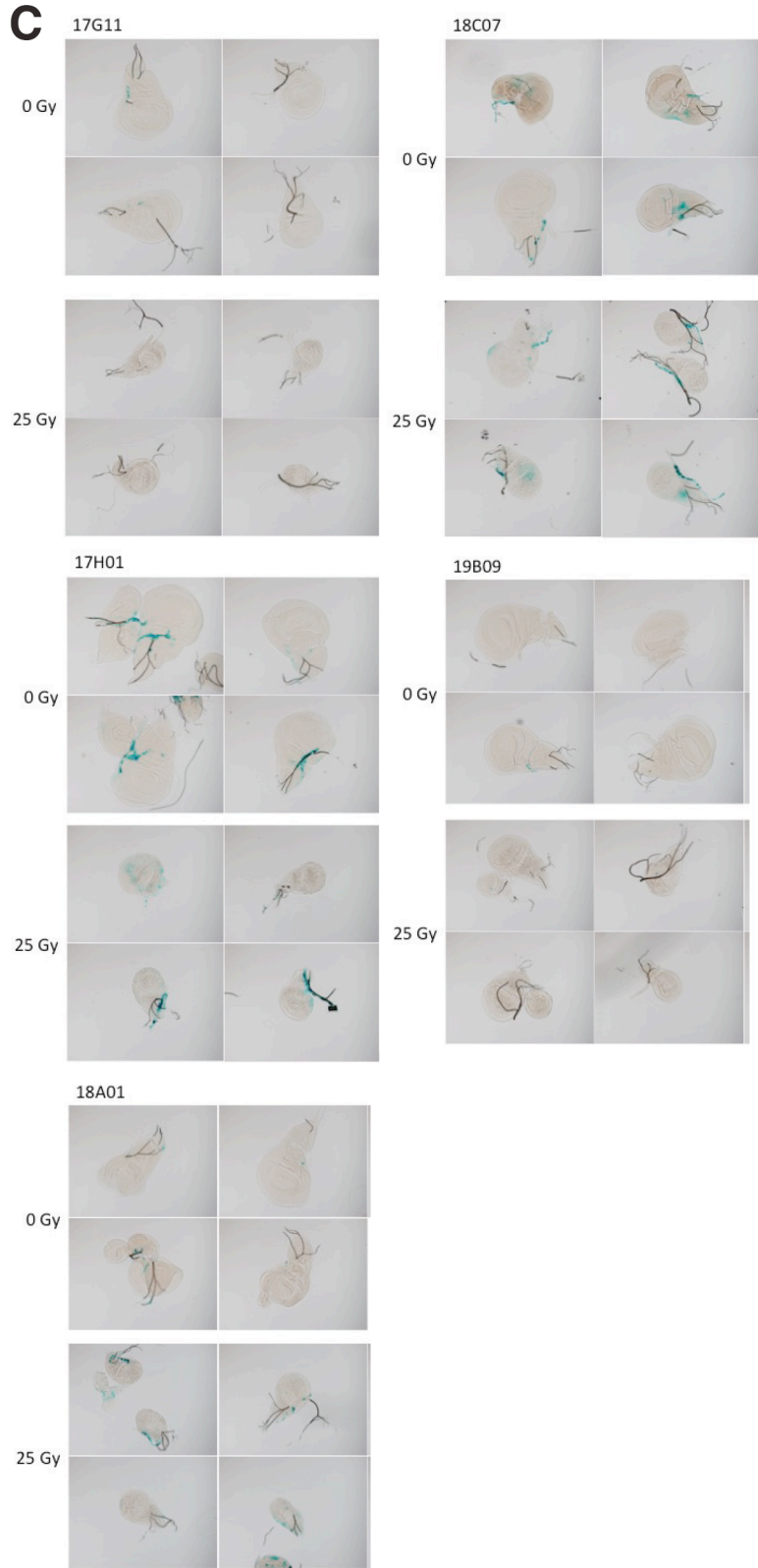


Figure A2-4. Expression of Lgr3-RNAi with the enhancer line 18A01 increases imaginal disc growth.

Expression of Lgr3-RNAi in the PG and CNS with 18A01-Gal4 (*18A01>Lgr3-RNAi*) increases growth imaginal disc growth in the absence of damage.

**** $p < 0.001$ calculated by two-tailed Student's t-test.

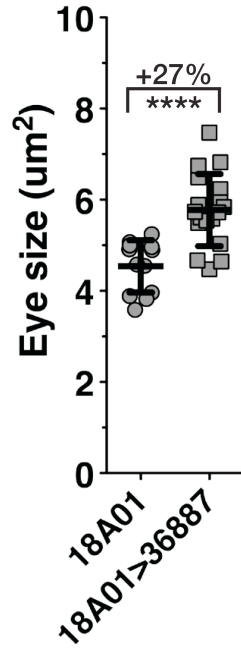


Figure A2-5. Expression of Gaq-RNAi in the PG does not rescue growth restriction after targeted irradiation.

Expression of the Gaq -RNAi, a target of GCPR signaling, in the PG (*phm>Gaq - RNAi*) does not rescue growth restriction. Larvae were damaged by targeted irradiation at 80hrs AED and size of the undamaged eye imaginal discs was measured at 104hrs AED. **** $p < 0.001$ calculated by two-tailed Student's t-test.

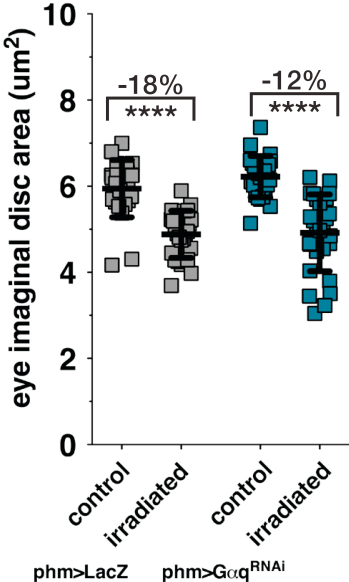


Figure A2-6. Irradiation increases calcium basal calcium levels and inhibits calcium pulsing and propagation.

Larvae expressing the calcium sensor GCaMP in the PG (*phm>GCaMP*) were irradiated at 80hrs AED with 25 Gy (not shielded) and imaged at 93hrs AED. Live larvae were immobilized under a coverslip and imaged for 5-10min. Control larvae (0 Gy) had dynamic pulses of signal that typically began in one cell and spread to adjacent cells before diminishing. This pulsing and propagation of signal looks reminiscent of gap-junction mediated cell-cell signaling. Each lobe of the PG typically pulsed independently. The irradiated larvae (25 Gy) had less pulsing cells, and when they did pulse, typically did propagate to neighboring cells (see frame 30 in 25 Gy). In contrast to the control, the irradiated larvae had a higher constant level of signal throughout imaging. This is reminiscent of increased level of calcium regulating closer of gap junctions (Orellana et al. 2012). Time stamps are in seconds.

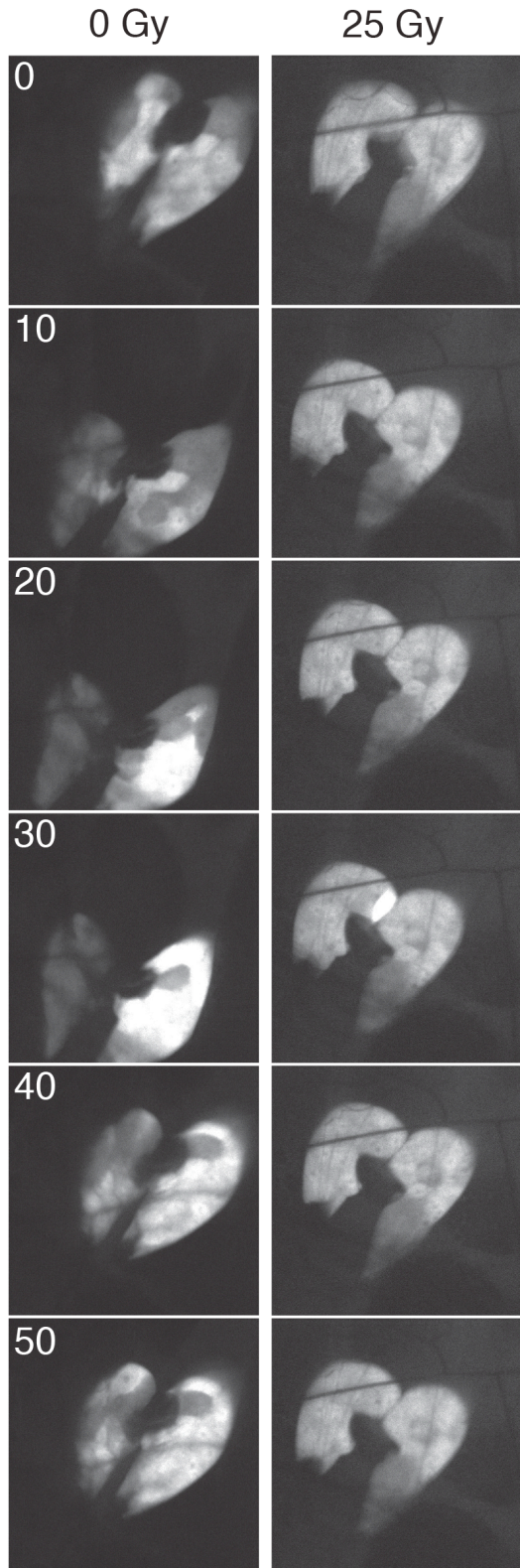


Figure A2-7. Expression of Lgr3-RNAi in neurons misregulates sgs3 expression.

Expression of *salavary-glad-secretion 3 (sgs3)* measured by semi-quantitative PCR in larvae expression Lgr3-RNAi in neurons (*elav>Lgr3-RNAi*). Larvae were harvested at 92, 104, and 116hrs AED. Lgr3-RNAi in the neurons increases *sgs3* expression more at 92hrs AED and decreases expression at 116hrs compared to control larvae (*elav>LacZ*). *Sgs3* is transcriptionally activated near the middle of the 3rd instar when regenerative capacity becomes restricted (Hackney, Zolali-Meybodi, and Cherbas 2012). These data further support the model that Lgr3 in neurons regulates ecdysone signaling. * $p < 0.05$ calculated by two-tailed Student's t-test.

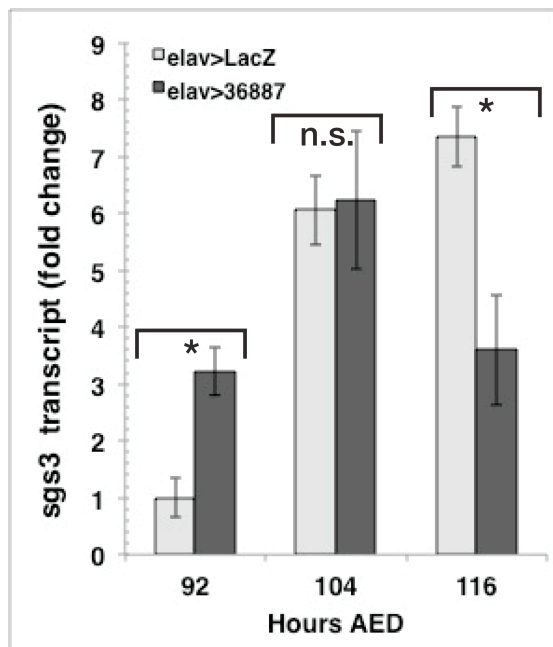


Figure A2-8. Lgr3-RNAi with *Dilp8* overexpression in neurons does not rescue growth but does rescue delay.

(A) Co-expression of Lgr3-RNAi with *Dilp8* in neurons (*elav>dilp8;LGR3-RNAi*) does not fully rescue imaginal disc growth restriction. Eye imaginal discs measured at 104hrs AED. (B) Co-expression of Lgr3-RNAi with *dilp8* in neurons completely rescues developmental delay. These data suggest that Dilp8 induced delay is solely regulated by Lgr3 in the neurons. However, *dilp8* induced growth restriction by expression in neurons is not solely regulated in the neurons. This may suggest that Dilp8 may be secreted by neurons, which is then restricting growth through signaling in the PG. ** $p < 0.01$, *** $p < 0.005$, **** $p < 0.001$ calculated by two-tailed Student's t-test.

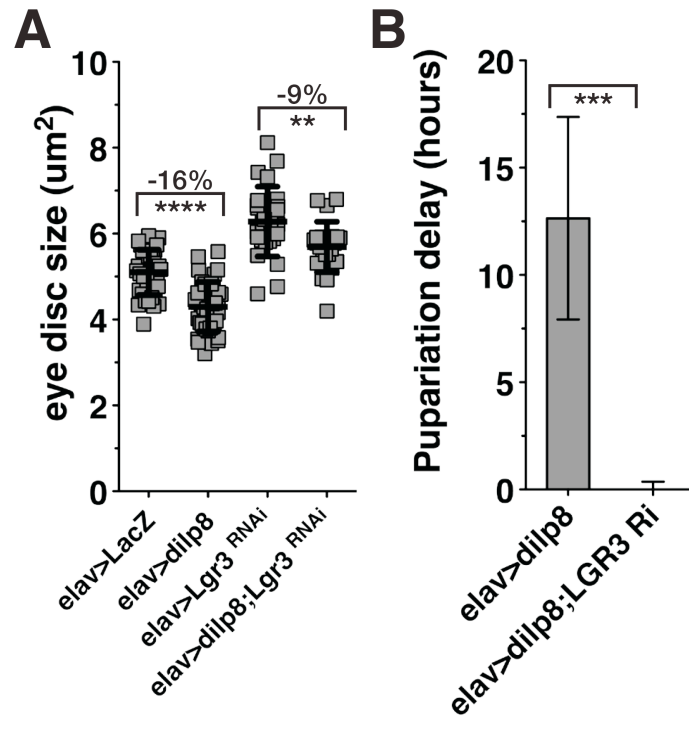


Figure A2-9. Lgr3-RNAi expression in neurons increases pupal death after development irradiation.

Larvae were irradiated at 80hrs AED with 17.5 Gy. Stage of death was measured as assay for defects in regenerative ability. Percent death in the larval stage was calculated from the total number of larvae irradiated of each genotype. n:

elav>LavZ = 30, *elav>Lgr3-RNAi* = 14, *phm* = 25, *phm>Lgr3-RNAi* = 23. Percent death at pupal stage was calculated from total number pupae that did not eclose into adults. Percent death at pre-pharate stage was calculated from total number of dead pupae that did not complete head-eversion or develop bristles. Percent death at pharate stage was calculated from total number of dead pupae that completed head-inversion or develop bristles.

stage of death:

	larva	pupae	pre-pharate	pharate
elav>LacZ	3%	17%	3%	14%
elav>Lgr3 RNAi	0%	43%	14%	29%
phm	0%	20%	0%	20%
phm>Lgr3 RNAi	0%	30%	4%	26%

Chapter 5

Discussion

5.1 Summary

The experiments in this dissertation were designed to examine the mechanisms of inter-organ communication that maintain allometry by coordinating developmental growth. Through the use of genetic and molecular approaches, I have defined a pathway by which distinct organs coordinate their growth during imaginal disc regeneration in *Drosophila melanogaster* larvae.

Damage to developing imaginal discs activates a regeneration checkpoint that 1) delays developmental progression and 2) reduces the growth rate of undamaged imaginal discs to coordinate regeneration with developmental growth. Developmental delay and growth coordination are both mediated by secretion of *Drosophila* insulin-like peptide 8 (Dilp8) from regenerating imaginal discs. I have demonstrated that growth coordination following imaginal disc damage is achieved through Dilp8 activation of nitric oxide synthase (NOS) in the prothoracic gland (PG), an endocrine organ in *Drosophila* larvae. Production of nitric oxide (NO) during the larval growth period inhibits growth by reducing synthesis of the steroid hormone ecdysone. Dilp8 regulation of ecdysone through NOS activity in the PG represents a novel pathway for growth coordination. Additionally, I have also demonstrated that NOS is not necessary for developmental delay. This provides the first evidence for a mechanistic

distinction between growth regulation and developmental delay during the regeneration checkpoint.

Taking a candidate-based approach I identified Lgr3, a relaxin receptor homologue and leucine-rich repeat-containing GPCR, as a putative receptor for Dilp8. I have shown that Lgr3 regulates growth coordination via multiple, tissue-specific mechanisms. Lgr3 in the PG mediates Dilp8 activation of NOS. Lgr3 in neurons regulates growth through a NOS-independent pathway. Furthermore, Lgr3 in neurons is necessary for the inducing developmental delay, while Lgr3 in the PG is not.

Together, this work has revealed some of the mechanisms by which the growth of individual tissues is coordinated. The regulation of steroid and peptide hormone signaling in this coordination mechanism is similar to the hypothalamic-pituitary-adrenal (HPA) axis of mammals, suggesting that regenerating organs function in an organ-endocrine axis to regulate developmental allometry. Further questions arise from this model of growth coordination. Of primary importance is how Lgr3 in the neurons regulates developmental time and growth; additionally, what is the intersection of the neural pathway with the Lgr3-NOS pathway in the PG? Also important is determining the pathway for Lgr3-NOS regulation of ecdysone biosynthesis. This chapter discusses several of these questions and how they might be addressed experimentally.

5.1.1 Is this model applicable outside the context of *Drosophila* regeneration?

While this work only addresses growth coordination during regeneration of imaginal discs in *Drosophila* larvae, a similar organ-endocrine axis may also function during homeostatic development across species.

A role for Lgr in growth coordination may also be conserved in mammals. The formation of morphological variation through sexual selection has been well studied in populations of wild Soay sheep. Recently, a polymorphism at Lgr8/RXFP2 (the mammalian homologue of the *Drosophila* Lgr3) in a population of Soay sheep has been demonstrated to be an important genetic determinant of horn size allometry and survival (Johnston et al. 2013). While Dilp8 may not be structurally conserved beyond dipterans (Garelli et al. 2012), the role for Lgr in regulation of allometry suggests that the genetic networks that regulate allometry may be conserved.

The Dilp8-Lgr3 pathway of inter-organ coordination may also regulate growth in the absence of damage. *Drosophila* mutant for Dilp8 (*dilp8* *-/-*) have increased variability of wing sizes across a population. This wing size variation is also seen between wings of the same animal, which are more asymmetric in the *dilp8* *-/-* than in controls (Garelli et al. 2012). Additionally, *Lgr3* *-/-* *Drosophila* also have the same population and individual asymmetry phenotypes (Garelli et al. 2015). This suggests that Dilp8 and Lgr3 coordinate growth and maintain bilateral symmetry during development in the absence of damage.

NOS regulation of ecdysone in the PG may also be involved in regulation of bilateral symmetry. However, could not to test this hypothesis, since I was unable to recapitulate the *dilp8* *-/-* phenotypes (A2-1). This is possibly due to a difference in culture conditions between labs, as differences in temperature or nutrients can change the severity of growth phenotypes (Mirth, Truman, and Riddiford 2005). Testing different culture conditions, such as higher temperature or richer media, may increase the severity of asymmetry in the *dilp8* *-/-*. If expression of NOS-RNAi in the PG has the same asymmetry phenotypes, this would suggest that coordination of symmetry is also regulated through the same pathway as the regeneration checkpoint.

5.1.2 What is the mechanism of NOS regulation of ecdysone biosynthesis?

In chapter 3, I found that NOS activity in the PG regulates ecdysone biosynthesis through transcriptional repression of Halloween genes. NO interacts reversibly with heme proteins through the iron moieties, and this interaction has been found to regulate the activity of nuclear hormone receptors (NHRs) (Minamiyama et al. 1997). Additionally, NO has been shown to react irreversibly with cytochrome P450 (CYP) enzymes (Minamiyama et al. 1997), inhibiting their enzymatic activity and shutting down the rate limiting steps of steroidogenesis (Drewett et al. 2002). Regulation of CYP enzymatic activity could be a direct mechanism by which NO inhibits ecdysone biosynthesis during regeneration. Ecdysone production is

regulated by positive feedback from Halloween gene transcription (Moeller et al. 2013). NO inhibition of CYPs may directly reduce ecdysone biosynthesis, thus inhibiting the positive feedback regulation that increases Halloween gene transcription. This activity may also explain the why *NOS* overexpression activates a developmental delay (Fig. 3-3). The sustained expression of *NOS* activity may inactivate CYPs at a rate that is higher than CYP synthesis itself.

The effect of *NOS* on this feedback regulation could be further tested by epistasis experiments. I have demonstrated that *NOS* overexpression inhibits Halloween gene transcription and ecdysone biosynthesis (Fig. 3-8). Examining at what point in the feedback pathway *NOS* regulates ecdysone production could be done by 1) testing whether overexpression of Halloween genes during *NOS* overexpression is able to rescue ecdysone production or 2) testing whether increased ecdysone titer is able to rescue the inhibition of Halloween gene transcription during *NOS* overexpression.

The combined results from these experiments would narrow down multiple models. One outcome where increased ecdysone levels do rescue Halloween gene expression, but overexpression of Halloween genes is not able to rescue ecdysone production, would suggest that *NOS* directly regulates CYP activity. Another outcome where Halloween gene expression does rescue ecdysone production, and increased ecdysone does not rescue Halloween gene expression, would suggest that *NOS* transcriptionally regulates Halloween genes

downstream of ecdysone. The other outcomes are that neither or both experiments can rescue gene expression or ecdysone. This result would suggest that NOS does not regulate the ecdysone feedback pathway, but instead regulates ecdysone production by another mechanism.

Through regulation of heme, NO also regulates the activity of the NHR E75 (Cáceres et al. 2011; D. M. Johnston et al. 2011). The isoform *E75B* is expressed only late in larval development, during the larval to pupal transition (Andres et al. 1993). *E75B* expression is suppressed during the regeneration checkpoint (Fig 3-9A). Isoform *E75A* is expressed earlier in larval development and is involved in early gene regulation that promotes ecdysone biosynthesis (Andres et al. 1993; Bialecki et al. 2002). Therefore, *E75A* may regulate growth coordination by functioning as a target of NOS. Experiments to test the role of *E75A* in growth coordination would include expressing RNAi specific for the *E75A* isoform in PG during *NOS* overexpression and targeted irradiation. *NOS* overexpression and irradiation damage during late larval development both are no longer able to delay development (Fig. 3-9, Halme 2010). If expression of *E75A*-RNAi in the PG rescues the inhibition of growth, this may suggest a mechanism that controls the temporal window when the regeneration checkpoint can be activated.

Forkhead box Class O (FoxO) is another candidate target of NO signaling. FoxO activity in the PG regulates ecdysone production (Koyama et al. 2014), and

FoxO has been found to be a target of NOS and soluble guanylate cyclase (sGC) signaling in neurodegenerative diseases (Kanao et al. 2012). To test whether FoxO is necessary for NOS-mediated growth coordination, I used an RNAi to deplete FoxO during targeted irradiation and *NOS* overexpression. In this preliminary data, I found that expression of FoxO-RNAi in the PG does not rescue growth coordination, nor does it block the ability of NOS to inhibit growth (A1-5B). However, I did find growth restriction induced by targeted damage (*Bx>eiger*) was significantly reduced in larvae mutant for FoxO (A1-5C). Together, these results suggest that FoxO may function in the undamaged imaginal discs to mediate growth restriction. Expressing FoxO-RNAi in the undamaged imaginal discs during targeted irradiation could test whether FoxO is necessary organ autonomously for growth restriction. Relative FoxO expression between different imaginal discs regulates how organs respond to restrictions in IIS (Tang et al. 2011). If FoxO-RNAi expressed in undamaged imaginal discs rescues growth restriction this would suggest a role for FoxO in regulating imaginal disc sensitivity to ecdysone.

Another mechanism of signaling by NO is through s-nitrosylation of glutathione, which creates the secondary messenger s-nitrosoglutathione (GSNO). In *Drosophila*, GSNO has been shown to activate nuclear translocation of transcription factors (Dijkers and O'Farrell 2009). Reduction of GSNO by glutathione-dependent formaldehyde dehydrogenase (Fdh) inhibits GSNO

signaling. Overexpression of *Fdh* in the PG during targeted irradiation could be used to test whether s-nitrosylation of glutathione is necessary for regulation of growth coordination and ecdysone biosynthesis regulation. Overexpression of *Fdh* will reduce GSNO activity. If GSNO is necessary for mediating NO signaling in the PG, then expression of *Fdh* would rescue growth coordination and ecdysone restriction. GSNO can regulate a number of pathways including cAMP, cGMP, and calcium. Experiments that examine the role of these pathways are discussed below.

5.1.3 What is the signaling pathway of Lgr3-NOS production?

In chapter 4, I found that the leucine-rich GPCR Lgr3 regulates Dilp8-mediated growth coordination and NO activity in the PG. GPCRs activate heterotrimeric G-protein complexes to regulate intercellular signaling. The main effector of these complexes is through the action of the $G\alpha$ subunits, of which *Drosophila* have six (Strathmann and Simon 1990; Katanayeva et al. 2010). $G\alpha$ subunits regulate multiple pathways including cyclic adenosine 3', 5'-monophosphate (cAMP), cyclic guanosine 3', 5'-monophosphate (cGMP), ion channels, and calcium channels (Strathmann and Simon 1990; Caers et al. 2012).

Signaling through $G\alpha$ subunits may mediate Lgr3 activation of NOS. Expression of RNAi lines against each $G\alpha$ subunit during targeted irradiation would test if they mediate growth coordination or NO production. Preliminary

experiments suggest that $G\alpha_q$ is not necessary for growth coordination during regeneration (A2-5). $G\alpha_s$ is another candidate due to its known function in regulating cAMP and calcium channels.

To identify the role of cAMP or cGMP in mediating Lgr3 regulation of ecdysone biosynthesis during regeneration, a pharmacological organ culture approach might be used to modify signaling in the PG. Dissected PGs can be cultured for several days (Colombani, Andersen, and Leopold 2012) and Halloween gene transcription can be measured by qRT-PCR or immunohistochemistry. This assay could be used to test the ability of cGMP or cAMP inhibitors to rescue inhibition of Halloween gene transcription after irradiation. Pharmacological enhancers could also be used to confirm the ability of cGMP or cAMP signaling to inhibit Halloween gene transcription.

To identify the mechanism by which Lgr3 increases NO production in the PG, the organ culture assay could be combined with the DAF2-DA fluorescent reporter assay (used in Fig 3-3, 3-5, and 4-4) to test the role of cAMP, cGMP, and calcium in activating NOS.

NOS activity is regulated by calcium. Preliminary imaging experiments suggest that irradiation increases basal calcium activity in the PG while suppressing calcium pulsing (A2-6). These observations can be further tested by the use of mutant alleles and RNAi expression to determine whether the calcium activity induced by irradiation is dependent on Dilp8, Lgr3, or $G\alpha$ subunits.

Injection experiments might also be used to test the sufficiency of synthetic Dilp8 to increase calcium signaling in cultured PGs. Additionally, hemolymph from irradiated larvae could be added to unirradiated PG cultures to test whether Dilp8 in the hemolymph is sufficient to regulate calcium signaling in the PG. GSNO also activates calcium signaling through the cGMP pathway. *Fdh* overexpression, which inhibits GSNO, could be used to test whether GSNO in the PG is necessary for calcium signaling in the PG after irradiation. Together, these experiments will begin to elucidate the signaling pathways by which Lgr3 regulates NOS activity in PG.

5.1.4 What is the mechanism of neuronal Lgr3 regulation of growth?

In chapter 4, I found that Lgr3 in neurons functions as a suppressor of imaginal disc growth. I also found that expressing Lgr3-RNAi in neurons rescues growth coordination during regeneration. This raises the question of how Lgr3 is necessary for regulation of growth coordination in both the PG and the neurons (Fig 4-4 and 4-7). Lgr3 has been observed to have high constitutive activity in the absence of any known ligand in comparison with Lgr1 or Lgr4 (Van Hiel et al. 2015), suggesting that Lgr3 in the neurons may regulate development independent of Dilp8. One possible mechanism is through regulation of the regeneration checkpoint, the developmental window when the regeneration can occur (Halme, Cheng, and Hariharan 2010). This model is supported by the

result that *Lgr3*-RNAi expression in neurons completely blocks the ability of larvae to delay during regeneration (Fig. 4-7A). Another model is that *Lgr3* negatively regulates DILP production in the IPCs, and that loss of this regulation increases ecdysone production and growth. However, this model does not fully explain why *Dilp8*-activation of NOS in the PG does not still reduce growth during regeneration. Therefore, *Lgr3* in the neurons may also regulate the ability of the PG to respond to the *Dilp8*-regenerative signal.

The competency for regeneration in *Drosophila* is lost as the animals near the end of the third instar of larval development. Consistent with these observations, preliminary data suggests that expression of *Lgr3*-RNAi in neurons increases the percentage of larvae that die at the pupal stage after treatment with irradiation, even in comparison to larvae that express *Lgr3*-RNAi in the PG (A2-9). This result suggests that the loss of *Lgr3* in neurons decreased regenerative capacity. Measuring regeneration defects in adult eyes and wings or measuring cell proliferation and death in imaginal discs after irradiation will further test whether *Lgr3*-RNAi in neurons changes the regenerative ability.

Ecdysone regulates the restriction of the regeneration checkpoint (Halme, Cheng, and Hariharan 2010). Consistent with this, I found that larvae expressing *Lgr3*-RNAi in neurons activate transcription of *E75* earlier than the control (Fig 4-5D). These preliminary results suggest that neuronal *Lgr3* regulates the timing of ecdysone signaling.

These experiments suggest a model in which neuronal *Lgr3* regulates the time of regenerative capacity. Loss of *Lgr3* in neurons prevents developmental delay (Fig. 4-7A) and may advance the period of development when the regeneration checkpoint can no longer restrict growth. This period of development is similar to the restriction point at which *NOS* misexpression no longer delays development or inhibits imaginal disc growth (Fig 3-8 and 9). This suggests that neuronal *Lgr3* may also regulate the ability of *NOS* to restrict growth. Overexpressing *NOS* in the PG while overexpressing *Lgr3*-RNAi in the neurons could test this model. If *NOS* is unable to restrict imaginal disc growth when *Lgr3*-RNAi is expressed in neurons, this would suggest that *Lgr3* in neurons may regulate the pathways in the PG that restrict *NOS* signaling.

One such pathway is the *E75* signaling pathway. *E75* is transcribed at the end of larval development, coinciding with the time in development when *NOS* no longer inhibits ecdysone signaling (Fig 3-8 and 3-9C,D). This period of development is similar to the restriction point at which regeneration no longer delays development (Halme, Cheng, and Hariharan 2010). Since *Lgr3* in the neurons regulates *E75* expression (Fig 4-5D) and *E75* activity regulates the effect of NO on ecdysone production (Cáceres et al. 2011; D. M. Johnston et al. 2011), this model also suggests that *Lgr3* may regulate the regeneration checkpoint by suppressing *E75*. Overexpressing *NOS* while overexpressing *E75* can test this role for *E75* regulation. If *NOS* is no longer able to restrict growth

when *E75* is expressed this would suggest that *Lgr3* in the neurons regulates the regeneration checkpoint capacity to restrict growth through regulation of *E75* expression.

5.1.5 How does regenerative growth continue during ecdysone restriction?

In chapter 3, I examined the pathway of ecdysone regulation that inhibits growth of undamaged imaginal discs during regeneration. Restriction of undamaged growth also occurs within a regenerating organ. When damage is induced by a clone of dying cells in an imaginal disc, the damage is regenerated by the neighboring cells while cell division distal from the damage is inhibited (Repiso, Bergantiños, and Serras 2013). These observations raise the question of how regenerative growth is permitted to continue while other cells and tissues are restricted. The growth of regenerating tissues may be regulated through ecdysone signaling. Experiments described here suggest that systemic *dilp8* expression increases the sensitivity of the imaginal discs and the larval tissues to ecdysone (Figure 3-10B and 11C). These observations suggest that *Dilp8* may function to regulate the growth of regenerating tissues by increasing their sensitivity to ecdysone.

Dilp8 and ecdysone may regulate tissue autonomous growth through the Hippo pathway. The nuclear scaffolding protein *Aac11* was recently shown to bind *Taiman*, a co-activator of ecdysone receptor (*EcR*), and promote imaginal

disc growth. Taiman can promote activation of Yorkie-target genes, while Aac11 is necessary for Yorkie-induced overgrowth, suggesting that ecdysone signaling may regulate the Hippo pathway (presented at the *Drosophila* Research Conference, Kenneth Moberg 2014, Zhang et al. 2015). Intriguingly, *taiman* has previously been found to regulate regenerative growth. *Taiman* is transcriptionally activated in damaged imaginal discs (Russell, Ostafichuk, and Scanga 1998). Also, *taiman* mutant clones are lost from regenerating mosaic tissues and reduce the regenerative capacity of the wildtype clones (Halme, unpublished data). Additionally, *yorkie* overexpression increases *dilp8* transcription by a Taiman and EcR dependent mechanism (Zhang et al. 2015). Whether Yorkie is dependent on Taiman and EcR to promote regenerative remains unknown.

Together, these data suggest a model in which the Hippo pathway and Dilp8 may regulate growth through modulating EcR. The Aac11/Taiman/EcR complex may regulate regenerative growth downstream or in parallel to the Hippo pathway. Making clones of *yorkie* $-/-$ cells and measuring their ability to activate *taiman* transcription in regenerating tissues can test whether Taiman is downstream of the Hippo pathway. Examining whether Dilp8 acts through Taiman and Yorkie to regulate imaginal disc growth can be tested with clones overexpressing *Dilp8*. Whether *Dilp8* overexpressing clones have increased sensitivity to changes in ecdysone and whether this is mediated by *taiman* or *yorkie* will determine if Dilp8 can regulate EcR and Hippo signaling. Testing if

Dilp8 regulates *taiman* can be done with clones overexpressing *Dilp8* and examining *taiman* expression. These experiments will further examine the ability of Dilp8 to regulate growth and possibly demonstrate novel interactions between regenerative, ecdysone, and Hippo signaling.

This model of tissue autonomous growth regulation by Dilp8 suggests that Lgr proteins may also be involved in the local regenerative process. In mammalian stem cell development, Lgr proteins maintain stem cell plasticity and multipotency (Barker, Tan, and Clevers 2013). Interestingly, I found that Lgr1-RNAi and Lgr2-RNAi increased the developmental delay in response to irradiation (Fig 4-2). This increased delay may be due to impaired regenerative ability of imaginal tissues. Therefore, Lgr proteins may also function in regulating the growth of regenerating tissues. To test whether Lgr proteins are autonomously required for regulating regenerative growth, clonal analysis could be used as described above to test: 1) the ability of clones expressing RNAi to regenerate after irradiation; 2) whether these clones are less sensitive to changes in ecdysone; and 3) whether Lgr proteins regulate EcR signaling or the Hippo pathway. A subclass of Lgr proteins are used as markers of stem cells in mammals (Barker, Tan, and Clevers 2013). While stem cells have not been identified in imaginal discs (Sustar et al. 2011) these experiments may reveal how Lgr proteins regulate developmental plasticity and multipotency during regeneration.

5.2 Conclusions

The precise regulation of size and proportion across nature is striking. Regulation of allometry is fundamental to the process of development and the generation of biological diversity. Misregulation of allometry can lead to birth defects and pathologies such as cardiovascular disease. Coordination of growth between organs ensures that all organs develop to the right size in a temporally coordinated manner.

In this work I present a model for growth coordination during regeneration in *Drosophila* larva. NOS in the PG and Lgr3 in the PG/neurons function as regulators of growth coordination by interpreting the damage signal Dilp8 from regenerating imaginal discs and reducing biosynthesis of the steroid hormone ecdysone to slow the growth rate of undamaged tissues. Lgr3 in the neurons also functions to coordinate regenerative growth with developmental time. Additionally, Dilp8 and Lgr3 regulation of bilateral symmetry also suggests that this pathway functions to coordinate growth in the absence of damage. This coordination mechanism is analogous to the HPA axis in mammals, suggesting that imaginal discs function in an organ-endocrine axis to regulate developmental allometry.

The delay of development during regeneration is similar to developmental delays seen during chronic inflammation. Significant delays in puberty and inhibition of growth are seen in pre-adolescent patients with chronic inflammatory diseases, such as rheumatoid arthritis or Crohn's disease. Therapies that treat the systemic effects of these pathologies will only be developed through a deeper understanding of the underlying networks that coordinate development.

The evidence that these mechanisms may be conserved across species suggests that these genes and networks may be part of an evolutionary substrate by which allometric diversity is generated. In this way, inter-organ growth coordination contributes to animals being the right size.

Literature Cited

- Alderton, WK, Cooper, CE, and Knowles, RG. 2001. "Nitric Oxide Synthases : Structure, Function and Inhibition." *Biochem J* 357: 593–615.
- Andres, AJ, and Cherbas, P. 1992. "Tissue-Specific Ecdysone Responses: Regulation of the Drosophila Genes Eip28/29 and Eip40 during Larval Development." *Development* 116 (4): 865–76.
- Andres, AJ, Fletcher, JC, Karim, FD, and Thummel, CS. 1993. "Molecular Analysis of the Initiation of Insect Metamorphosis: A Comparative Study of Drosophila Ecdysteroid-Regulated Transcription." *Developmental Biology*.
- Barker, N, Tan, S, and Clevers, H. 2013. "Lgr Proteins in Epithelial Stem Cell Biology." *Development* 140 (12): 2484–94.
- Bathgate, RAD, Halls, ML, van der Westhuizen, ET, Callander, GE, Kocan, M, and Summers, RJ. 2013. "Relaxin Family Peptides and Their Receptors." *Physiological Reviews* 93 (1): 405–80.
- Bauer, PM, Buga, GM, and Ignarro, LJ. 2001. "Role of p42/p44 Mitogen-Activated-Protein Kinase and p21waf1/cip1 in the Regulation of Vascular Smooth Muscle Cell Proliferation by Nitric Oxide." *Proc Natl Acad Sci* 98 (22): 12802–7.
- Bialecki, M, Shilton, A, Fichtenberg, C, Segraves, WA, and Thummel, CS. 2002. "Loss of the Ecdysteroid-Inducible E75A Orphan Nuclear Receptor Uncouples Molting from Metamorphosis in Drosophila." *Developmental Cell* 3 (2): 209–20.
- Bos, M, Burnet, B, Farrow, R, and Woods, RA. 1976. "Development of Drosophila on Sterol Mutants of the Yeast *Saccharomyces Cerevisiae*." *Genet. Res. Comb.* 28: 163–97.
- Boulan, L, Martín, D, and Milán, M. 2013. "Bantam miRNA Promotes Systemic Growth by Connecting Insulin Signaling and Ecdysone Production." *Current Biology* 23 (6): 473–78.
- Brennan, CA, Ashburner, M, and Moses, K. 1998. "Ecdysone Pathway Is Required for Furrow Progression in the Developing Drosophila Eye." *Development* 125 (14): 2653–64.

- Bryant, PJ. 1971. "Regeneration and Duplication Following Operations in Situ on the Imaginal Discs of *Drosophila Melanogaster*." *Developmental Biology* 26 (4): 637–51.
- Bryant, PJ. 1975. "Pattern Formation in the Imaginal Wing Disc of *Drosophila Melanogaster*: Fate Map, Regeneration and Duplication." *J Exp Zool* 193 (1): 49–77.
- Burris, TP. 2008. "Nuclear Hormone Receptors for Heme: REV-ERBalpha and REV-ERBbeta Are Ligand-Regulated Components of the Mammalian Clock." *Molecular Endocrinology* 22 (7): 1509–20.
- Cáceres, L, Necakov, AS, Schwartz, C, Kimber, S, Roberts, IJH, and Krause, HM. 2011. "Nitric Oxide Coordinates Metabolism, Growth, and Development via the Nuclear Receptor E75." *Genes & Development* 25 (14): 1476–85.
- Caers, J, Verlinden, H, Zels, S, Vandersmissen, HP, Vuerinckx, K, and Schoofs, L. 2012. "More than Two Decades of Research on Insect Neuropeptide GPCRs: An Overview." *Frontiers in Endocrinology* 3: 1–30.
- Callier, V, and Nijhout, HF. 2013. "Body Size Determination in Insects: A Review and Synthesis of Size- and Brain-Dependent and Independent Mechanisms." *Biological Reviews* 88 (4): 944–54.
- Champlin, DT, and Truman, JW. 1998. "Ecdysteroids Govern Two Phases of Eye Development during Metamorphosis of the Moth, *Manduca Sexta*." *Development* 125 (11): 2009–18.
- Chávez, VM, Marqués, G, Delbecque, JP, Kobayashi, K, Hollingsworth, M, Burr, J, Natzle, JE, and O'Connor, MB. 2000. "The *Drosophila* Disembodied Gene Controls Late Embryonic Morphogenesis and Codes for a Cytochrome P450 Enzyme That Regulates Embryonic Ecdysone Levels." *Development* 127 (19): 4115–26.
- Chawla, A, Repa, JJ, Evans, RM, and Mangelsdorf, DJ. 2001. "Nuclear Receptors and Lipid Physiology: Opening the X-Files." *Science* 294 (5548): 1866–70.
- Colombani, J, Andersen, DS, and Leopold, P. 2012. "Secreted Peptide Dilp8 Coordinates *Drosophila* Tissue Growth with Developmental Timing." *Science* 336 (6081): 582–85.

- Colombani, J, Bianchini, L, Layalle, S, Pondeville, E, Dauphin-Villemant, C, Antoniewski, C, Carré, C, Noselli, S, and Léopold, P. 2005. "Antagonistic Actions of Ecdysone and Insulins Determine Final Size in *Drosophila*." *Science* 310 (5748): 667–70.
- Conlon, I, and Raff, M. 1999. "Size Control in Animal Development Review." *Cell* 96: 235–44.
- Delanoue, R, Slaidina, M, and Léopold, P. 2010. "The Steroid Hormone Ecdysone Controls Systemic Growth by Repressing dMyc function." Delanoue, Rénaud, Maija Slaidina, and Pierre Léopold. 2010. 'The Steroid Hormone Ecdysone Controls Systemic Growth by Repressing dMyc Function in *Drosophila* Fat Cells.' *Developmental Cell* 18 (6): 1012–21.
- Derbyshire, ER, and Marletta, MA. 2012. "Structure and Regulation of Soluble Guanylate Cyclase." *Annual Review of Biochemistry* 81 (1): 533–59.
- Dewes, E. 1975. "Entwicklungsleistungen Implantierter Ganzer Und Halbierter Männlicher Genitalimaginalscheiben von *Ephesia kuehniella* Z. Und Entwicklungsdauer Der Wirtstiere." *Wilhelm Roux Arch Entwickl Mech Org* 178: 167–83.
- DiGregorio, PJ, Ubersax, JA, and O'Farrell, PH. 2001. "Hypoxia and Nitric Oxide Induce a Rapid, Reversible Cell Cycle Arrest of the *Drosophila* Syncytial Divisions." *J Biol Chem* 276 (3): 1930–37.
- Dijkers, PF, and O'Farrell, PH. 2009. "Dissection of a Hypoxia-Induced, Nitric Oxide-Mediated Signaling Cascade." *Molecular Biology of the Cell* 20 (18): 4083–90.
- Drewett, JG, Adams-Hays, RL, Ho, BY, and Hegge, DJ. 2002. "Nitric Oxide Potently Inhibits the Rate-Limiting Enzymatic Step in Steroidogenesis." *Molecular and Cellular Endocrinology* 194 (1-2): 39–50.
- Edgar, BA. 2006. "How Flies Get Their Size: Genetics Meets Physiology." *Nat Rev Genet* 7 (12): 907–16.
- Elphick, MR. 1997. "Localization of Nitric Oxide Synthase Using NADPH Diaphorase Histochemistry." *Methods Mol Biol* 72: 153–58.
- Emlen, DJ, Warren, IA, Johns, A, Dworkin, I, and Lavine, LC. 2012. "A Mechanism of Extreme Growth and Reliable Signaling in Sexually Selected Ornaments and Weapons." *Science* 337 (6096): 860–64.

- Estrada, C, Gómez, C, Martín-Nieto, J, De Frutos, T, Jiménez, A, and Villalobo, A. 1997. "Nitric Oxide Reversibly Inhibits the Epidermal Growth Factor Receptor Tyrosine Kinase." *The Biochemical Journal* 326: 369–76.
- Francis, GA, Fayard, E, Picard, F, and Auwerx, J. 2003. "Nuclear Receptors and the Control of Metabolism." *Annual Review of Physiology* 65: 261–311.
- Garelli, A, Gontijo, AM, Miguela, V, Caparros, E, and Dominguez, M. 2012. "Imaginal Discs Secrete Insulin-Like Peptide 8 to Mediate Plasticity of Growth and Maturation." *Science* 336 (6081): 579–82.
- Garelli, A, Heredia, F, Casimiro, AP, Macedo, A, Nunes, C, Koyama, T, and Gontijo, AM. 2015. "Dilp8 Requires the Neuronal Relaxin Receptor Lgr3 to Couple Growth to Developmental Timing."
- Garg, UC, and Hassid, A. 1989. "Nitric Oxide-Generating Vasodilators and 8-Bromo-Cyclic Guanosine Monophosphate Inhibit Mitogenesis and Proliferation of Cultured Rat Vascular Smooth Muscle Cells." *Journal of Clinical Investigation* 83 (5): 1774–77.
- Géminard, C, Arquier, N, Layalle, S, Bourouis, M, Slaidina, M, Delanoue, R, Bjordal, M, et al. 2006. "Control of Metabolism and Growth through Insulin-like Peptides in *Drosophila*." *Diabetes* 55 (SUPPL. 2): 5–8.
- Gibbs, SM, and Truman, JW. 1998. "Nitric Oxide and Cyclic GMP Regulate Retinal Patterning in the Optic Lobe of *Drosophila*." *Neuron* 20 (1): 83–93.
- Gilbert, LI, and Rewitz, KF. 2009. "The Function and Evolution of the Halloween Genes: The Pathway to the Arthropod Molting Hormone." *Evolution*, 231–69.
- Grönke, S, Clarke, DF, Broughton, S, Andrews, TD, Partridge, L. 2010. "Molecular evolution and functional characterization of *Drosophila* insulin-like peptides". *PLOS Genetics*. 6(2).
- Gu, M, and Brecher, P. 2000. "Nitric Oxide-Induced Increase in p21^{Sdi1/Cip1/Waf1} Expression During the Cell Cycle in Aortic Adventitial Fibroblasts." *Arteriosclerosis, Thrombosis, and Vascular Biology* 20 (1): 27–34.
- Hackney, JF, Zolali-Meybodi, O, and Cherbas, P. 2012. "Tissue Damage Disrupts Developmental Progression and Ecdysteroid Biosynthesis in *Drosophila*." *PLoS ONE* 7 (11).

- Halme, A, Cheng, M, and Hariharan, IK. 2010. "Retinoids Regulate a Developmental Checkpoint for Tissue Regeneration in *Drosophila*." *Current Biology* 20 (5). Elsevier Ltd: 458–63.
- Hartenstein, V. 2006. "The Neuroendocrine System of Invertebrates: A Developmental and Evolutionary Perspective." *Journal of Endocrinology* 190 (3): 555–70.
- Hill, JA, and Olson, EN. 2008. "Cardiac Plasticity." *The New England Journal of Medicine* 358 (13): 1370–80.
- Hodgetts, RB. 1977. "Ecdysone Titrers during Postembryonic *Melanogaster* Development of *Drosophila*." *Genetics* 317: 310–17.
- Hölldobler, B, and Wilson, EO. 1990. *The Ants*. Harvard University Press.
- Irvine, KD, and Harvey, KF. 2015. "Control of Organ Growth by Patterning and Hippo Signaling in *Drosophila*." *Cold Spring Harbor Perspectives Biol* 7: 1–16.
- Jaszczak, JS, Wolpe, JB, Dao, AQ, and Halme, A. 2015. "Nitric Oxide Synthase Regulates Growth Coordination During *Drosophila* *Melanogaster* Imaginal Disc Regeneration." *Genetics* early onli (June 16th).
- Jindra, M, Palli, SR, and Riddiford, LM. 2011. "The Juvenile Hormone Signaling Pathway in Insect Development." *Annual Review of Entomology* 58 (1): 181–204.
- Johnston, DM, Sedkov, Y, Petruk, S, Riley, KM, Fujioka, M, Jaynes, JB, and Mazo, A. 2011. "Ecdysone- and NO-Mediated Gene Regulation by Competing EcR/Usp and E75A Nuclear Receptors during *Drosophila* Development." *Molecular Cell* 44 (1). Elsevier Inc. 51–61.
- Johnston, SE, Gratten, J, Berenos, C, Pilkington, JG, Clutton-Brock, TH, Pemberton, JM, and Slate, J. 2013. "Life History Trade-Offs at a Single Locus Maintain Sexually Selected Genetic Variation." *Nature* 502 (7469). Nature Publishing Group: 93–95.
- Kanao, T, Sawada, T, Davies, SA, Ichinose, H, Hasegawa, K, Takahashi, R, Hattori, N, and Imai, Y. 2012. "The Nitric Oxide-Cyclic GMP Pathway Regulates FoxO and Alters Dopaminergic Neuron Survival in *Drosophila*." *PLoS ONE* 7 (2): 1–13.

- Karim, FD, and Thummel, CS. 1992. "Temporal Coordination of Regulatory Gene Expression by the Steroid Hormone Ecdysone." *The EMBO Journal* 11 (11): 4083–93.
- Katanayeva, N, Kopein, D, Portmann, R, Hess, D, and Katanaev, VL. 2010. "Competing Activities of Heterotrimeric G Proteins in Drosophila Wing Maturation." *PLoS ONE* 5 (8).
- Kawahara, K, Gotoh, T, Oyadomari, S, Kuniyasu, A, Kohsaka, S, Mori, M, and Nakayama, H. 2001. "Nitric Oxide Inhibits the Proliferation of Murine Microglial MG5 Cells by a Mechanism Involving p21 but Independent of p53 and Cyclic Guanosine Monophosphate." *Neuroscience Letters* 310 (2-3): 89–92.
- Koyama, T, Rodrigues, M a, Athanasiadis, A, Shingleton, AW, and Mirth, CK. 2014. "Nutritional Control of Body Size through FoxO-Ultraspiracle Mediated Ecdysone Biosynthesis." *eLife* 3: 1–20.
- Kuzin, B, Roberts, I, Peunova, N, and Enikolopov, G. 1996. "Nitric Oxide Regulates Cell Proliferation during Drosophila Development." *Cell* 87 (4): 639–49.
- Lacin, H, Rusch, J, Yeh, RT, Fujioka, M, Wilson, BA, Zhu, Y, Robie, AA, et al. 2014. "Genome-Wide Identification of Drosophila Hb9 Targets Reveals a Pivotal Role in Directing the Transcriptome within Eight Neuronal Lineages, Including Activation of Nitric Oxide Synthase and Fd59a/Fox-D." *Developmental Biology* 388 (1): 117–33.
- Liu, X, Miller, MJS, Joshi, MS, Sadowska-Krowicka, H, Clark, D a, and Lancaster, JR. 1998. "Diffusion-Limited Reaction of Nitric Oxide with Erythrocytes vs Free Hemoglobin." *Faseb Journal* 12 (4): A82–A82.
- Livak, KJ, and Schmittgen, TD. 2001. "Analysis of Relative Gene Expression Data Using Real-Time Quantitative PCR and the 2(-Delta Delta C(T)) Method." *Methods* 25 (4): 402–8.
- Lorenz, M, Hewing, B, Hui, J, Zepp, A, Baumann, G, Bindereif, A, Stangl, V, and Stangl, K. 2007. "Alternative Splicing in Intron 13 of the Human eNOS Gene: A Potential Mechanism for Regulating eNOS Activity." *FASEB J* 21 (7): 1556–64.
- Lozinsky, O V, Lushchak, O V, Kryshchuk, NI, Shchypanska, NY, Riabkina, AH, Skarbek, S V, Maksymiv, I V, Storey, JM, Storey, KB, and Lushchak, VI.

2013. "S-Nitrosoglutathione-Induced Toxicity in *Drosophila Melanogaster*: Delayed Pupation and Induced Mild Oxidative/nitrosative Stress in Eclosed Flies." *Comparative Biochemistry and Physiology - A Molecular and Integrative Physiology* 164 (1). Elsevier B.V. 162–70.
- Lozinsky, O V, Lushchak, O V, Storey, JM, Storey, KB, and Lushchak, VI. 2012. "Sodium Nitroprusside Toxicity in *Drosophila Melanogaster*: Delayed Pupation, Reduced Adult Emergence, and Induced Oxidative/nitrosative Stress in Eclosed Flies." *Archives of Insect Biochemistry and Physiology* 80 (3): 166–85.
- Lu, H, and Bilder, D. 2005. "Endocytic Control of Epithelial Polarity and Proliferation in *Drosophila*." *Nature Cell Biology* 7 (12): 1232–39.
- Madhavan, K, and Schneiderman, H. 1969. "Hormonal Control of Imaginal Disc Regeneration in *Galleria Mellonella* (Lepidoptera)." *Biol. Bull.* 137: 321–31.
- Martín, FA, and Morata, G. 2006. "Compartments and the Control of Growth in the *Drosophila* Wing Imaginal Disc." *Development* 133 (22): 4421–26.
- Marvin, KA, Reinking, JL, Lee, AJ, Pardee, K, Krause, HM, and Burstyn, JN. 2009. "Nuclear Receptors Homo Sapiens Rev-Erb-Beta and *Drosophila Melanogaster* E75 Are Thiolate-Ligated Heme Proteins Which Undergo Redox-Mediated Ligand Switching and Bind CO and NO." *Biochemistry* 48 (29): 7056–71.
- McBrayer, Z, Ono, H, Shimell, M, Parvy, JP, Beckstead, RB, Warren, JT, Thummel, CS, Dauphin-Villemant, C, Gilbert, LI, and O'Connor, MB. 2007. "Prothoracicotropic Hormone Regulates Developmental Timing and Body Size in *Drosophila*." *Developmental Cell* 13 (6): 857–71.
- Metcalf, D. 1964. "Restricted Growth Capacity of Multiple Spleen Grafts." *Transplantation* 2 (3): 387–92.
- Minamiyama, Y, Takemura, S, Imaoka, S, Funae, Y, Tanimoto, Y, and Inoue, M. 1997. "Irreversible Inhibition of Cytochrome P450 by Nitric Oxide." *J Pharmacol Exp Ther* 283 (3): 1479–85.
- Mirth, C, Truman, JW, and Riddiford, LM. 2005. "The Role of the Prothoracic Gland in Determining Critical Weight for Metamorphosis in *Drosophila Melanogaster*." *Current Biology* 15 (20): 1796–1807.

- Mirth, CK, and Shingleton, AW. 2012. "Integrating Body and Organ Size in *Drosophila*: Recent Advances and Outstanding Problems." *Frontiers in Endocrinology* 3 (APR): 1–13.
- Mirth, CK, Tang, HY, Makohon-Moore, SC, Salhadar, S, Gokhale, RH, Warner, RD, Koyama, T, Riddiford, LM, and Shingleton, AW. 2014. "Juvenile Hormone Regulates Body Size and Perturbs Insulin Signaling in *Drosophila*." *Proc Natl Acad Sci U S A* 111 (19): 7018–23.
- Moeller, ME, Danielsen, ET, Herder, R, O'Connor, MB, and Rewitz, KF. 2013. "Dynamic Feedback Circuits Function as a Switch for Shaping a Maturation-Inducing Steroid Pulse in *Drosophila*." *Development* 140 (23): 4730–39.
- Moen, RA, Pastor, J, and Cohen, Y. 1999. "Antler Growth and Extinction of Irish Elk." *Evolutionary Ecology Research* 1 (2): 235–49.
- Nässel, DR, Liu, Y, and Luo, J. 2015. "Insulin/IGF Signaling and Its Regulation in *Drosophila*." *General and Comparative Endocrinology*. Elsevier Inc.
- Nathan, C, and Xie, Q. 1994. "Nitric Oxide Synthases: Roles, Tolls, and Controls." *Cell* 78: 915–18.
- Nijhout, FH, and Grunert, LW. 2010. "The Cellular and Physiological Mechanism of Wing-Body Scaling in *Manduca sexta*." *Science* 330 (6011): 1693–95.
- Nijhout, HF. 2003. "The Control of Body Size in Insects." *Developmental Biology* 261 (1): 1–9.
- Nijhout, HF, and Emlen, DJ. 1998. "Competition among Body Parts in the Development and Evolution of Insect Morphology." *Proc Natl Acad Sci U S A* 95 (7): 3685–89.
- Nijhout, HF, Smith, WA, Schachar, I, Subramanian, S, Tobler, A, and Grunert, LW. 2007. "The Control of Growth and Differentiation of the Wing Imaginal Disks of *Manduca sexta*." *Developmental Biology* 302 (2): 569–76.
- Oldham, S, Montagne, J, Radimerski, T, Thomas, G, and Hafen, E. 2000. "Genetic and Biochemical Characterization of dTOR, the *Drosophila* Homolog of the Target of Rapamycin." *Genes & Development* 14 (21): 2689–94.
- Oliveira, MM, Shingleton, AW, and Mirth, CK. 2014. "Coordination of Wing and Whole-Body Development at Developmental Milestones Ensures

- Robustness against Environmental and Physiological Perturbations.” *PLoS Genetics* 10 (6).
- Orellana, JA, Sánchez, HA, Schalper, KA, Figueroa, V, and Sáez, JC. 2012. “Regulation of Intercellular Calcium Signaling Through Calcium Interactions with Connexin-Based Channels.” In *Advances in Experimental Medicine and Biology*, 740:777–94.
- Parker, NF, and Shingleton, AW. 2011. “The Coordination of Growth among *Drosophila* Organs in Response to Localized Growth-Perturbation.” *Developmental Biology* 357 (2). Elsevier B.V. 318–25.
- Parkin, CA, and Burnet, B. 1986. “Growth Arrest of *Drosophila Melanogaster* on Erg-2 and Erg-6 Sterol Mutant Strains of *Sacchomyces Cervisiae*.” *J. Insect Physiol.* 5: 463–71.
- Pauli, A, Althoff, F, Oliveira, RA, Heidmann, S, Schuldiner, O, Lehner, CF, Dickson, BJ, and Nasmyth, K. 2008. “Cell-Type-Specific TEV Protease Cleavage Reveals Cohesin Functions in *Drosophila* Neurons.” *Developmental Cell* 14 (2). Elsevier Inc. 239–51.
- Peunova, N, Scheinker, V, Cline, H, and Enikolopov, G. 2001. “Nitric Oxide Is an Essential Negative Regulator of Cell Proliferation in *Xenopus* Brain.” *J Neurosci* 21 (22): 8809–18.
- Pfeiffer, BD, Jenett, A, Hammonds, AS, Ngo, T-TB, Misra, S, Murphy, C, Scully, A, et al. 2008. “Tools for Neuroanatomy and Neurogenetics in *Drosophila*.” *Proc Natl Acad Sci U S A* 105 (28): 9715–20.
- Pollex, RL, and Hegele, RA. 2004. “Hutchinson-Gilford Progeria Syndrome.” *Clinical Genetics* 66 (5): 375–81.
- Poodry, CA, and Woods, DF. 1990. “Control of the Developmental Timer for *Drosophila* Pupariation.” *Roux’s Archives of Developmental Biology* 199 (4): 219–27.
- Porcheron, P, Moriniere, M, Grassi, J, and Pradelles, P. 1989. “Development of an Enzyme Immunoassay for Ecdysteroids Using Acetylcholinesterase as Label.” *Insect Biochemistry* 19 (2): 117–22.
- Postlethwait, JH, and Schneiderman, HA. 1970. “Induction of Metamorphosis by Ecdysone Analogues: *Drosophila* Imaginal Discs Cultured in Vivo.” *The Biological Bulletin* 138 (1): 47–55.

- Rahn, P. 1972. "Untersuchungen Zur Entwicklung von Ganz Und Teilimplantaten Der Flugelimaginalscheibe von *Ephesia Kuhnii* Z." *Wilhelm Roux' Archiv Für Entwicklungsmechanik Der Organismen* 170: 48–82.
- Regulski, M, Stasiv, Y, Tully, T, and Enikolopov, G. 2004. "Essential Function of Nitric Oxide Synthase in *Drosophila*." *Current Biology* 14 (20): R881–R882.
- Regulski, M, and Tully, T. 1995. "Molecular and Biochemical Characterization of dNOS: A *Drosophila* Ca²⁺/calmodulin-Dependent Nitric Oxide Synthase." *Proc Natl Acad Sci U S A* 92 (20): 9072–76.
- Reinking, J, Lam, MMS, Pardee, K, Sampson, HM, Liu, S, Yang, P, Williams, S, et al. 2005. "The *Drosophila* Nuclear Receptor E75 Contains Heme and Is Gas Responsive." *Cell* 122 (2): 195–207.
- Repiso, A, Bergantiños, C, and Serras, F. 2013. "Cell Fate Respecification and Cell Division Orientation Drive Intercalary Regeneration in *Drosophila* Wing Discs." *Development* 140 (17): 3541–51.
- Roof, SR, Biesiadecki, BJ, Davis, JP, Janssen, PML, and Ziolo, MT. 2012. "Effects of Increased Systolic Ca²⁺ and B-Adrenergic Stimulation on Ca²⁺ Transient Decline in NOS1 Knockout Cardiac Myocytes." *Nitric Oxide* 27 (4). Elsevier Inc. 242–47.
- Russell, MA, Ostafichuk, L, and Scanga, S. 1998. "Lethal P-lacZ Insertion Lines Expressed during Pattern Respecification in the Imaginal Discs of *Drosophila*." *Genome* 41 (1): 7–13.
- Schubiger, G. 1971. "Regeneration, Duplication and Transdetermination in Fragments of the Leg Disc of *Drosophila Melanogaster*." *Developmental Biology* 26 (2): 277–95.
- Segraves, WA, and Hogness, DS. 1990. "The E75 Ecdysone-Inducible Gene Responsible for the 75B Early Puff in *Drosophila* Encodes Two New Members of the Steroid Receptor Superfamily." *Genes & Development* 4 (2): 204–19.
- Simmons, LW, and Emlen, DJ. 2006. "Evolutionary Trade-off between Weapons and Testes." *Proc Natl Acad Sci U S A* 103 (44): 16346–51.

- Simpson, P, Berreur, P, and Berreur-Bonnenfant, J. 1980. "The Initiation of Pupariation in *Drosophila*: Dependence on Growth of the Imaginal Discs." *J Embryol Exp Morphol* 57: 155–65.
- Sisk, CL, and Foster, DL. 2004. "The Neural Basis of Puberty and Adolescence." *Nature Neuroscience* 7 (10): 1040–47.
- Smith-Bolton, RK, Worley, MI, Kanda, H, and Hariharan, IK. 2009. "Regenerative Growth in *Drosophila* Imaginal Discs Is Regulated by Wingless and Myc." *Developmental Cell* 16 (6). Elsevier Ltd: 797–809.
- Stasiv, Y, Regulski, M, Kuzin, B, Tully, T, and Enikolopov, G. 2001. "The *Drosophila* Nitric-Oxide Synthase Gene (dNOS) Encodes a Family of Proteins That Can Modulate NOS Activity by Acting as Dominant Negative Regulators." *Journal of Biological Chemistry* 276 (45): 42241–51.
- Stern, DL, and Emlen, DJ. 1999. "The Developmental Basis for Allometry in Insects." *Development* 126 (6): 1091–1101.
- Stieper, BC, Kupershtok, M, Driscoll, M V, and Shingleton, AW. 2008. "Imaginal Discs Regulate Developmental Timing in *Drosophila Melanogaster*." *Developmental Biology* 321 (1): 18–26.
- Straßburger, K, Tiebe, M, Pinna, F, Breuhahn, K, and Teleman, AA. 2012. "Insulin/IGF Signaling Drives Cell Proliferation in Part via Yorkie/YAP." *Developmental Biology* 367 (2). Elsevier: 187–96.
- Strathmann, M, and Simon, MI. 1990. "G Protein Diversity: A Distinct Class of Alpha Subunits Is Present in Vertebrates and Invertebrates." *Proc Natl Acad Sci U S A* 87 (23): 9113–17.
- Sustar, A, Bonvin, M, Schubiger, M, and Schubiger, G. 2011. "*Drosophila* Twin Spot Clones Reveal Cell Division Dynamics in Regenerating Imaginal Discs." *Developmental Biology* 356 (2). Elsevier Inc. 576–87.
- Tang, HY, Smith-Caldas, MSB, Driscoll, M V, Salhadar, S, and Shingleton, AW. 2011. "FOXO Regulates Organ-Specific Phenotypic Plasticity in *Drosophila*." *PLoS Genetics* 7 (11).
- Tennyson, AG, and Lippard, SJ. 2011. "Generation, Translocation, and Action of Nitric Oxide in Living Systems." *Chemistry and Biology* 18 (10). Elsevier Ltd: 1211–20.

- Thomas, DD, Liu, X, Kantrow, SP, and Lancaster, JR. 2001. "The Biological Lifetime of Nitric Oxide: Implications for the Perivascular Dynamics of NO and O₂." *Proc Natl Acad Sci U S A* 98 (1): 355–60.
- Tsutsui, M, Shimokawa, H, Morishita, T, Nakashima, Y, and Yanagihara, N. 2006. "Development of Genetically Engineered Mice Lacking All Three Nitric Oxide Synthases." *J Pharmacol Sci* 102 (2): 147–54.
- Tumaneng, K, Schlegelmilch, K, Russell, RC, Yimlamai, D, Basnet, H, Mahadevan, N, Fitamant, J, Bardeesy, N, Camargo, FD, and Guan, K-L. 2012. "YAP Mediates Crosstalk between the Hippo and PI(3)K–TOR Pathways by Suppressing PTEN via miR-29." *Nature Cell Biology* 14 (12). Nature Publishing Group: 1322–29.
- Van Hiel, MB, Vandersmissen, HP, Proost, P, and Vanden Broeck, J. 2014. "Cloning, Constitutive Activity and Expression Profiling of Two Receptors Related to Relaxin Receptors in *Drosophila Melanogaster*." *Peptides* 68. Elsevier Inc. 83–90.
- Villalobo, A. 2006. "Nitric Oxide and Cell Proliferation." *FEBS Journal* 273 (11): 2329–44.
- Warren, JT, Yerushalmi, Y, Shimell, MJ, O'Connor, MB, Restifo, LL, and Gilbert, LI. 2006. "Discrete Pulses of Molting Hormone, 20-Hydroxyecdysone, during Late Larval Development of *Drosophila Melanogaster*: Correlations with Changes in Gene Activity." *Developmental Dynamics* 235 (2): 315–26.
- Wingrove, JA, and O'Farrell, PH. 1999. "Nitric Oxide Contributes to Behavioral, Cellular, and Developmental Responses to Low Oxygen in *Drosophila*." *Cell* 98 (1): 105–14.
- Yakubovich, N, Silva, E a, and O'Farrell, PH. 2010. "Nitric Oxide Synthase Is Not Essential for *Drosophila* Development." *Current Biology* 20 (4): R141–R142.
- Yamanaka, N, Rewitz, KF, and O'Connor, MB. 2013. "Ecdysone Control of Developmental Transitions: Lessons from *Drosophila* Research." *Annual Review of Entomology* 58 (1): 497–516.
- Zhang, C, Robinson, BS, Xu, W, Yang, L, Yao, B, Zhao, H, Byun, PK, Jin, P, Veraksa, A, Moberg, KH. 2015. "The Ecdysone Receptor Coactivator Taiman Links Yorkie to Transcriptional Control of Germline Stem Cell Factors in Somatic Tissue". *Developmental Cell*. 34(2):168-80.

Zoncu, R, Efeyan, A, and Sabatini, DM. 2011. "mTOR: From Growth Signal Integration to Cancer, Diabetes and Ageing." *Nat Rev Mol Cell Biol* 12 (1): 21–35.